# Single-Cell Analysis of the Physiology of Mechanosensation in Bacteria

Thesis by

Maja Bialecka-Fornal

In Partial Fulfillment of the Requirements

for the Degree of

Doctor of Philosophy


California Institute of Technology

Pasadena, California

2013

(Defended April 29, 2013)

© 2013
Maja Bialecka-Fornal
All Rights Reserved

# Acknowledgements

The five years spent at Caltech were a truly amazing experience for me, thanks to the people I had the chance to interact with. I feel honored and privileged to have had the opportunity to become part of the Caltech community and participate in the wonderful scientific journey called graduate school.

First and foremost, I would like to deeply thank my advisor, Rob Phillips, without whom I would never be able to get through graduate school. No words can express how much being in his group has positively influenced me and how much I appreciate his mentorship. He is an infinite source of insights into how to become a better scientist, as well as a better person in everyday life, being always there for me, ready to discuss new ideas. I couldn't have asked for a better teacher.

I would like to acknowledge my thesis committee: Doug Rees, Henry Lester, Grant Jensen, and Dianne Newman, whom I would like to thank for their helpful advice and guidance. I feel very lucky to have had the chance to interact with members of the Phillips lab: Stephanie Barnes, Helen Bermudez, James Boedicker, Justin Bois, Rob Brewster, Yi-Ju Chen, Sidney Cox, Hernan Garcia, Christoph Haselwandter, Kelsey Homyk, Stephanie Johnson, Daniel Jones, Heun Jin Lee, Martin Linden, Chao Liu, Geoff Lovely, Gita Mahmoudabadi, Sarah Marzen, Katie Miller, Pradeep Ramesh, Manuel Razo, Mattias Rydenfelt, Linda Scott, Damien Soghoian, Linda Song, Arbel Tadmor, Tristan Ursell, Dave Van Valen, Franz Weinert, and Dave Wu – a group of passionate people who inspired me in many ways. Among them, I am particularly indebted to Heun Jin Lee who spent countless hours as my scientific mentor, collaborator, and friend.

The research projects I worked on could not have been completed without the help of Morgan Beeby, Suzy Black, Ian Booth, Bill Clemons, Hannah DeBerg, Rob Egbert, Michael Elowitz, Chris Gandhi, Hernan Garcia, Steve Mayo, Alasdair McDowall, Sam Miller, Akiko Rasmussen, Sergei Sukharev, and Troy Walton.

I would like to thank the instructors and students at the Woods Hole Physiology course for pursuing science with incredible passion. I would like to specially acknowledge Jennifer Lippincott-Schwartz, Dan Fletcher, Mike Sheetz, and Linda Kenney. I am deeply indebted to the NIH and Caltech Provost for funding. There exists a number of people who have helped me along my scientific path through grad school, whom I did not mention here by name, but I would like to warmly thank them for their support.

Finally, I would like to thank my family, especially my husband Bartosz, for their constant help and support. This would not have been possible without you.

# Abstract

*Escherichia coli* is one of the best studied living organisms and a model system for many biophysical investigations. Despite countless discoveries of the details of its physiology, we still lack a holistic understanding of how these bacteria react to changes in their environment. One of the most important examples is their response to osmotic shock. One of the mechanistic elements protecting cell integrity upon exposure to sudden changes of osmolarity is the presence of mechanosensitive channels in the cell membrane. These channels are believed to act as tension release valves protecting the inner membrane from rupturing. This thesis presents an experimental study of various aspects of mechanosensation in bacteria. We examine cell survival after osmotic shock and how the number of MscL (Mechanosensitive channel of Large conductance) channels expressed in a cell influences its physiology. We developed an assay that allows real-time monitoring of the rate of the osmotic challenge and direct observation of cell morphology during and after the exposure to osmolarity change. The work described in this thesis introduces tools that can be used to quantitatively determine at the single-cell level the number of expressed proteins (in this case MscL channels) as a function of, e.g., growth conditions. The improvement in our quantitative description of mechanosensation in bacteria allows us to address many, so far unsolved, problems, like the minimal number of channels needed for survival, and can begin to paint a clearer picture of why there are so many distinct types of mechanosensitive channels.

# Contents

**Acknowledgements** **iii**

**Abstract** **v**

**1 Introduction** **1**

1.1 Mechanosensation and mechanotransduction . . . . . 2

1.2 Evolution of sensors and membrane channels . . . . . 3

**2 Mechanosensation in *Escherichia coli*** **5**

2.1 *Escherichia coli* as a model organism . . . . . 5

2.2 Bacterial anatomy . . . . . 7

2.3 Turgor pressure measurement in *E. coli* . . . . . 8

2.4 Stimuli and forces *E. coli* might be exposed to . . . . . 10

2.4.1 Osmosis . . . . . 12

2.4.2 Adaptation to increasing osmotic pressure . . . . . 15

2.4.3 Reaction to decrease in osmotic pressure . . . . . 16

2.4.4 Examples of "real" osmotic shocks . . . . . 19

2.5 Family of mechanosensitive channels in *E. coli* . . . . . 21

2.6 Standard ways of studying MS channels in bacteria . . . . . 23

2.6.1 Theoretical modeling . . . . . 23

2.6.2 Electrophysiology . . . . . 26

2.6.3 Plating assay . . . . . 30

2.7 Unanswered questions - motivation for further studies . . . . . 32

2.7.1 How many channels are there in a cell? . . . . . 32

2.7.2 What is the role of MS channels in cell physiology? . . . . . 33
2.7.3 What is the role of single-cell stochasticity? . . . . . 33

**3 Single-cell response to medium exchange 35**
3.1 The mystery of seven channels . . . . . 35
3.2 Single-cell observation . . . . . 37
3.3 Rate dependence . . . . . 40
3.4 Death mechanisms . . . . . 43
3.5 Discussion on the rate dependence phenomenon . . . . . 49

**4 Counting the number of MscL channels per cell 52**
4.1 Published results . . . . . 55
4.2 Regulation of MscL expression . . . . . 57
4.3 Strain construction and counting methods . . . . . 60
4.3.1 Western blots . . . . . 62
4.3.2 Fluorescence microscopy . . . . . 65
4.4 Results . . . . . 67
4.4.1 Mean number . . . . . 67
4.4.2 Distribution in the population . . . . . 70
4.4.3 Summary . . . . . 72

**5 Minimal number of channels needed for survival 75**
5.1 Number and variety paradox . . . . . 75
5.2 Bulk results using $\Delta rpoS$ strain . . . . . 76
5.3 RBS modification . . . . . 79

**6 Hypothesis of an alternative function of MS channels 84**
6.1 Overexpression of one type of MS channel guarantees survival . . . . 84
6.2 Experimental hints at an alternative function of MS channels . . . . . 86

**7 Future directions 92**
7.1 Monitoring channels' activity *in vivo* . . . . . 92

7.1.1 What are calcium-sensitive proteins? . . . . . 93
7.1.2 Preliminary results . . . . . 93
7.2 Volume change measurement . . . . . 96
7.2.1 Experimental design . . . . . 97
7.2.2 Preliminary results . . . . . 100
7.2.3 Possible variations . . . . . 102
7.3 High resolution imaging: cryo-EM . . . . . 105

**8 Conclusions** **110**

**Appendices** **113**

**A Modified protocol for the plating assay** **114**

**B Flow cell assembly** **117**

**C MLG910 strain: chromosomal integration strategy** **120**

**D Gamma fitting parameters** **122**

**Bibliography** **127**

# Chapter 1

# Introduction

In order to survive, all living organisms have to respond to stimuli from the environment by activating mechanisms that will allow them to adapt to new conditions. The molecular elements used to detect, recognize, and transmit these signals are therefore crucial for controlling homeostasis and cell survival.

Mechanosensing structures are present across all kingdoms of life. The best known example from the Plantae kingdom is *Dionaea muscipula* (Venus Flytrap) (Figure 1.1A). This carnivorous plant has multiple hair cells on the inner surface of each half of the leaf. They serve as mechano-motion detectors that need two closely-spaced stimuli (20 seconds) [1] to close the trap. This narrow time window minimizes the chance of accidental activation. Another well-studied example is the reaction of the worm *Caenorhabditis elegans* (Figure 1.1B) to a touch stimulus. This worm has six touch receptor neurons, which are part of a mechanoreceptive complex [2]. The transduction apparatus is formed by a mechanically sensitive ion channel connected to both intracellular and extracellular matrix proteins.

The ability to react to a mechanical stimulus is present in humans as well. One of the better known examples in medicine is Babinski's response [3]. This test is used to identify a disease of the spinal cord and brain in adults. The patient's foot is stimulated with a blunt instrument. In case of malfunction of the nervous system, the hallux will show an upward response as the stimulus is not inhibited by the cerebral cortex (Figure 1.1C). Interestingly, in infants the response to this test is simply a

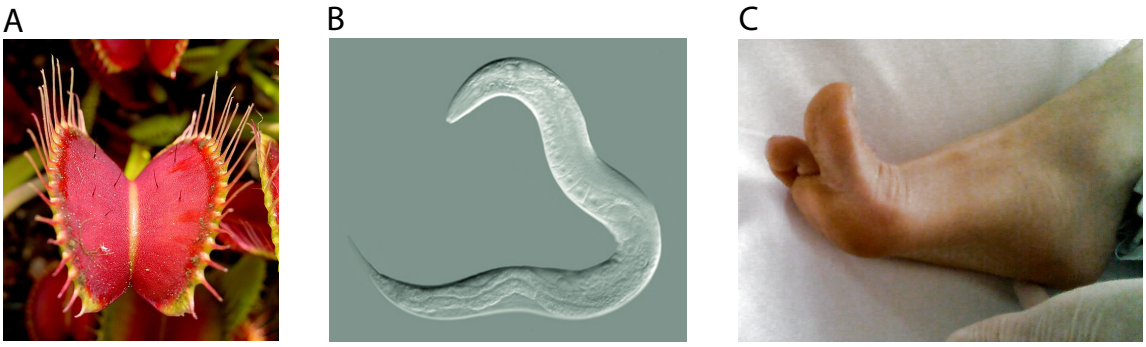


Figure 1.1: Examples of mechanosensing structures in various organisms. (A) A trap of *Dionaea muscipula* (Venus Flytrap). The hair cells are used as mechano-motion detectors which transduce the signal, closing the trap (photo by Noah Elhardt [4]); (B) The worm *Caenorhabditis elegans* has six touch receptor neurons, which react to touch stimulus (photo by Bob Goldstein [5]); (C) Babinski's response to stimulation of the patient's foot with a blunt instrument is used in medicine for identification of neuronal malfunctioning (photo by Medicus of Borg [6]).

primitive reflex, as the nerve cells are not fully myelinated at an early age.

## 1.1 Mechanosensation and mechanotransduction

Stimuli from the environment may be quite different in nature, e.g., mechanical, chemical or physical. In this thesis we will concentrate only on mechanical stimuli.

As discussed above, the structure and location of the sensor varies depending on the organism. However, there are some features which all mechanosensing systems in different organisms have in common. To achieve proper sensitivity and a fast response, these mechanical stimuli are directed to specific channels, where they are translated into a flow of ions. For example, the voltage-gated and mechanosensitive superfamilies of channels respond to electrostatic membrane potentials and to membrane tension caused by mechanical stimuli, respectively. The ligand-gated superfamily of channels is activated in response to specific interactions with small molecules, such as $\gamma$-aminobutyrate or glycine. All types of channels can open rapidly and amplify the signal. A general model of a mechanotransduction complex (Figure 1.2) consists of a mechanosensitive ion channel connected to extracellular and intracellular matrix

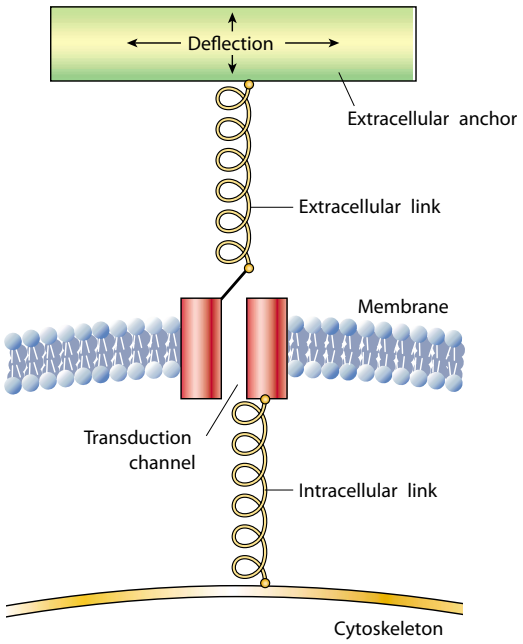


Figure 1.2: A general model of a mechanotransduction complex [2]. A channel is linked to intracellular (cytoskeleton) and extracellular matrix proteins. When the force is applied to the extracellular structure, the relative displacement of these elements gates the channel due to the increase of the tension.

proteins. The channel is activated (its open probability changes) when it detects the change in the tension caused by the deflection of an extracellular structure with respect to the intracellular one. In bacteria, channels that respond to tension change in the membrane are called mechanosensitive (MS) channels.

## 1.2 Evolution of sensors and membrane channels

Channels are mediators between the cell interior and exterior. Such a connection is essential for many functions, e.g.: transport of ions, nutrients, and waste products; cellular growth and volume regulation; transmission of environmental signals to the cell interior. This is why these structures are believed to have evolved very early [7]. Most channels have selectivity encoded in the amino acid sequence and preferentially conduct only one type of ion, e.g., $Na^+$, $Ca^{2+}$, $Cl^-$, or a specific neutral species like water. This diversity is required for adaptation (to different nutritional sources or

environmental conditions) and a more complex signal transduction in multicellular organisms.

Mechanical force can be sensed universally and MS channels, being transducers of mechanical stress, are believed to be among the oldest signal transduction molecules known. They might have evolved as early as 3.5 Gyr ago [8, 9]. MS channels are present in the membranes of organisms from the three domains of life: bacteria, archaea, and eukaryotes [9, 10, 11, 12, 13, 14].

# Chapter 2

# Mechanosensation in *Escherichia coli*

## 2.1 *Escherichia coli* as a model organism

*Escherichia coli* (*E. coli*), originally named *Bacterium coli commune*, was isolated and brought to scientific attention by Theodor Escherich in 1885 [15]. His motivation and devotion to finding an agent which caused childhood diarrhea (very serious illness at the time) resulted in isolating various bacterial strains from fecal matter samples from children (Figure 2.1). The ease of culture made *E. coli* the most popular bacterium, even though it is only a minor ingredient of the intestinal flora of an adult human (between 0.2% and 1.5% of the total number of cells) [16]. Escherich's work with *E. coli* led to many fundamental biochemical discoveries and advanced molecular biology.

*E. coli* is an aerobic, Gram-negative, non-sporulating, rod-shaped bacteria that can be commonly found in animal feces and lower intestines of mammals. It can also be found in environments of higher temperature, such as the edge of hot springs. *E. coli* can be classified into hundreds of variants on the basis of different serotypes, which are recognized based on the O (cell wall (somatic)), H (flagella), and K (capsular) antigens. Enteric *E. coli* can be classified into six categories based on its virulence properties, such as enterotoxigenic *E. coli* (ETEC), enteropathogenic *E. coli* (EPEC), enteroinvasive E. *coli* (EIEC), enterohemorrageic *E. coli* (EHEC), enteroadherent aggregative *E. coli* (EAggEC), and verotoxigenic *E. coli* (VTEC) [17].

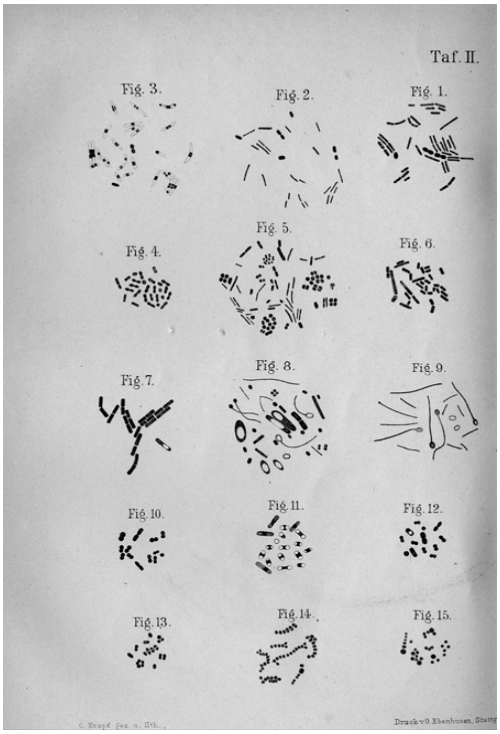


Figure 2.1: Photograph of the original figure from Escherich's book from 1886 showing various bacterial species and difference in their morphology. Fig. 4: *Bacterium coli commune* from a 6 day old potato culture; Fig. 6: *Bacterium coli commune* from an 8 day long culturing on a gelatin plate; Fig. 7: *Bacillus subtilis*, one bacterium at the stage of spore formation; Fig. 10: *Bacterium lactis aerogenes* from an 8 day long culturing in a gelatin tube. Photographs were taken by Charles Workman [15].

The presence of *E. coli* in human intestines helps with the digestion processes, food breakdown and absorption, as well as vitamin K production. Some strains of *E. coli*, however, can cause severe infections, e.g., enteroaggregative *E. coli*. One of the most common cases is the urinary tract infection. The most infective *E. coli* strain found so far is O157:H7 and it causes food poisoning, bloody diarrhea and even kidney failure. It produces a Shiga-like toxin which inactivates 60S ribosomal subunits of most eukaryotic cells. This in turn blocks mRNA translation and leads to cell death. The non-pathogenic strains used in the lab for research purposes, such as *E. coli* K-12, are so distant from their ancestors that they have lost their ability to survive in the human intestine [15].

## 2.2 Bacterial anatomy

Based on the cell surface structure, bacteria can be divided into two groups: Gram-positives and Gram-negatives. *E. coli* belongs to the second group, which means that its envelope consists of two independent membranes (cytoplasmic and outer membrane) and the peptidoglycan mesh between them. The cell envelope is not only a milieu of many biochemical processes, but it also protects the cell and its content from destructive and sudden impulses from the environment, e.g., water potential changes.

The cell is built of multiple elements, which may show different properties when isolated from the organism compared to their functioning in the intact cell. One such example is the cell membrane geometry: in a living cell it is limited by the peptidoglycan; without it, the membrane forms a spherical structure (Figure 2.2).

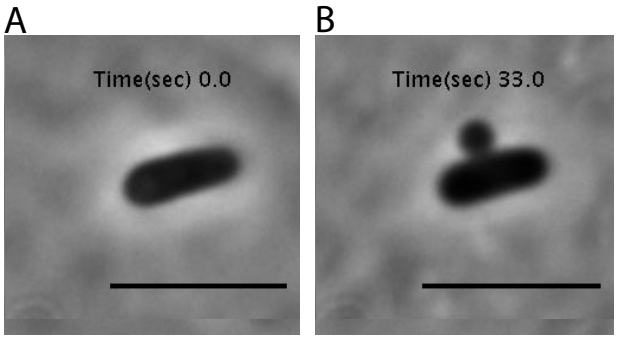


Figure 2.2: Single *E. coli* cell before (A) and after (B) osmotic downshock. The cells were grown in 0.5 M NaCl medium in the presence of a low concentration of ampicillin. The presence of antibiotic is thought to cause point defects in the peptidoglycan layer by inhibiting the enzyme transpeptidase. (A) Cell before the shock does not show any morphological defects; (B) Cell after the osmotic downshock into 0 M medium. The increase in the turgor pressure "pushed" the inner membrane through the damaged region peptidoglycan layer. The visible membrane "bleb" indicates that in the absence of peptidoglycan the membrane prefers a spherical geometry. The scale bars are 2 $\mu$m.

One should remember that culture conditions in the laboratory are often radically different from the natural habitat of the organism and, thus, one needs a sophisticated experimental design to capture the physiology under natural conditions.

Isaac and Ware [18] showed that the Gram-negative cells exhibit considerable elas-

ticity, whereas the Gram-positive organisms show a far greater resistance to stretching. The *E. coli* cell envelope can become as much as 100% longer when stretched along the major axis. Wang *et al.* [19] reported the results of an experiment on *E. coli* which suggests that MreB (bacterial actin homologue) contributes almost as much to the cell stiffness as the peptidoglycan layer, indicating an important role of the bacterial cytoskeleton homologue. These results imply that in order to resist mechanical perturbations bacteria could (apart from activating physiological mechanisms) increase the peptidoglycan density (or cross-linking) or increase the amount of MreB.

## 2.3 Turgor pressure measurement in *E. coli*

Bacteria accumulate ions and molecules necessary for growth in the cytoplasm. As a result, the osmolarity (solute concentration defined as the number of osmoles of solute per liter of solution) inside bacteria is higher than the osmolarity of the growth medium. This differential osmotic pressure is called turgor pressure. It pushes the membrane against the peptidoglycan layer maintaining bacterial shape, and is believed to be the driving force for bacterial growth [20]. Changes in the outer osmolarity (of the environment) influence the osmolarity inside the cell due to water moving across the membrane. Such a stress on the membrane activates various mechanisms: inducing the expression of osmoregulatory genes [21] in the case of an increase in external osmolarity, or opening of mechanosensitive channels in the case of a decrease in external osmolarity [22]. Turgor pressure regulates several functions in bacteria: signal transduction systems, periplasmic transport functions, synthesis of porins in the outer membrane, and expression of genes in the transport system responsible for the $K^+$ uptake [21, 23, 24]. For all of these reasons there have been many attempts to measure the turgor pressure (Table 2.1). However, the measured values vary a lot.

The turgor pressure in Gram-positive bacteria is much higher than in Gram-negative bacteria. This difference can be explained by the different thicknesses of the peptidoglycan layer in these two groups of organisms. However, the measured values

| Organism | Value [atm] | Method | Ref. |
|---|---|---|---|
| ***Gram-positive bacteria*** | | | |
| *Staphylococcus aureus* | 20 – 30 | water uptake | [25] |
| *Bacillus subtilis* | 18.8 | hypersaline treatment | [26] |
| *Enterococcus hirae* | 3.95 – 5.9 | AFM | [27] |
| ***Cyanobacteria*** | | | |
| *Anabaena flos-aquae, Nodularia sp* sp. | 0.79 – 1.78 | gas vesicles collapse | [28] |
| *Microcystis* sp. | 6.4 – 10.9 | gas vesicles collapse | [29] |
| ***Gram-negative bacteria*** | | | |
| *E. coli* | 5 – 6 | | [25] |
| *E. coli* | 5 – 10 | lysozyme | [30] |
| *E. coli* | 0.7 – 3.1 | amount of water | [31] |
| *E. coli* | 0.26 | AFM | [32] |
| *E. coli, Salmonella typhimurium* | 3.5 | solute distribution | [33] |
| *Ancylobacter aquaticus* | 1.85 | gas vesicles collapse | [34] |
| *Ancylobacter aquaticus* | 1.06 | gas vesicles collapse | [35] |
| *Pelodictyon phaeoclathratiforme* | 3.26 | gas vesicles collapse | [36] |
| *Magnetospirillum gryphiswaldense* | 0.84 – 1.48 | AFM | [37] |
| *Pseudomonas aeruginosa* | 0.1 – 3.95 | AFM | [27] |

Table 2.1: Comparison of the turgor pressure measured using various methods in Gram-positive, Cyanobacteria, and Gram-negative bacteria. A significant difference in measured values is observed not only when comparing different groups of organisms (e.g., Gram-positive and Gram-negative bacteria), but among the representatives of the same group as well.

or the turgor pressure vary a lot even among the species from the same group. In the case of Gram-negative bacteria the reported values differ by up to two orders of magnitude (0.1 – 10 atm, Table 2.1). As mentioned above, turgor pressure plays an important role in many physiological reactions and regulations. The lack of information on the exact value of this parameter has a lot of consequences for our ability to predict and model the reaction of the cell to a given stimulus. Due to the variation in measured turgor pressure values we don't know how hard the membrane is pressed against the peptidoglycan layer or how much support it gets from the cell wall. This, in turn, makes it impossible to accurately predict the reaction of a cell to exposure to a medium of a given osmolarity or measure how fast the cell can adapt to this change. Depending on the difference between the internal concentration of solutes and the medium the cell was shocked with, the rate of the water efflux/influx will change and

the reaction to this stimulus may occur at different time scales. As mentioned above, stress on the membrane activates various osmoprotective mechanisms. Without an accurate measurement of the pressure change due to water diffusion one cannot quantitatively study and describe the details of cell reaction to osmotic challenges. One of the possible explanations for the source of the variation in the measured turgor pressure values is that the cell is in a dynamic state, readily adapting to shifts in environmental conditions or mechanical stimuli introduced by the techniques used for the measurement, which may result in turgor pressure changes occurring very fast, at the time scales shorter than the time needed for the measurement.

## 2.4 Stimuli and forces *E. coli* might be exposed to

To gain a holistic view of bacterial physiology, i.e., how it changes under the influence of various stresses and what the factors influencing cell survival are, one should study the environmental specimens. However, these specimens are very challenging to work with, the main reason being the lack of tools to define the number of bacterial species in the environmental sample and their physiological state (alive or dead). The two main methods used – plate count and direct microscopy count – are not completely satisfactory (Figure 2.3). In the case of plate counting there is no single medium which can be used to culture bacteria from the environmental sample, so the counting results are biased depending on the species present in the specimen. The direct microscopy count captures the number of all species, however, it does not provide any information on the ability of the bacteria to grow, metabolize, respire, or divide. The situation is further complicated by the discovery of a viable yet nonculturable stage, postulated to be a mechanism of bacterial survival, in which bacteria are alive but do not undergo cell division [38]. Not only the count but also the "normal" physiological state of bacteria in the environment are hard to define. The most popular view is that the microbes are in a dynamic state and they adapt to a continuously changing environment by genotypic and phenotypic modifications [38]. In the environment, both the chemical and physical parameters may change at the same time depending

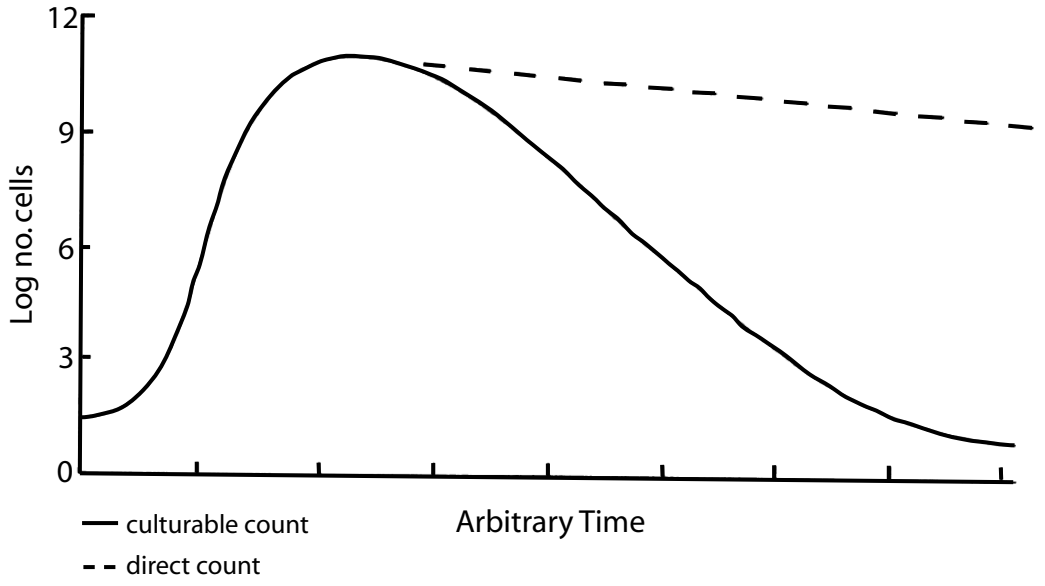


Figure 2.3: Difference in the number of bacteria estimated by the plate counting method and direct microscopy. The plate counting method introduces the bias towards organisms which can be cultured in the laboratory setting. The microscopy counts are more accurate in term of number of cells, however, they do not provide any information on their physiological state. The difference in counts from these two methods represents viable but not dividing cells [38].

on the local microenvironment, time of the year, or the presence of other species. The most important one, however, is water availability. Water is necessary for survival of all living organisms. This is why all animals evolved osmoregulatory mechanisms, controlling the composition and volume of internal fluids. The development of this control system facilitated the differentiation of freshwater and terrestial animals [39].

All of these obstacles discussed above limit the studies on the response of a cell to given stimuli to observations of only a single isolated aspect of bacterial physiology using a laboratory strain. This work focuses on the survival of *E. coli* after exposure to water potential changes. The ease of growing *E. coli* in a laboratory setting made it the best studied living organism and a model organism to monitor the pollution of water. Information on the survival of *E. coli* in a given environment is of special interest, since it is used as an indicator of a potential danger from fecal contamination.

Despite our knowledge on *E. coli*'s physiology, genetics, and biochemistry, we lack

a general understanding of how it behaves and survives in its natural habitats. The habitats of *E. coli* can be divided into two groups: host-associated and open. However, one should remember that the genomes of different forms of *E. coli* may vary even by 20%, which results in different phenotypes from changing patterns of gene expression [40]. This variation may be the effect of experiencing a biphasic lifestyle (host-independent and host-associated phases) and, as a consequence, exposure to various evolutionary pressures (biotic and abiotic [41]). These two environments are very different. *E. coli* living in the human intestine is under pressure from the biotic factors: competitors, cheaters, or host defense mechanisms. Bacteria entering the human digestive system with food are exposed to low pH when entering the stomach. In the intestine they are exposed to big variations in water content: the moisture content of feces may oscillate between 53 and 92% [42]. Bacteria in the urinary tract experience significant variations in the osmolarity, roughly 900 mOsm (Figure 2.4). Also, the composition of the *E. coli* population in the intestine is constantly changing with no dominant serotype [43] and may vary significantly depending on the source of the sample [44].

The challenges in the open environment are very different: temperature, UV radiation, low concentration of nutrients, and fluctuating osmolarity and water level. Survival depends on how well *E. coli* can cope with rapidly changing conditions and adapt to them. The most important factor is water availability. Without proper water activity, cells desiccate very quickly (15 – 60 hours) [45]. If there is enough moisture, *E. coli* can survive many days in the environment: in sea water [41, 46, 47], fresh water [47], as well as the beach sand [48].

### 2.4.1 Osmosis

Osmosis is the net movement of a solvent (or solvents) across a partially permeable membrane (ideally, permeable to the solvent, but not to the solute) into a region of higher solute concentration, in order to equalize the solute concentrations on both sides. It was discovered in 1748 by L'Abbé Nollet [49]. The first quantitative mea-

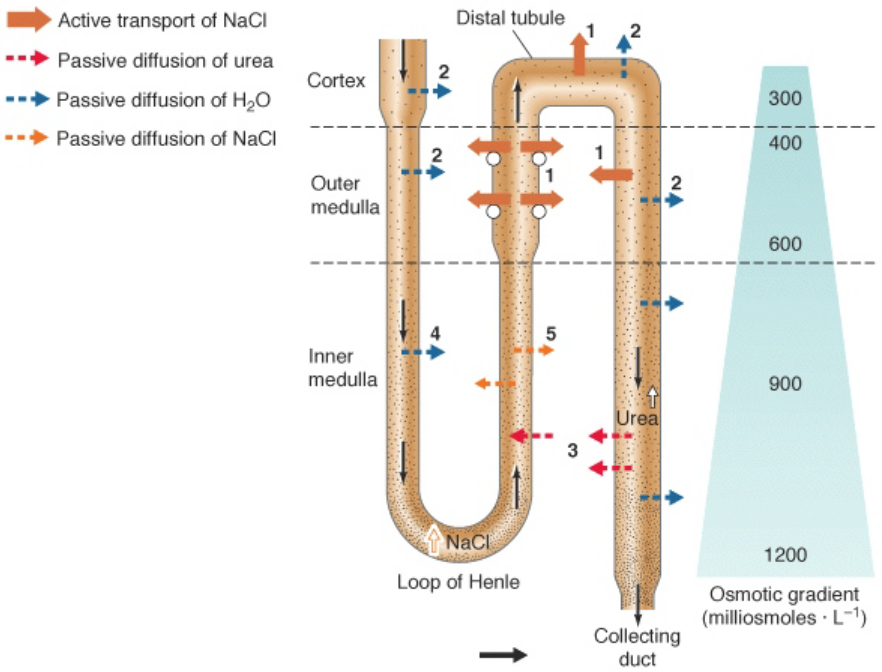


Figure 2.4: The osmolarity changes which bacteria may be exposed to when living in the urinary tract. The content of the urine changes significantly due to resorption of valuable molecules (e.g., proteins and sugars). Active transport of NaCl and diffusion of urea, water, and NaCl increase urine osmolarity from 300 to 1200 mOsm. Figure adapted from [50].

surements were carried out between 1826 and 1846 by René Joachim Henri Dutrochet (who was the first to use terms "endosmosis" and "exosmosis" [51], Figure 2.5A) and Karl Vierordt [52]. They concluded that the rate of osmosis depends on both the nature of the salt and the concentration of the solution. Later, it was shown that also the type of membrane separating the two solutions plays an important role. This fact was subsequently used by Thomas Graham for the separation of different substances by dialysis [53] (Figure 2.5B). In 1864, Moritz Traube obtained a precipitation membrane permeable to water (tannic acid and non-setting glue) forming a coating on a drop and, thus, initiating studies of the "endosmotic force" [54]. Jacobus Henricus van't Hoff called the membrane which is permeable only to the solvent a semi-permeable membrane (there is no membrane that is completely impermeable to the solute) [55].

The osmotic pressure is defined as an equivalent of the excess pressure which must

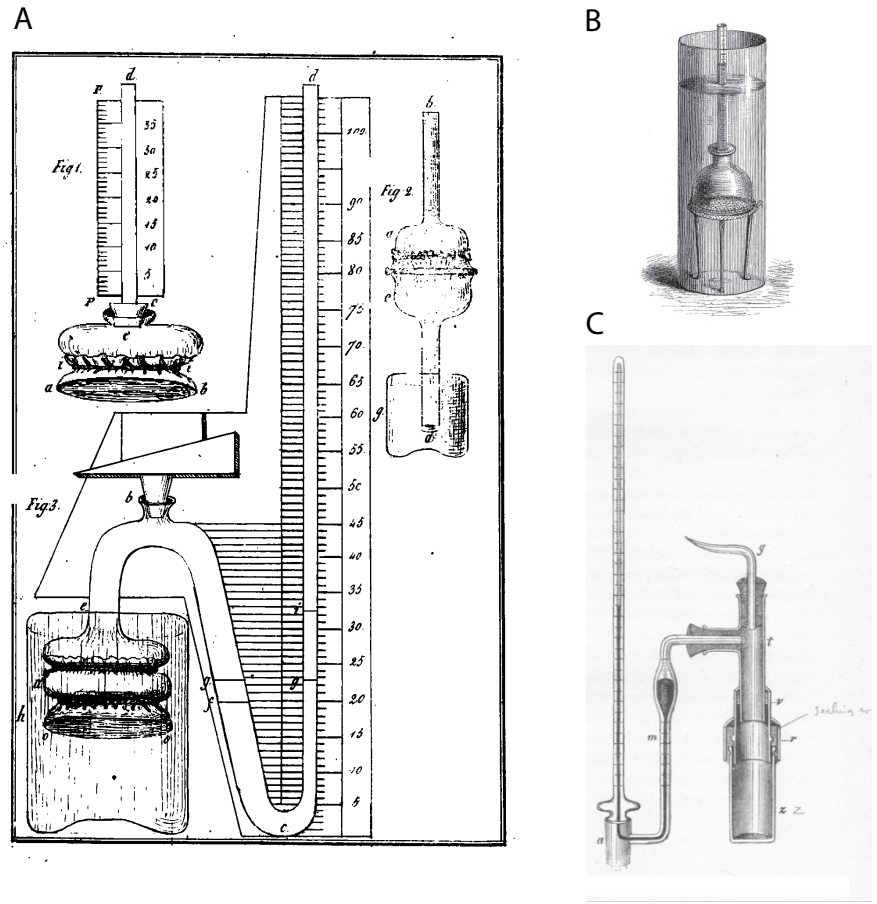


Figure 2.5: Examples of osmometers. (A) Osmometer used by Dutrochet [56]. This type of an osmometer was used for the first quantitative measurements of osmosis; (B) Osmometer used by Graham [53]. After the discovery that the type of the membrane separating two solutions plays an important role, this type of osmometer was used by Graham to study the separation of various substances by dialysis ; (C) Osmometer used by Pfeffer [57]. Formation of a membrane in the wall of porous earthenware pots significantly increases the range of values which can be measured in this type of the osmometer.

be imposed in order to prevent the solvent from passing through the perfectly semi-permeable membrane. In 1877, Wilhelm Pfeffer introduced a device which made a measurement of the osmotic pressure of several atmospheres possible and practicable (he formed a membrane in the wall of porous earthenware pots) [57] (Figure 2.5C). He showed that the osmotic pressure was proportional to the concentration and it increased with rising temperature. The subsequent very important step in studies on osmosis was van't Hoff's theory of dilute solutions from 1885. Applying thermodynamics and stating that the physical properties of a dilute solution are identical

with that of a gas, van't Hoff deduced that *the osmotic pressure of a solution is equal to the pressure which the dissolved substance would exercise in the gaseous state if it occupied a volume equal to the volume of the solution* [58]. The first direct determination of osmotic pressure was carried out by Wilhelm Pfeffer and later perfected by Harmon Northrop Morse [59].

### 2.4.2 Adaptation to increasing osmotic pressure

*E. coli* cells can grow in a variety of environments, from very aqueous to those with high salt concentration. The bacterial growth in environments with such a wide range of osmolarities is a great challenge for cell physiology. A very high membrane permeability for water compared to other molecular species (permeability coefficient for water: $10^{-6}$ to $10^{-2}$ cm/s depending on the cell type; permeability coefficient for $Na^+$: $10^{-12}$ cm/s [60, 61]) makes *E. coli* sensitive to osmolarity changes in the environment. In case of an increase in osmolarity the cell has to retain water necessary for growth and biochemical reactions by, e.g., increasing the osmolarity of the cytoplasm. At the same time, the solutes accumulated in the cytoplasm (by transport or synthesis) to reduce these osmotically induced changes can't destabilize the homeostasis of the cell or cause a disruption of biochemical processes (this is why they are called compatible solutes). Such solutes include $K^+$, amino acids (glutamate, proline) and their derivatives (peptides), quaternary amines (glycine betaine, carnitine), sugars (sucrose, trehalose), and tetrahydropyrimidines (ectoines) [62].

*E. coli* exhibits both passive and active responses to change in the external osmolarity. Upon transition to an environment of higher osmolarity, *E. coli* reacts passively by losing cytoplasmic water and decreasing turgor pressure, which may lead to plasmolysis. This triggers an active response. In order to increase the osmolarity of the cytoplasm, *E. coli* accumulates potassium ions through a constitutive, low affinity Trk system and an inducible, high affinity Kdp system expressed when turgor pressure is low [63, 64]. The amount of accumulated $K^+$ depends on the osmolarity of the external medium (0.11 M for each 0.2 Osm increase in external osmolarity,

maximum uptake rate being 10pmol/cm$^2$s) [63, 64]. Simultaneously, to balance the electric charge of accumulated $K^+$, cells synthesize glutamate. A 0.5 M NaCl upshock induces an increase of glutamate concentration to 300 nmol/mg dry mass within 10 minutes [65].

In the next phase, to avoid very high internal ionic strength, *E. coli* substitutes potassium and glutamate with zwitterionic (a molecule with a positive and a negative electrical charge) or neutral solutes (neutral and zwitterionic solutes are more favorable to protein stability). A 0.5 M NaCl upshock induced synthesis of the disaccharide trehalose to a concentration of 300 nmol/mg dry mass within 2 hours [65]. The second phase response may be much faster if the compatible solutes are present in the medium. The most common zwitterions are glycine betaine and proline [21, 62, 66]. These compounds can be accumulated in the periplasm at a high concentration. For example, uptake of glycine betaine through a high affinity betaine transport proU of more than 1 $\mu$ mol/mg of dry mass translates to cytoplasmic concentration of close to 1 M [65, 67]. Glycine betaine can also improve a diminished growth rate due to the presence of high salt concentration [67].

### 2.4.3 Reaction to decrease in osmotic pressure

Bacteria are very often exposed to sudden changes in osmolarity of the surrounding fluids. Membranes are most permeable to water (permeability coefficient varies from $10^{-6}$ to $10^{-2}$ cm/s depending on the cell type [60, 61]) and least permeable to charged molecules like ions (permeability coefficient for $Na^+$ is $10^{-12}$ cm/s [60]). However, membrane permeability (measure of the ability of a membrane to allow molecules to pass through it) is not high enough to release tension from the membrane fast enough and prevent it from rupturing.

Osmotic shock was used in microbiology laboratories as a method of depleting cells of a given molecule of interest (metabolite, ion or enzyme) without damaging the cells [68, 69]. However, the mechanism of this phenomenon was unknown. Epstein and Schultz [63] proposed that the variety and non-specificity of the released compounds

are due to their leakage through the hole in the cell wall and membrane produced by the tension.

The discovery of MS channels, especially MscL (Mechanosensitive channel of Large conductance), made them a perfect candidate to explain this phenomenon. The size and types of the molecules which might be released through these channels was studied using various methods (Table 2.2), however, some controversy concerning the size and the mechanism of release still remains. Schleyer *et al.* [70] looked at the amino acids that *E. coli* releases during osmotic shock. Surprisingly, aspartate and glutamate were released whereas alanine, lysine, and arginine were not. Ajouz et al. [65] have shown that thioredoxin (11.5 kDa), and Berrier *et al.* [71] have shown that the heat shock protein DnaK (41 kDa) and elongation factor Tu (52 kDa) are released during osmotic shock through MscL channels. However, the work by van den Bogaart *et al.* [72] contradicted these results. They have shown that MscL can release proteins up to at least 6.5 kDa, but not bigger. In their experiments, liposomes (artificially-prepared lipid vesicles) with MscL reconstituted were monitored for the release of fluorescently labeled species upon channel activation. Molecules with a mass bigger than 6.5 kDa, i.e., thioredoxin (11.5 kDa), histidine-containing protein HPr (9 kDa), and $\alpha-$lactalbumin (14 kDa), all labeled with Alexa fluor 633 ($\sim$ 1 kDa), were not released from the liposomes upon MscL gating. Using the crystal structure of thioredoxin, histidine-containing protein HPr, and $\alpha-$lactalbumin, the sizes of these molecules (25 x 30 x 35 Å, 32 x 32 x 33 Å, and 52 x 32 x 34 Å, respectively) are comparable to or bigger than the estimated size of the MscL pore. Based on channel conductance and the fact that poly-L-lysines with a diameter bigger than 37 Å blocked the conductance of the channel, the size of the MscL pore is estimated to be 26-46 Å [73, 74].

One possible explanation of the discrepancy between van den Bogaart's and previous results is that part of the molecules is being released through small holes in the membrane. The work of Vazquez-Laslop *et al.* [75] has shown that the polypeptides

| Molecule | Mass | Amount | Shock | Method | Ref. |
|---|---|---|---|---|---|
| potassium | 39 Da | 60% | 1000 mOsm | flame photometer | [63] |
| potassium | 39 Da | 85% | 0.2 M NaCl | valinomycin electr. | [76] |
| potassium | 39 Da | 85% | 0.25 M NaCl | flame photomety | [70] |
| potassium | 39 Da | 50-85% | 0.2 M NaCl | valinomycin electr. | [65] |
| amino acids | | 80% | 10x dilution | radioactivity | [77] |
| $PO_4^{3-}$ | 95 Da | 100% | | radioactivity | [77] |
| TMG | 210 Da | 80% | 0.5 osm | radiolabeling | [78] |
| galactose | 180 Da | 40% | 10x dilution | radiolabeling | [78] |
| nucleotides | $\sim$ 300 Da | 40% | 500 mOsm | UV absorption | [78] |
| ATP | 507 Da | 76% | 0.2 M NaCl | luciferin/luciferase | [76] |
| ATP | 507 Da | 5% | | [79] | [70] |
| lactose | 342 Da | 82% | 0.2 M NaCl | radiolabeling | [76] |
| glutamate | 145 Da | 83% | 0.2 M NaCl | enzymatic assay | [76] |
| glutamate | 145 Da | 75% | 0.4 M NaCl | phenol method | [70] |
| glutamate | 145 Da | 80% | 0.5 M NaCl | enzymatic assay | [65] |
| $Rb^+$ | 85 Da | 93% | 0.2 M NaCl | radiolabeling | [76] |
| trehalose | 342 Da | 75% | 0.4 M NaCl | phenol method | [70] |
| trehalose | 342 Da | 70% | 0.5 M NaCl | phenol method | [65] |
| aspartate | 1333 Da | 80% | 0.4 M NaCl | phenol method | [70] |
| glycine betaine | 117 Da | 90% | 0.5 M NaCl | radiolabeling | [65] |
| thioredoxin[1,2] | 14.8 Da | 100% | 0.5 M NaCl | enzymatic assay | [65] |
| DnaK[1] | 41 kDa | 60% | 20% sucrose | immunoblotting | [71] |
| DnaK[1] | 41 kDa | | | immunoblotting | [80] |
| RFP | 862 Da | 44% | 20% sucrose | fluorescence | [80] |
| EF-Tu[1] | 52 kDa | 70% | 20% sucrose | immunoblotting | [71] |
| Est55[1] | 55 kDa | 89% | 20% sucrose | p-nitrophenyl butyrate | [81] |
| glutathione[3] | 307 Da | 35% | | fluorescence-burst | [72] |
| R9C[3] | 1 kDa | 50% | | fluorescence-burst | [72] |
| insulin[3] | 5.7 kDa | 60% | | fluorescence-burst | [72] |
| BPTI[3] | 6.5 kDa | 30% | | fluorescence-burst | [72] |
| protein content[1] | | 10% | 20% sucrose | electrophoresis | [75] |
| DsbA*[1] | 23 kDa | 90% | 0.5 M sucrose | enzymatic assay | [82] |
| DsbC*[1] | 25 kDa | 73% | 0.5 M sucrose | enzymatic assay | [82] |

Table 2.2: Molecules released from *E. coli* cells during osmotic shock. TMG = $\text{methyl}-\beta-\text{D}-\text{thiogalactoside}$, RFP = trimethylpyrrocorphin and sirohydrochlorin, BPTI = bovine pancreas trypsin inhibitor, Est55 = carboxylesterase of *Geobacillus stearothermophilus*, EF-Tu = elongation factor Tu, R9C = bradykinin R9C, DsbA* and DsbC* = leaderless (signal sequence deleted). The phenol method is described in [83]. [1] = in the presence of EDTA, [2]= contradicted by [72], [3] = labeled with Alexa 633 (1089 Da).

released during osmotic shock are identical with those released during electroporation. It is known that electroporation causes formation of pores in biological membranes that can be healed [84, 85]. The similarity in protein release for these two techniques may indicate that osmotic shock also causes transient holes in the cell membrane. Molecular dynamics studies [86] have shown that at a loading rate of 660kN/(m × s) the membrane ruptures before the MscL channel gets activated. However, once the internal and external pressures are equalized, the liposome can close itself by healing the rupture. There exists no experimental proof yet that this is also true for an *E. coli* exposed to osmotic shock, but the membrane sealing was experimentally demonstrated for red blood cells [87].

### 2.4.4 Examples of "real" osmotic shocks

Bacteria can be found inside and on the surface of the human body, as a part of the regular microflora or as an effect of infection. The largest population of bacteria can be found in the intestine, in the mouth, and on the skin. These bacteria have to be in osmotic equilibrium with the surrounding fluids (intracellular or extracellular). An interesting problem to consider is the osmotic pressure change which these cells are exposed to when diluted with water. As an example, the osmolarity change for bacteria inhabiting three different regions of the human body (mouth, intestine, and urinary tract) can be calculated using equation (2.1), where $\Delta\pi$ is the osmotic pressure change, $R$ is the gas constant, $T$ is the temperature, and $\Delta C$ is the concentration change.

$$\Delta\pi = RT\Delta C. \tag{2.1}$$

The distribution of water in the human body varies a lot between the compartments: about 80% of total water is cell water (intracellular fluids), 12% is the blood in circulation, and about 5.6% in the plasma (the liquid which remains when blood cells and other solid particles have been removed) [39]. The osmolarity of the fluids secreted from the human body (e.g., tears, saliva or sweat) is similar to that of the

blood, but the composition may vary significantly due to diffusion and resorption. For example, the osmolarity and the content of urine changes significantly between the beginning (where it is close to the osmolarity of other physiological fluids) and the end of a nephron (where it is mostly water, urea, and ions). Most of the water and solutes (e.g., proteins, sugar, or NaCl) that are filtered in the nephron are resorbed. Active transport and diffusion change both the composition and the osmolarity of the urine (Figure 2.4). Interestingly, the composition of saliva and sweat depends on the rate of secretion. For example, the amount of sodium in saliva increases with increasing rate of flow (from 20 mM at 3 mL/min to 90 mM at 40 mL/min) [39]. Assuming that sodium is the only osmolyte in the saliva, one can estimate the osmolarity to vary between 20 and 90 mOsm. Using this value and $T = 310$ K (body temperature) to solve equation 2.1, one obtains an estimate of the osmotic pressure change that bacteria inhabiting our mouth are exposed to when one drinks a glass of water that varies between 0.5 and 2.3 atm.

Feces represent the sum of the indigestible parts of ingested food, digestive juices and cells shed by the mucous membrane lining of the digestive canal. In human, the total quantity of liquid passing into the gut probably amounts to 10 liters a day, of which all but about 100 ml are resorbed [39]. The typical stool osmolarity is 290-300 mOsm per kg [88], however, the moisture content of the feces may range between 53 and 92% [42]. The osmolarity of the intestinal content depends on the diet (the products of bacterial fermentation) and the amount of undigested or unabsorbed food in the intestine (which increase the osmolarity of the intestinal content causing lesser water reabsorption and smaller change in the concentration of ions [42, 89]). Taking 290-300 mOsm per kg as a typical osmolarity of the stool, the osmolarity change which the bacteria are exposed to when going into water is about 7.7 atm.

The osmolarity of human urine ranges between $70 - 1200$ mOsm/L [90]. Table 2.3 lists the osmolarity of infected urine samples from eight different individuals. These samples were diluted into water. Using equation (2.1), the osmotic pressure the bacteria were exposed to was estimated to be on average above 20 atm. For comparison,

the recommended pressure of the car tire is 2 atm.

| urine number | osmolarity [mOsm/L] | osmotic pressure [atm] | viable bacteria/mL | | |
|---|---|---|---|---|---|
| | | | before lysis | after lysis | % survival |
| 1 | 500 | 12.9 | 200 | 20 | 10 |
| 2 | 1126 | 29 | 11600 | 2600 | 22.4 |
| 3 | 1016 | 26.2 | 7000 | 860 | 12.3 |
| 4 | 1012 | 26 | 2300 | 470 | 20.4 |
| 5 | 996 | 25.7 | 15000 | 3200 | 21.3 |
| 6 | 1056 | 27.2 | 2148000 | 548000 | 25.5 |
| 7 | 980 | 25.2 | 810000 | 12400 | 1.53 |
| 8 | 904 | 23.3 | 2470 | 160 | 6.5 |

Table 2.3: Osmotic fragility of spheroplasts induced in human urine *in vitro*. All samples were diluted $1:40000$ into water. The atmospheric pressure change the bacteria were exposed to was calculated using equation (2.1). The survival count measured was based on plating. Adapted from [91].

As shown by these examples, the osmotic pressure difference which bacteria can be exposed to varies a lot ($5 \times 10^{-4} - 20$ atm). Despite being a single-celled organism, *E. coli* can survive a wide variety of pressure changes (Table 2.3).

## 2.5 Family of mechanosensitive channels in *E. coli*

Mechanosensitive (MS) channels were discovered in 1987 [92], resulting in the proposal that they may play a crucial role in sensing osmolarity through changes in turgor pressure and protecting cells from osmotic shock. This discovery led to a very active development of research in the mechanotransduction and osmoregulation field. Subsequent discoveries demonstrated that the channels are gated by a mechanical stimulus, but left the questions concerning the mechanism and physiological relevance of MS channel functioning unanswered, creating at the same time even more interest in the subject.

The results of further studies led to a conclusion that there are different types of mechanosensitive channels. Berrier *et al.* [76] observed the activity of channels having

different conductances upon application of suction pressure on the giant spheroplasts of *E. coli*. Moreover, activity of only some of these channels could be inhibited by the addition of $Gd^{3+}$ ions. These results suggested not only the existence of multiple types of mechanosensitive channels in *E. coli*, but also demonstrated that they have different properties. Another piece of evidence for the existence of different mechanosensitive channels in the cell membrane (and their physiological role) was reported by Ajouz *et al.* [93]. The authors were investigating the efflux of various molecules due to osmotic downshock in the wild type and $mscL^-$ strains of *E. coli*. The release of some species was not disturbed in the $mscL^-$ strain, which demonstrates the involvement of different channels in the rescue of the cell during an osmotic shock. Another surprising result was that the efflux of glycine betaine occurred only upon about a 200 mM change in the external NaCl concentration, which suggested the existence of different thresholds for various channels. This was soon proven to be the case using patch-lamp technique [94].

The discovery of the gene encoding the MscL protein by Sukharev *et al.* [95] enabled the introduction of crystallography techniques to study MS channels. The first crystallographic structure of an MscL homolog was reported in 1998 by Chang *et al.* [96]. The authors identified an MscL homolog in the bacterium *M. tuberculosis* (Tb-MscL) which exhibits an overall 37% sequence identity to *E. coli* MscL (Eco-MscL). Tb-MscL is a homopentamer consisting of two domains, a TM domain and a cytoplasmic domain. The TM1 helix that forms the pore of the channel is one of the most highly conserved regions in the sequences of the MscL protein. To this day, crystal structures of a few MscL and MscS homologs have been solved in different conformational states [97, 98, 99].

Levina *et al.* [22] identified two genes (*yggB* (now called *mscS*) and *kefA*) contributing to MscS activity. They were also the first to demonstrate a physiologically important phenotype due to loss of mechanosensitive channel activity. They demonstrated that cells with *mscL* and *mscS* genes deleted do not survive exposure to 0.5 M NaCl osmotic shock at a high rate. This result revealed the role of these channels

in providing protection against osmotic shock. More recently, more genes coding proteins having mechanosensitive channel activity were characterized: *ybdG* [100], *ynaI*, *ybiO*, and *yjeP* [101] reaching the total number of 7 different types of MS channels in *E. coli* (Table 2.4).

| Gene | Year of characterization | Reference |
|---|---|---|
| *mscL* | 1994 | [95] |
| *yggB* | 1999 | [22] |
| *kefA* | 1999, 2002 | [22, 102] |
| *ybdG* | 2010 | [100] |
| *ynaI* | 2012 | [101] |
| *ybiO* | 2012 | [101] |
| *yjeP* | 2012 | [101] |

Table 2.4: Genes coding the activity of all seven mechanosensitive channels in *E. coli*. The first gene coding MS channel activity (*mscL*) was identified seven years after the discovery of MS channels. The last three mechanosensitive genes (*ynaI*, *ybiO*, and *yjeP*) were identified 25 years after the discovery of MS channels.

## 2.6 Standard ways of studying MS channels in bacteria

### 2.6.1 Theoretical modeling

One of the methods used to study mechanosensitive channels is theoretical modeling, predicting the reaction of the channel (gating probability) to a given perturbation.

A single channel is modeled as a two-state protein. It can be in a closed state, characterized by the energy $E_{closed}$, or in an open state, characterized by the energy $E_{open}$. The equilibrium between these two states depends on the value of the external driving force, in this case the tension $\tau$, pictured as a loading device (Figure 2.6).

In the absence of tension ($\tau$=0) the closed state will be favored since it has lower energy. However, as the tension increases the value of the external driving force increases, which can be pictured as the increasing weight of the loading devices. As

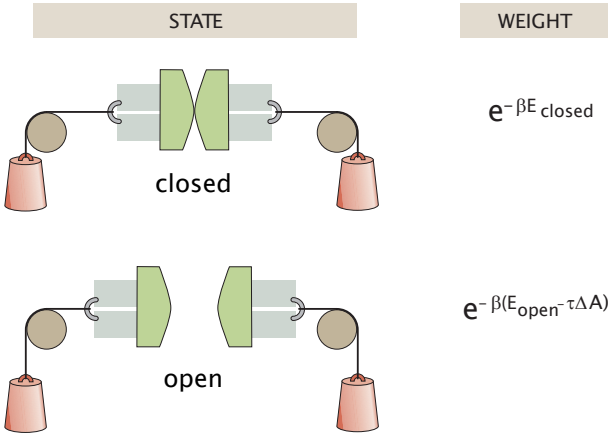


Figure 2.6: Mechanosensitive channel modeled as a two-state protein. The closed state has energy $E_{closed}$ and the open state is characterized by energy $E_{open}$. The external force is pictured as a loading device attached to the channel. The lowering of the loading device (open state) stabilizes the open state by descreasing its energy value by $\tau\Delta A$. Figure adapted from [60].

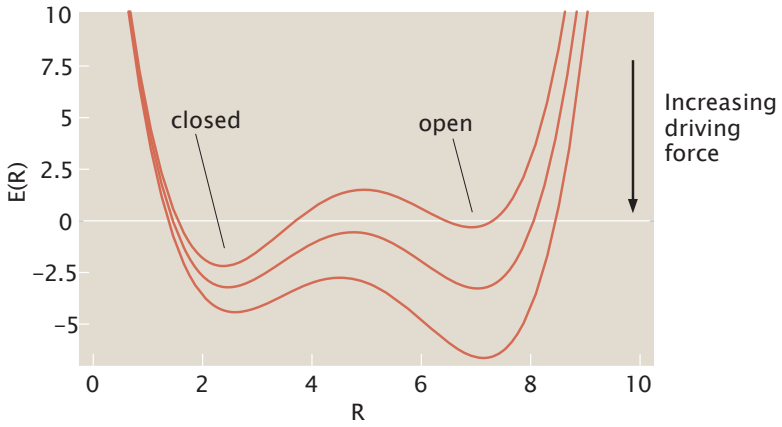


Figure 2.7: Energy landscape of the two-state channel as a function of its radius. The curves correspond to different values of the externally applied force (tension). Depending on its value, the balance between open and closed state can be shifted. For small values of tension the closed state is energetically favorable (first curve). As the tension increases, the open state decreases its energy and the balance shifts towards this state being more stable (last curve). Figure adapted from [60].

a consequence, the channel opens and the potential energy of the loading device is reduced by the value $\tau\Delta A$, where $\Delta A$ is the areal change due to channel opening. This additional term stabilizes the open state by lowering its energy (Figure 2.7).

Using this theoretical model we can quantitatively predict the state of the channel by calculating its gating probability. To do so, one can use the Boltzmann distribution, which states that finding the a state with a given energy $E$ is

$$p(E) = \frac{e^{-\beta E}}{Z}, \tag{2.2}$$

where $Z$ is called the partition function and is a sum of all possible states (it is a normalization constant determined by the requirement that the sum of all probabilities is equal to 1). We can calculate the probability of the channel being in an open state as a function of applied tension $\tau$ as

$$p_{open} = \frac{e^{-\beta(E_{open}-\tau\Delta A)}}{e^{-\beta(E_{open}-\tau\Delta A)} + e^{-\beta E_{closed}}} = \frac{1}{1 + e^{-\beta(\tau\Delta A - E_{gate})}}, \tag{2.3}$$

where $E_{gate} = E_{closed} - E_{open}$ is the gating energy.

As already mentioned, the tension in the membrane is the external stimulus that changes the state (closed or open) of the protein. However, the protein may also influence the energy of the membrane [103]. The conformation of the protein depends on the tension value applied through the bilayer; however, the opening of the channel causes deformation of the surrounding lipid membrane. One can thus model the free energy of the protein-membrane system as the sum of energies associated with the state (conformation) of the protein and energies associated with the deformation of the membrane. Surprisingly, the values of these energies are very similar to the energy difference between the channel conformational states [104, 105]. This suggests that the mechanical properties of the lipid bilayer surrounding the protein will have a great impact on the channel gating.

The application of tension to a membrane can result in changes in its thickness and/or curvature. The two most important parameters are the hydrophobic mismatch between the protein core and surrounding lipids (variation in membrane thickness), and midplane bending [106]. Thus, by changing membrane properties, e.g., the length of the lipid tails, one can influence the gating probability by modifying the tension

required to open mechanosensitive channels.

### 2.6.2 Electrophysiology

The application of patch-clamp techniques to giant spheroplasts of *E. coli* led to the discovery of mechanosensitive channels [92]. Delcour *et al.* [107] were the first to report successful reconstitution of bacterial mechanosensitive channels into liposomes, which showed that the small size of bacteria is no longer a factor that excludes electrophysiology from the possible experimental techniques in this field (Figure 2.8 A). The parameters for channels characterized in spheroplasts and reconstituted in liposomes are very similar [95]. The same activity of a protein in its natural environment (spheroplasts with all the other proteins present and natural *E. coli*'s lipids) and in the artificial environment (liposomes) indicates that the gating tension is transmitted through the only element these two environments have in common, the lipid bilayer, and that protein-lipid interactions play a fundamental role in channel gating. The reconstitution of MscL into various lipid environments (synthetic phosphatidylcholine (PC) containing monosaturated chains of 14, 16, 18, 20, and 22 carbons) further proved that gating of the channel is influenced by the surrounding lipids. The pressure needed to activate MscL was lower in the PC16 (phosphatidylcholine with chains of 16 carbons) environment when compared to the PC20 (phosphatidylcholine with chains of 20 carbons) environment (Figure 2.8 B). Interestingly, the shape of the pressure dependence curve remains the same, with the curve being shifted by some value [108]. Based on the experimental data the authors concluded that the two physical mechanisms influencing MS channel gating are hydrophobic mismatch between the protein and the lipid environment (which can be controlled by reconstitution into lipid vesicles with different acyl chain lengths) and the bilayer curvature (which can be modified by unsymmetrical addition of, e.g., lysophosphatidylcholine (LPC)) [108].

The observation that channels in patches formed with large diameter pipettes were activated at lower pressures [74], as well as the application of the reconstitution

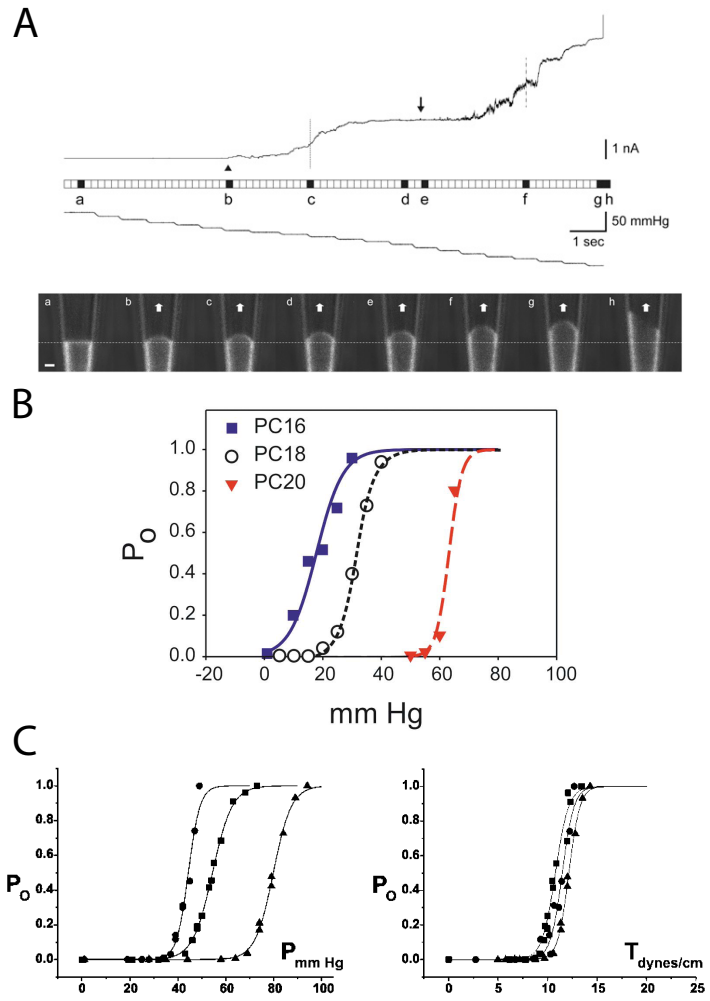


Figure 2.8: Characterization of mechanosensitive channels in *E. coli* by the electropysiological measurement. (A) The current traces of MscS and MscL reconstituted into liposomes. The images beneath the trace show the geometry of the patch for a given value of the applied pressure. The data obtained by simultaneous measurement of the current and a function of applied pressure (electrophysiology) and observation of patch geometry (confocal microscopy) allows one to calculate the tension (equation 2.4) and correlate this value with the number of observed MS channel activities: (a) resting state, (b) opening of the first MscS channel, (c) midpoint activation of MscS, (d) saturation of MscS activity, (e) opening of the first MscL channel, (f) midpoint activation of MscL, (g) saturation of MscL activity, and (h) rupture of the patch. Scale bar is 1 $\mu m$. Adapted from [110]. (B) Probability of MscL activation as a function of applied pressure for three different lipid environments. Shorter lipid tails lower the energy needed for MscL channel activation. Adapted from [108]. (C) Comparison of the probability of MscL activation as a function of applied pressure and tension. The collapse of all curves when plotted as a function of tension shows that tension, not pressure, is the parameter affecting MscL activation. Adapted from [109].

technique and simultaneous imaging of the curvature of the patch, allowed us to conclude that the parameter regulating the MscL gating is tension, not pressure [74, 108, 109] (Figure 2.8 C). The image of the patch enables a measurement of its radius ($R$) for a given value of the applied pressure ($p$). Knowing this relationship, one can calculate the tension ($\tau$) using Laplace's law

$$\tau = \frac{pR}{2}. \tag{2.4}$$

The existence of various conductances in *E. coli* membranes was reported [76, 94], suggesting the existence of various types of MS channels. However, only the identification of the genes coding proteins with MS channels activity allowed the detailed characterization of individual channels (Table 2.5). Until 2012 it was believed that there is a hierarchy in the opening of MS channels, meaning that the tension required to open a given channel is correlated with its conductance. The experimental results indicated that the first channel to open was the one showing MscM activity, and, as the tension increases, MscS and MscK would gate before the MscL opening, which gates near the membrane rupture threshold [111]. However, the characterization of YjeP, YnaI, and YbiO channels proved that this rule is no longer valid (Figure 2.9). YjeP gates at a tension close to that needed to activate MscS or MscK, but it has a much lower conductance. YnaI and YbiO gate at the tension near the one needed to activate MscL, but their conductances are 100 pS, 900 pS, and 3000 pS, respectively [101]. Interestingly, the electrophysiological activity of YbdG can't be observed unless the mutation in $\beta$ domain is introduced (V229A) [101].

It was known that negative pressure is necessary to observe the opening of mechanosensitive channels, but soon other factors, increasing or decreasing open probability, appeared in the literature. Martinac *et al.* [112] studied the impact of amphipathic compounds (molecules having a hydrophobic and hydrophilic character) on channel gating. Cationic amphipaths (e.g., chlorpromazine CPZ) are believed to locate themselves in the inner leaflet of the bilayer, whereas anionic amphipaths (e.g., trinitrophenol TNP) – in the outer leaflet. Insertion of such molecules into the membrane

| Channel | Size [aa] | $P_L$:$P_X$ | Current amplitude [pA] | Conductance [pS] |
|---|---|---|---|---|
| MscL | 136 | 1 | 90 | 3000 |
| MscS | 286 | 1.6 | 25 | 1250 |
| MscK | 1120 | 1.85 | 17.5 | 875 |
| YbdG | 415 | – | 7.5 | 300 (*) |
| YnaI | 343 | 1.05 | 2 | 100 |
| YbiO | 741 | 1.21 | 17 | 900 |
| YjeP | 1107 | 1.64 | 5-8 | 350 |

Table 2.5: Characterization of mechanosensitive channels in *E. coli* using electrophysiological techniques. The size of the protein does not correlate well with its conductance or gating tension measured with respect to the MscL activation tension ($P_L$ : $P_X$). There is also lack of correlation between the gating tension and the conductance of the channel, suggesting that the increase in tension value does not guarantee opening of the channels which allow a bigger flux of material through a single channel. (*) the mutation in the $\beta$ domain (V229A) in necessary for electrophysiological activity of YbdG. Table constructed based on [101].

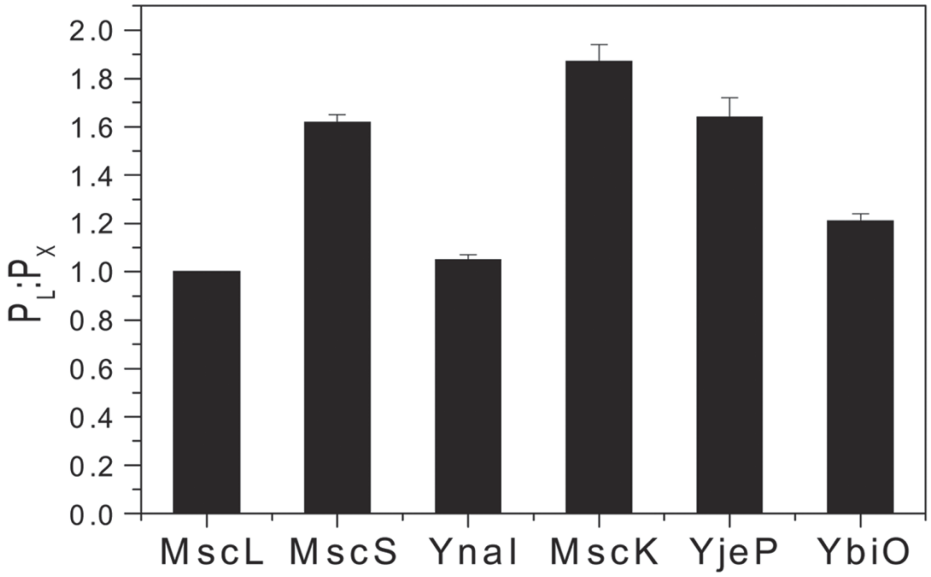


Figure 2.9: Comparison of the relative pressure needed to activate various MS channels. The values for MscS homologs ($P_X$) are reported with respect to the activation pressure of MscL ($P_L$ : $P_X$). Values larger than 1 mean that the tension needed to activate a given channel is lower than the tension needed to activate MscL channel. Figure adapted from [101].

impacts the curvature and, as a consequence, lowers the activation threshold to open the channel. Also, addition of lysophosphatidylcholine (LPC) or cholesterol influ-

ences the gating of both MscL and MscS [110] and the presence of ethyl or propyl parabens causes their spontaneous activation (the effect is reversible) [113]. Recent studies show that MscL can be engineered to show light-gated activity through the modification of the protein (G22C mutant and a cysteine-reactive spiropyran photoswitch) [114] or through reconstitution into a lipid vesicle containing a light-sensitive lipid mimic undergoing trans-cis isomerization [115].

### 2.6.3 Plating assay

Protection against osmotic shock as a function of mechanosensitive channels in cell physiology was postulated at the time these channels were discovered [92], and the assay testing this assumption was published only 12 years later [22].

To test the role of a given channel (or the lack of such) in cell physiology downshock assay is used (also known as survival assay or plating assay). A single colony is inoculated into 5 ml of LB and grown overnight. Next morning, the culture is diluted into 20 ml of fresh LB to a final $OD_{600}$ of 0.05. Once the culture reaches an $OD_{600}$ of 0.3, it is diluted 1:10 into LB supplemented with 0.5 M NaCl and grown again to $OD_{600} \sim 0.3$. The culture is then diluted 1:20 into LB (shock) and LB supplemented with 0.5 M NaCl (control) and incubated for 10 min at 37°C. After the incubation serial dilutions are made into the medium of the same osmolarity (0 M NaCl for the shock sample and 0.5 M NaCl for the control). A small aliquot of each serial dilution (5 $\mu$l) is spotted on an agar plate of matched osmolarity (0 M NaCl for the shock sample and 0.5 M NaCl for the control). Plates are incubated overnight and the next day the survival rate is calculated based on the number of colonies for a shock sample normalized to a number of colonies for the control sample (Figure 2.10).

This basic assay can be modified by changing the type of medium used or the amplitude of the shock. However, there are some parameters that cannot be controlled or observed in this bulk assay, e.g., the rate of the shock or the variation in response of individual cells. The way the assay is performed may introduce some systematical errors. When counting the colonies one assumes that each colony started from one

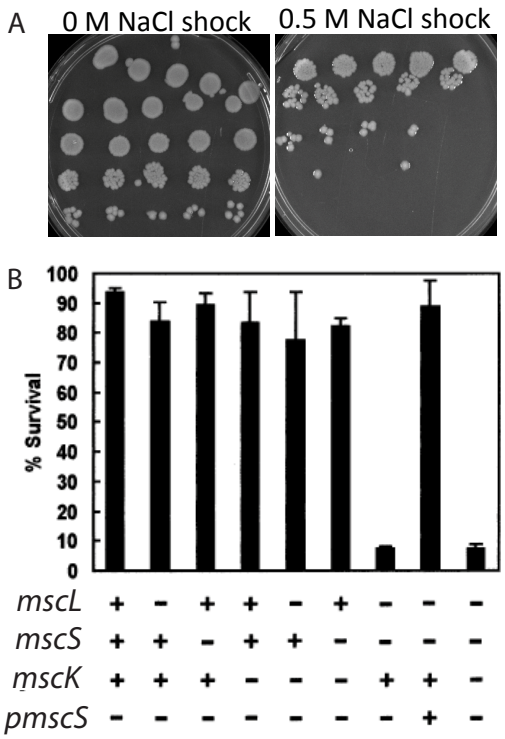


Figure 2.10: Survival of mechanosensitive channel mutants after exposure to osmotic shock. (A) Agar plates showing growth of colonies after overnight incubation for the shock sample (0.5 M NaCl shock) and the control sample (0 M NaCl shock). Rows represent aliquots of the same dilution, columns represent serial dilutions. (B) Survival rate for strains expressing MscL, MscS, and/or MscK from the chromosome, and/or from the plasmid (pmscS) after exposure to a 0.5 M NaCl shock. The survival rate is calculated based on the number of colonies of cells exposed to osmotic challenge which grew after the recovery period, normalized by the number of colonies for control samples (not exposed to osmotic challenge). Adapted from [22].

cell. This may not be the case if two or more cells formed a minicluster, resulting in a single colony after an overnight incubation. Another source of error when calculating the survival rate is the normalization factor. The control sample is grown on a high salt plate, which may limit growth of some percentage of the cells. Also, the normalization by $OD_{600}$ of a given sample when it was exposed to osmotic shock may introduce a systematical error. The same $OD_{600}$ does not always correspond to the same number of cells for a given strain [116], so this parameter should be controlled for (for the modified plating assay protocol with comments see Appendix A).

Other types of survival assays were published as an alternative (Table 2.6), how-

ever, they did not gain as much interest as the assay described above.

| Type of assay | Reference |
|---|---|
| colony count | [22] |
| amount of $A_{260}$ absorbing material released | [22] |
| Live/Dead BacLight dyes and plate reader | [117] |
| microscopy and staining | [118] |
| flow cytometry and staining | [118] |
| amount of released DNA (fluorescence) | [119] |
| light scattering with a stopped-flow device | [120] |

Table 2.6: Various techniques used to calculate the number of cells surviving an osmotic shock. The colony count method is the most popular one. The readout of this method is cellular growth. The other methods are based on the amount of released material (measured by absorbance or fluorescence) or the integrity of cell envelope (staining methods).

## 2.7 Unanswered questions - motivation for further studies

### 2.7.1 How many channels are there in a cell?

A broad variety of methods was used to characterize the physiological role and the behavior of mechanosensitive channels under given conditions. These channels are well characterized at the molecular level: we know the gating probability and conductance (from electrophysiological measurement and theoretical modeling), the crystal structure, molecular species that can be released through these channels, and the size of the pore in an open configuration [65, 74, 96]. At the cellular level, the role of these channels was characterized through the cell viability assay after exposure to osmotic challenge [22]. However, we lack information on the total number of channels expressed in a cell under given circumstances to fully understand the connection between the molecular picture and the cellular response, . Having this information and the previously measured gating tension along with the conductance, one can determine the number of open channels and the amount of transport through them at given conditions. Depending on the number of open channels, the physiological response

of the cell to a given osmotic stimulus will vary. If this number is constant, the cells in the population should respond differently depending on their size. As shown by numerous biophysical models, both the number of such channels and their variability can impact many physiological processes, including osmoprotection, channel gating probability, and channel clustering. [121].

### 2.7.2 What is the role of MS channels in cell physiology?

From the very first moment MS channels in bacteria were discovered, their importance in osmoregulation was postulated [92], and only a few years later a proof of their function as defense mechanisms against the osmotic shock was experimentally affirmed [22]. It is known that wild-type cells express seven types of mechanosensitive proteins [101] and the reason for this variety should be explained by studying their response to the same perturbation. Bulk osmotic shock experiments revealed that the presence of MscL or MscS [22], or an overexpression of one of the MscS homologs (in the absence of other mechanosensitive channels), can rescue the cell from a hypoosmotic shock [100, 101]. This fact indicates that all of the channels have a potential to rescue the cell from a very severe osmotic downshock, and, theoretically, the presence of all of them is not crucial.

The identification of genes coding all mechanosensitive channels in *E. coli* (Table 2.4) opens the possibility of creating a strain carrying any desired combination of MS channels. The comparison of the physiological behavior or response to osmotic shock for various mutants makes it possible to study the physiological relevance of variouis MS channels, their response to the same perturbation, time scale of this response, their sensitivity, and potential interactions.

### 2.7.3 What is the role of single-cell stochasticity?

The majority of physiological experiments are performed on cell cultures in the exponential phase of growth. It is argued that the physiological condition of each cell in this phase of growth is identical. This assumption, however, is far from being true,

even if cells are genetically identical [122]. There are many possible explanations for the phenotypic heterogeneity of an isogenic population: various "ages" of the cells, the cell cycle stage (fluctuations in the transcriptional activity), different volume or density of cells in a population, or, finally, intrinsic (stochastic effects in transcription, translation, or replication) and extrinsic (fluctuations in the number of polymerases or ribosomes) noise in gene expression. Whatever the source of such variation is, it may result in a differential sensitivity to stress among the members of a given population.

The role of this single-cell stochasticity is unclear. One of the explanations for the diverse patterns of gene expression resulting in phenotypic subpopulations is fitness advantage. The conditions in the natural environment tend to fluctuate, so if the distribution of phenotypes is broad, the chances that one of the subpopulations will remain viable increase. Such a scenario means that bacteria are able to anticipate and adjust to sudden changes in the environment. Another possibility is that cells may vary not only in the gene expression profile but also other physiological parameters, e.g., the growth rate. This suggests that members of the same population may react to changes in the environment at different time scales. One subpopulation may be able to respond to a very fast change, whereas the other subpopulation may respond only to persistent and slow change in the environment.

Observation of the response to a given stimulus, e.g., the osmotic shock, at the single-cell level is necessary in order to study whether genetically identical cells show a similar type and time scale of reaction when disturbed. Systematic, reproducible, and precise measurements should be performed to observe whether the cell reaction to a given stimulus is identical every time. These measurements, along with simultaneous MS channel counting, would reveal whether the *mscL* gene expression differs from cell to cell and how it impacts cell survival. It would also answer the question whether this heterogeneity is "static" (doesn't change with varying conditions) or "dynamic" (the width of the distributions changes with the environmental conditions, suggesting that cells sense and response to external changes).

# Chapter 3

# Single-cell response to medium exchange

## 3.1 The mystery of seven channels

Mechanosensation is a ubiquitous phenomenon found across all domains of life. In bacteria, one of the manifestations of such processes is in the context of osmoprotection, where it has been proposed that the presence of MS channels in the cell membrane allows these cells to survive an osmotic shock. These channels gate in response to an increase in membrane tension and prevent membrane rupture by mediating a net efflux of water and small molecules. The first bacterial mechanosensitive channels were discovered in 1987 [92] and in the intervening period a whole battery of such channels has been discovered with seven different mechanosensitive channels now demonstrated experimentally in *E. coli* [101]. These channels have been characterized with electrophysiological measurements (Table 2.5). Interestingly, the characterization of YjeP, YnaI, and YbiO violates the hierarchy rule for opening MS channels, which hypothesizes that the tension required to open a given channel correlates with its conductance. One of the puzzles left unresolved in the wake of the discovery of this mechanosensitive protein diversity is why there are so many distinct mechanosensitive channels in *E. coli* and what their significance for cell physiology is. The work presented here partially addresses these questions.

The physiology of MS channels has been studied extensively over the last 20 years.

Specifically, until now the survival of cells subjected to osmotic shock has been mainly characterized in bulk assays, in which a large population of cells is shocked and the resulting survival fraction is measured through colony counting. The comparison of the survival rate for various deletion mutants has made it possible to study the contribution of a particular channel to cell survival after exposure to a 0.5 M NaCl shock. Based on these studies, the presence of MscL or MscS is believed to provide osmoprotection at near wild-type level [22].

These assays, although very informative, reflect the population response to a large amplitude (0.5 M NaCl) and not well-controlled rate of change in the medium osmolarity (about 1 s). These conditions may seem extreme when compared to the osmolarity changes which *E. coli* may be exposed to in its natural habitat. For example, the osmotic challenge due to rainfall will be different for *E. coli* in the shallow marine water when compared to one in an open ocean. In addition, some of the channel properties may be too subtle to be discovered by means of this assay. For example, the inactivation of MscS channels in the patch clamp measurement can be observed only when the pressure is applied gradually [120].

It is well known that variations in water potential cause perturbations in cell physiology. Specifically, the kinetics of the decrease or increase in the external water potential were found to have great influence on cell survival [123, 124, 125]. Bacterial viability is strongly related to the water potential gradient between the cell and the external medium, which is related to the water flow across the membrane. However, to our knowledge, no work has analyzed the role of various MS channels for cell survival as a function of various kinetics of osmotic treatment. As a result, we have developed a single-cell video microscopy approach, in which individual bacteria are subjected to highly controlled osmotic shocks, and their resulting growth dynamics is monitored for hours afterwards.

## 3.2 Single-cell observation

The physiology of MS channels has been studied extensively over last twenty years. However, until now the survival of cells subjected to an osmotic shock has mainly been characterized in bulk assays, in which a large population of cells is shocked and the resulting survival fraction is measured through colony counting [22]. The measurement of the mean response of the cell population makes this assay blind to many parameters, e.g., variety of responses among cells from a given population, or the time and mechanism of cell envelope rupture. In addition, the kinetics of the addition of a shock medium is not well-controlled, which may result in observing only one (out of many possible) types of cell responses.

In this work, we present a single-cell method for measuring cell survival after an osmotic challenge and the influence of the kinetics of the osmotic treatment on the survival of various MS channel deletion mutants. This method allows us to control the medium exchange rate and perform a quantitative measurement of the osmolarity gradient based on fluorescence signal change. The observation of single cells as a function of the recovery time after an osmotic challenge allows for an accurate determination of the fate of individual cells (death or division), as well as the time interval between the osmotic challenge occurrence and cell death.

The experiments are performed in a simple flow cell mounted on the microscope (Figure 3.1) (the details of the assembly method of the flow cell are described in Appendix B). The chamber was primed with a charged polymer polyethylenimine diluted 1:400 to attach cells to the bottom of the chamber (glass coverslip), and then washed with water. Two input ports were primed with the media of different osmolarity: one with a 0.5 M NaCl LB, the second one with a 0 M NaCl LB. Cells were loaded into a chamber at a constant speed of 100 $\mu$l/min through the input port primed with high salt medium. After about a five-minute long incubation the excess of unattached cells was removed by flushing the 0.5 M NaCl medium and introducing a small air bubble (the bubble treatment did not affect cell survival). The number and condition of cells before the shock was documented at twenty different positions

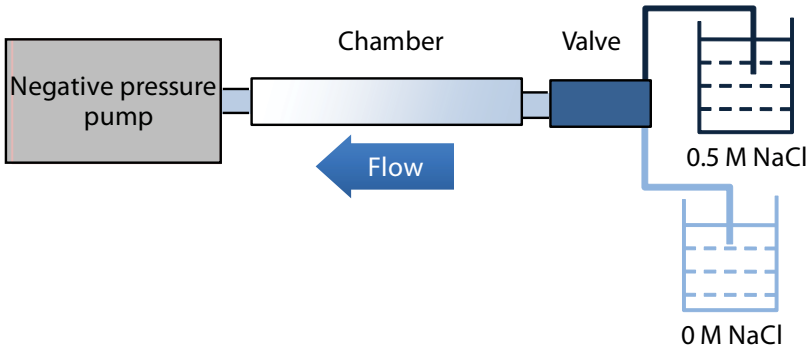


Figure 3.1: A schematic picture of the experimental setup used for the single-cell observation of *E. coli* mutants exposed to a well-controlled osmotic challenge. The inputs of the flow cell are connected to reservoirs with high (0.5 M NaCl) and low (0 M NaCl) osmolarity media. The osmolarity of the medium in the viewing chamber is controlled by the valve. The constant flow of medium through the experimental system is guaranteed by the connection to the syringe pump through the output of the flow cell. The details of the assembly method are described in Appendix B.

in the chamber. Next, the real time medium exchange calibration was recorded for one of the positions.

In order to monitor the rate of the medium exchange, both high and low salt media were supplemented with 250 nM calcium-sensitive Rhod-2 dye. The shock medium (0 M NaCl LB) was also supplemented with 100 $\mu$M $CaCl_2$ to create a difference in the fluorescence signal between these two media. The fluorescence signal of the medium in the flow cell was recorded in real time during cell exposure to osmotic challenge. The rate of medium exchange was measured based on the signal intensity change as the high salt medium (low signal) was substituted by the low salt medium (high signal). The quantitative measurement of the rate exchange was performed by curve fitting to the recorded signal ($fluo$) (Figure 3.2). The minimum (0.5 M NaCl medium) and the maximum (0 M NaCl medium) signal level was calculated as the average value ($fluo_{min}$ and $fluo_{max}$, respectively). The standard deviation for both means was calculated as well ($\Delta fluo_{min}$ and $\Delta fluo_{max}$, respectively). The difference between these two values was taken as the fluorescence signal change corresponding to a 0.5 M NaCl osmolarity drop ($fluo_{max}$ - $fluo_{min}$). Next, a linear fit was performed to the middle part of the trace ($fluo = a \times time + b$), where $fluo$ and $b$ are measured

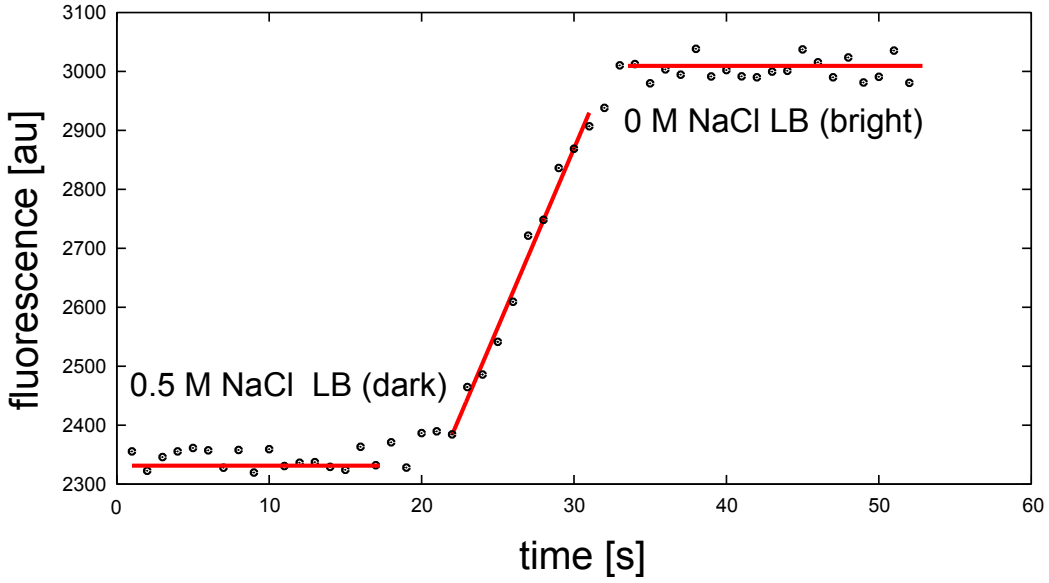


Figure 3.2: Fluorescence signal of the medium as a function of time during the medium exchange in a flow chamber. The medium is changed from 0.5 M NaCl LB with 250 nM calcium-sensitive Rhod-2 dye (dark) to 0 M NaCl LB with 250 nM calcium-sensitive Rhod-2 dye and 100 $\mu$M $CaCl_2$ (bright). The rate is calculated by fitting a straight line to three regions: minimal fluorescence level, maximal fluorescence level and the middle of the calibration curve. The error analysis is discussed in the text.

in arbitrary units (called here counts), *time* is measured in seconds, and $a$ is measured in counts per second. The uncertainties in determining the slope ($a$) and the intercept ($b$) of the fitted curve were obtained from the fitting as well ($\Delta a$ and $\Delta b$, respectively). The correlation coefficient $R^2$ was kept higher than 0.95 (if the correlation coefficient of the linear fit was lower than 0.95, the fit was performed to only a part of the middle of the trace). The rate ($R$) was calculated by dividing the slope of the fitted curve ($a$) by the value of the recorded signal ($fluo$). The uncertainty in the rate determination ($\Delta R$) was calculated by error propagation:

$$\frac{\Delta X}{X} = \sqrt{\left(\frac{\partial f}{\partial A} \times \Delta A\right)^2 + \left(\frac{\partial f}{\partial B} \times \Delta B\right)^2}, \tag{3.1}$$

where $X = f(A, B)$, and $\Delta A$ and $\Delta B$ are $A$ and $B$ errors, respectively. For our

function this calculation resulted in the following equation:

$$\frac{\Delta R}{R} = \sqrt{\left(\frac{a \times \Delta fluo_{max}}{(fluo_{max} - fluo_{min})^2}\right)^2 + \left(\frac{a \times \Delta fluo_{min}}{(fluo_{max} - fluo_{min})^2}\right)^2 + \left(\frac{\Delta a}{fluo_{max} - fluo_{min}}\right)^2}. \tag{3.2}$$

After the calibration, the shock medium (0 M NaCl LB) was substituted with a medium of the same osmolarity, but without the dye and $CaCl_2$. The recovery of cells was recorded by taking snapshots at previously chosen positions, one snapshot per minute during a two to three hour period. In order to supply enough nutrients and oxygen to the recovering cells, the 0 M NaCl LB medium was pumped through the chamber during the recovery phase at a constant speed of 10 $\mu$l/min.

The survival rate and the fate of each individual cell was determined based on the data collected during the recovery phase. A cell was counted as a survivor based on its division (Figure 3.3, cells marked with an arrow). The rest of the cells were classified as dead (Figure 3.3, cells marked with a star) or intact, non-dividing cells (Figure 3.3, cells marked with a triangle). The dead cells were further divided into subclasses (described later). The percentage of the population which survived the shock was calculated as the ratio of the number of dividing cells to the total number of cells from twenty fields of view. The error in the calculated survival rate was taken as the fraction of intact, non-dividing cells with respect to the total number of cells.

## 3.3 Rate dependence

One of our principal findings is that the kinetics of medium exchange is an important factor in determining the survival probability of cells subjected to an osmotic challenge. Specifically, the percentage of cells surviving the osmotic shock depends on the rate of medium exchange. The number of surviving cells varies for different MS channel deletion mutants (Figure 3.4). The fact that bacterial viability is strongly related to the water potential gradient between the cell and the external medium, which is related to the water flow across the membrane, suggests that mechanosensi-

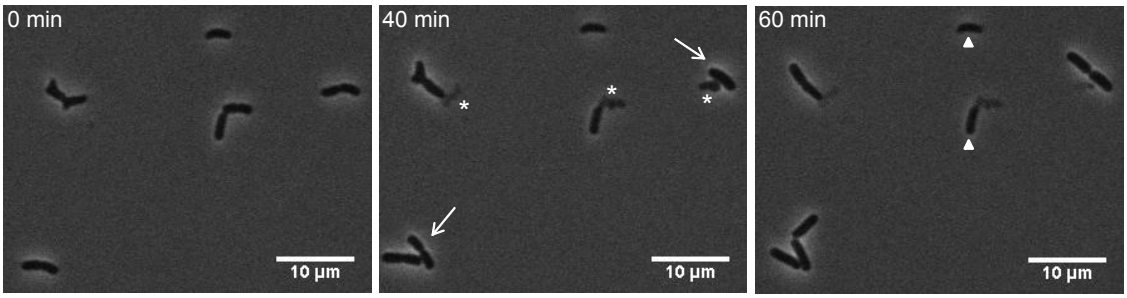


Figure 3.3: Image sequence showing the recovery of MJF465 cells exposed to a 0.5 M NaCl shock at 100 $\mu$L/min. Cells can be classified into 3 groups: cells that survived the shock and divide (marked with an arrow), cells which are intact, but do not divide (marked with a triangle), and cells that died as a result of the osmotic challenge (marked with a star). As discussed in the text, the dead cells can be further classified based on their morphology.

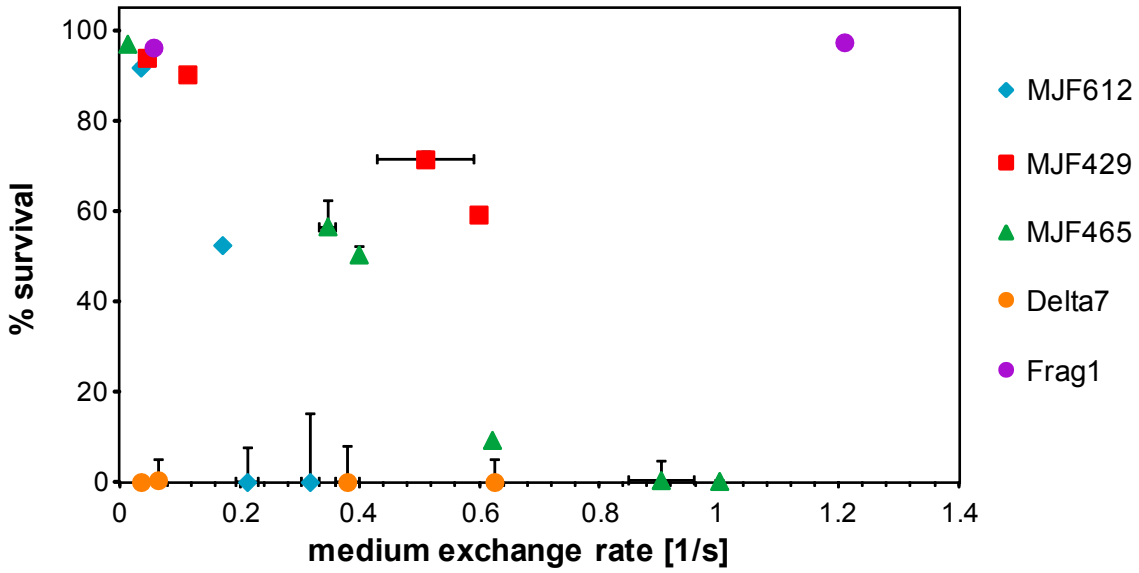


Figure 3.4: Survival as a function of the rate of medium exchange. Strains Frag1 (wild-type), MJF429 ($\Delta mscS$ $\Delta mscK$), MJF465 ($\Delta mscL$ $\Delta mscS$ $\Delta mscK$), MJF612 ($\Delta mscL$ $\Delta mscS$ $\Delta mscK$ $\Delta ybdG$), and MJF641 (all seven mechanosensitive channels knocked-out) were exposed to a 0.5 M NaCl shock performed at various rates of medium exchange. The survival depends on the rate of the osmotic challenge as well as on the type of MS channels present.

tive channels play an important role in protecting the integrity of the cell envelope. The role which a background strain used for MS channel deletion mutants may have on cell survival is discussed in section 3.5 below.

Strain Frag1 (wild-type) was used as a positive control and, as expected, survives at a level close to 100% for the whole range of medium exchange rates tested (for a comparison with the previously published values, see Figure 2.10 and Table 3.1). Strains MJF429 ($\Delta mscS$ $\Delta mscK$), MJF465 ($\Delta mscL$ $\Delta mscS$ $\Delta mscK$), and MJF612 ($\Delta mscL$ $\Delta mscS$ $\Delta mscK$ $\Delta ybdG$) show various survival levels (0% - 90%) depending on the kinetics of medium exchange. Only strain MJF641, which has all seven mechanosensitive channels deleted, did not survive a 0.5 M NaCl osmotic shock, even at the slowest shock rate tested.

| Strain | Osmotic shock [M NaC] | Survival [%] | Reference |
|---|---|---|---|
| Frag1 | 0.5 | 94 ± 1.2 | [22] |
| | 0.25 | 96 ± 27 | [100] |
| MJF429 | 0.5 | 82 ± 2.6 | [22] |
| MJF465 | 0.5 | 7.6 ± 1.2 | [22] |
| | 0.3 | 6.5 ± 1.5 | [126] |
| | 0.25 | 6.3 ± 6.3 | [100] |
| MJF612 | 0.25 | 3.9 ± 3.6 | [100] |
| MJF641 | 0.3 | 0.5 ± 0.1 | [101] |
| | 0.3 | 0.5 ± 0.3 | [101] |
| | 0.3 | 0.6 ± 0.1 | [101] |

Table 3.1: Previously published survival results obtained by a standard plating assay for strains used in this study. These survival rates differ significantly from the results obtained through the single-cell assay with a controlled rate of medium exchange. The rate of osmotic challenge is not controlled in a standard plating assay.

The slopes of the curves showing the survival level as a function of the medium exchange rate vary depending on the strain used. In general, the more types of channels that are deleted, the steeper the slope of the survival curve (Figure 3.4), meaning that the cells are increasingly sensitive to the rate of the osmotic shock. The two channels having the largest conductances, namely MscL and MscS, were proved to provide protection from osmotic shock previously [22]. The other types of channels were shown experimentally to provide protection only if overexpressed from a plasmid [100, 101]. Our work presents the first, to our knowledge, results suggesting that all types of MS channels can provide some level of protection (depending on the medium

exchange rate) at the native level of expression.

Comparing the medium exchange time (and rate) resulting in a 50% survival for a given strain illustrates the idea that various channels provide protection at different time scales (Table 3.2). The comparison between the MJF429 ($\Delta mscS$ $\Delta mscK$) and MJF465 ($\Delta mscL$ $\Delta mscS$ $\Delta mscK$) strains suggests that the presence of MscL channels protects against a 0.5 M osmolarity change occurring over less than 1.7 s (50% survival for medium exchange over 2.5 s for strain MJF465 versus less than 1.7 s for strain MJF429), whereas YbdG provides enough protection to guarantee a 50% survival after a 0.5 M osmolarity change occurring over 2.5 s (50% survival for medium exchange over 5.8 s for strain MJF612 ($\Delta mscL$ $\Delta mscS$ $\Delta mscK$ $\Delta ybdG$) versus 2.5 s for strain MJF465). Channels YbiO, YjeP, and YnaI acting together may be sufficient for protection against a 0.5 M osmolarity change over more than 5.8 s.

| Strain | Time of medium exchange [s] | Rate of medium exchange [1/s] |
|---|---|---|
| Frag1 | $\ll 1$ | $\gg 1$ |
| MJF429 | $< 1.7$ | $> 0.6$ |
| MJF465 | $\sim 2.5$ | $\sim 0.4$ |
| MJF612 | $\sim 5.8$ | $\sim 0.2$ |
| MJF641 | $\gg 30$ | $\ll 0.03$ |

Table 3.2: Time and rate of medium exchange at which all tested strains show 50% survival. The survival of various MS channels deletion mutants depends on the rate of osmotic challenge. This suggests that all mechanosensitive channels may contribute to cell survival. However their contribution to cell protection against osmolarity change varies depending on the rate.

## 3.4 Death mechanisms

As noted above, the bulk assay used in previous work [22] to study the role of MS channels in cell physiology was focused on the mean response of the population of cells exposed to a rapid change in the medium osmolarity. Moreover, the lack of direct observations of the morphology of the cells during and after the shock led to many assumptions about the fate of these cells, the most popular being that cells lyse

as an effect of rupture of all three layers of cell envelope and release their content [22, 119] (for cartoons illustrating this assumed fate of the cell after an osmotic shock see [126] and [127]). It has only recently been proposed that the cell lysis may result in the existence of various morphological forms and the rupture of all three layers of the cell envelope does not have to occur (for the cartoon illustrating various possible scenarios see [128]).

The results presented in this work are based on the observation of individual cells during and after a controlled osmolarity change. Direct observation allowed us to notice various changes in cell morphology leading to cell death (Figure 3.5).

As mentioned earlier, the cells classified in our assay as dead were further divided into four subgroups based on their morphology. The most common observed change was the formation of a membrane bleb (Figure 3.5A), similar to those formed in cells treated with antibiotics introducing defects in the peptidoglycan structure (Figure 2.2). Formation of a visible bleb was interpreted as the existence of a rupture in the peptidoglycan layer. The second most common phenotype was a slow loss of phase contrast ("fading away") without clear signs of cell envelope disruption (Figure 3.5C). This was interpreted as a loss of the cytoplasmic content. Such a loss may be the effect of the excess depolarization of the cell. The functioning of many transporters important for the homeostasis of the cell is known to depend on the gradient across the cell membrane and, in the case of depolarization, they may not function properly [129]. The other two types are: cells showing morphological changes which we interpret as membrane rupture without formation of the bleb, and bursting cells (Figure 3.5B and 3.5D, respectively) were a much smaller fraction of the cell population, typically up to 20%. This type of cell death was interpreted as a loss of membrane integrity. However, the release of cell content happening at different time scales, very slowly or very rapidly, suggests that the size of the hole in the membrane in these two cases might have been very different. The interpretation of the reason for the existence of these various death mechanisms needs further investigation and the arguments presented here should be treated as hypotheses that require experimental investigation.

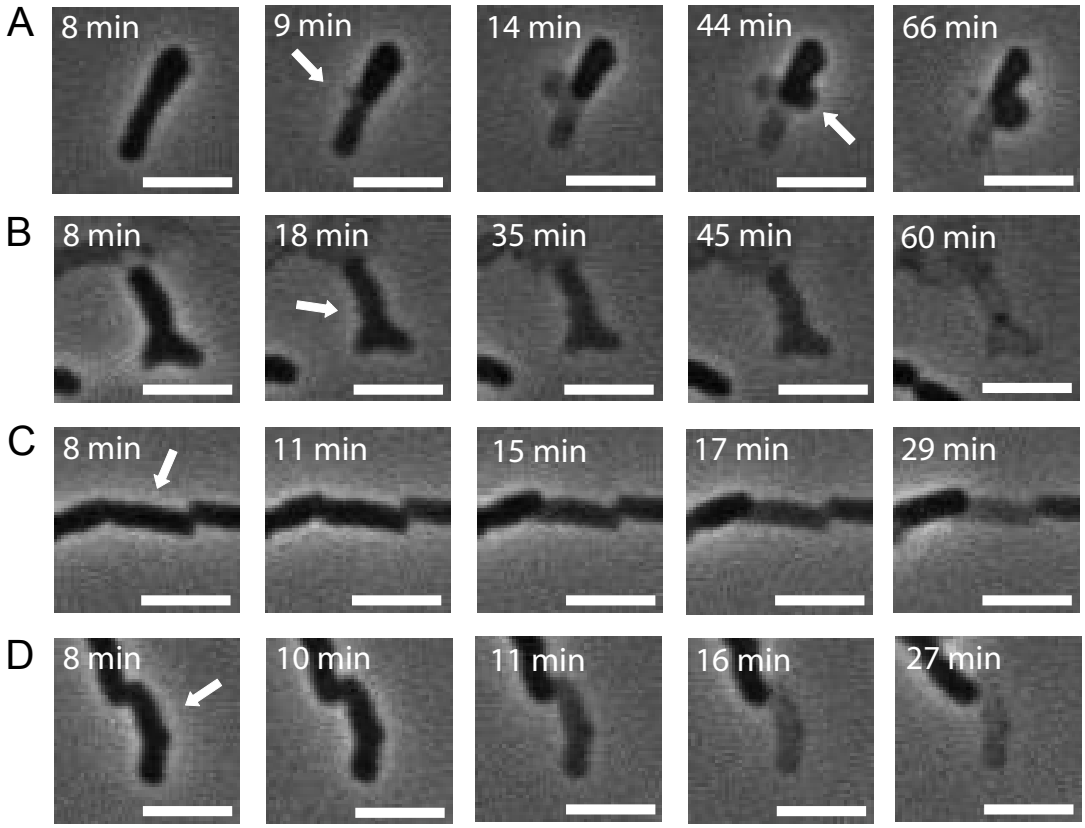


Figure 3.5: Image sequences showing typical cell morphology changes after exposure to osmotic challenge leading to cell death as a function of time. (A) Bleb formation, arrows indicate the region of the cell where the blebs were formed; (B) Morphological change interpreted as a membrane rupture without formation of a bleb. The arrow indicates the location of a potential rupture; (C) Cell releasing its content ("fading") without a clear sign of envelope damage. Arrow indicates the cell of interest; (D) Bursting cell. The content of the cell gets suddenly released. Arrow indicates the cell of interest.)

Interestingly, the abundance of a given type of change in cell morphology due to the osmotic challenge does not seem to be correlated with the rate of osmotic exchange (Figure 3.6). For all three strains tested (MJF465, MJF612, and MJG641) the percentage of a given type of morphological change was rather constant in most of the cases. In all cases cells forming blebs were the most abundant and the cells showing signs of potential membrane rupture were least abundant. This lack of correlation with the rate of the medium osmotic shock suggests that there might be a few mechanisms involved in the formation of these phenotypes.

The observation of cell recovery as a function of time allows us to establish the

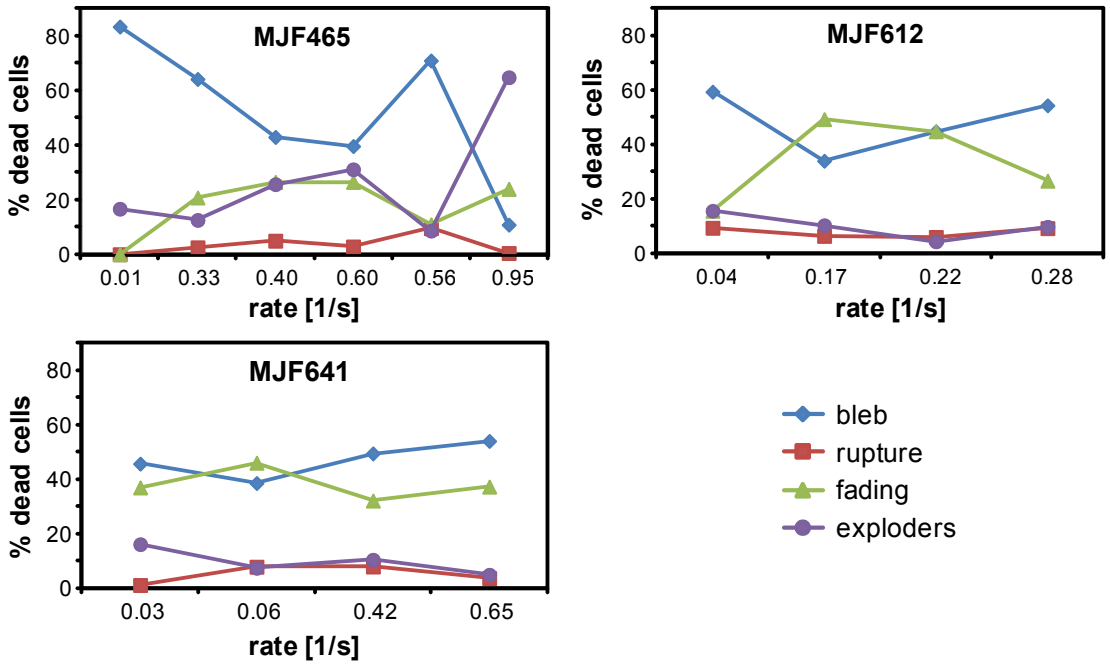


Figure 3.6: The percentage of cells showing a given morphology change as a function of the rate of medium exchange for three strains: strain MJF465 ($\Delta mscL\ \Delta mscS\ \Delta mscK$), MJF612 ($\Delta mscL\ \Delta mscS\ \Delta mscK\ \Delta ybdG$), and MJF641 (all seven mechanosensitive channels deleted). In all cases the death mechanism is not correlated with the rate of the osmotic challenge and the most common morphological change leading to cell death is bleb formation.

time after the shock at which every cell died with a one minute precision. Such an analysis was performed for strain MJF465 (Figure 3.7). The histograms of the "time of death" of blebbing cells were constructed for four samples shocked at different rates, resulting in various survival levels of the cells. Interestingly, we find that in many cases the death is not due to nearly instantaneous cell envelope rupture at the moment of exposure to an osmotic challenge. Specifically, only a few cells "explode" during the medium exchange. The majority of cells die long after the osmotic challenge took place, about 10-20 minutes after. Such a delay between the osmotic challenge and the death of cells may suggest the existence of damage of the cell envelope (membrane or peptidoglycan layer). This means that in most of the cases the sudden change in medium osmolarity causes irreversible injury to the membrane or peptidoglycan layer, which the cell is trying to recompense for over some time.

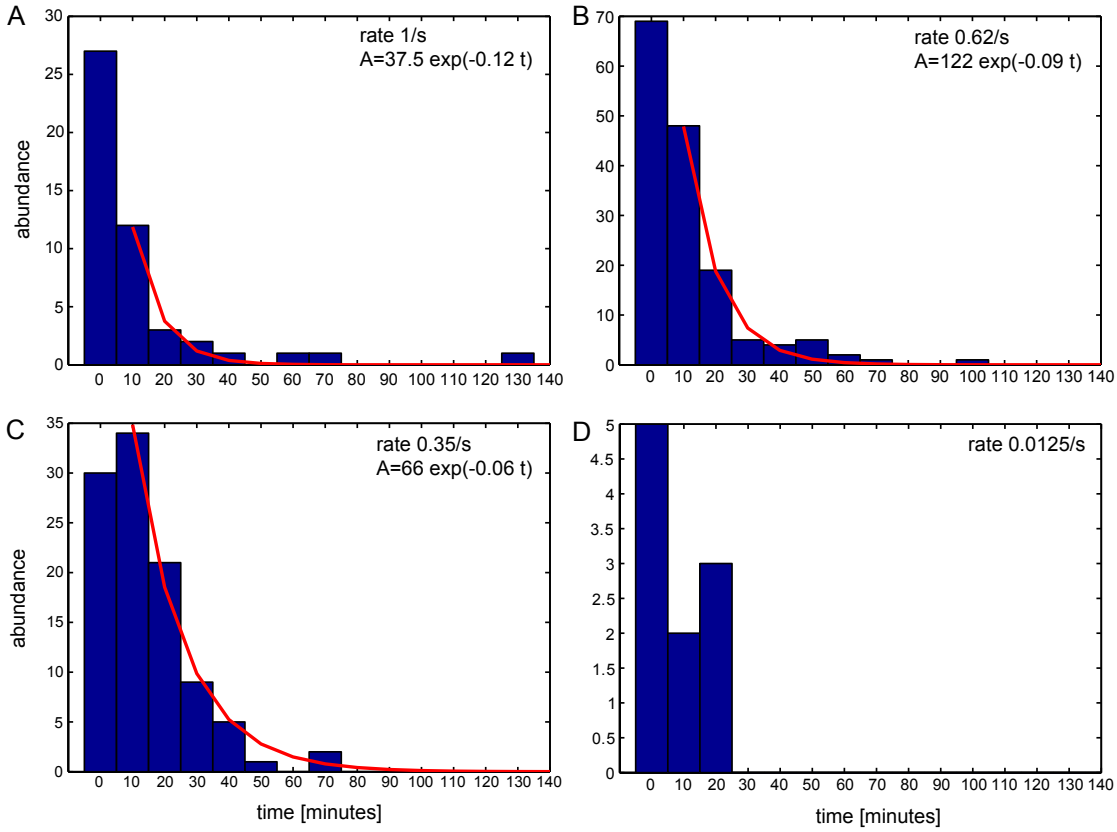


Figure 3.7: Histograms showing the "time of death" of blebbing MJF465 cells exposed to 0.5 M NaCl osmotic challenge performed at various rates: 1 $s^{-1}$ (A), 0.62 $s^{-1}$ (B), 0.35 $s^{-1}$ (C), and 0.0125 $s^{-1}$ (D). The exponential decay function ($Y = Aexp(-Bt)$) was fitted to the histograms (the first bin was neglected for fitting). Only the last histogram does not have a fit due to the small number of bins. The fitting parameters are listed in Table 3.3 and discussed in the text.

As discussed earlier, the rate of medium exchange does not seem to influence the mechanism by which the cells die. However, the analysis of the distribution of death times for cells shocked at different rates allows us to comment on whether or not the rate influences the time interval between the osmotic challenge and cell death. To address this question, we performed an exponential fit to the histograms. The first bin was not taken into account for the fitting due to the uncertainty in determining the time of death of some cells. We define $t = 0$ as the beginning of the movie showing cell recovery process. However, some of the cells are already dead at this point. They might have died during the medium exchange or during the time needed to rearrange the experimental system from the calibration mode to recovery data collection. In the

analysis, these cells are treated as if they died at $t = 0$, even though they were dead earlier. That is why, to avoid the error due to an inaccurate death time assignment for these cells, we decided to neglect the first bin.

The fitting of an exponential decay function (abundance = Aexp($-$B $\times$ time)) to our histograms gave us the fitting parameters $A$ and $B$, which then allowed us to calculate the time needed for a $1/e$ drop:

$$e^{(-Bt_2)} = \frac{1}{e} \times e^{(-Bt_1)} = e^{(-Bt_1-1)}$$
$$e^{(-Bt_2+Bt_1+1)} = 1, \tag{3.3}$$

where $\Delta t = t_2$ - $t_1$ is the time after which the abundance drops by a factor of $1/e$. Equation 3.3 is correct only if

$$-Bt_2 + Bt_1 + 1 = 0, \tag{3.4}$$

which gives us

$$t_2 - t_1 = \Delta t = \frac{1}{B}. \tag{3.5}$$

The values of the fitting parameters and the times after which one observes a $1/e$ drop are listed in Table 3.3. Interestingly, the rate of the shock seems to influence the time between the osmotic challenge and cell death. The lower the rate the longer the time needed to observe a $1/e$ drop. This suggests that cells exposed to an osmotic challenge at high rates tend to die sooner compared to cells exposed to a slower rate of medium exchange. This in turn implies that injuries due to a rapid medium exchange are more serious and the cells lose their homeostasis earlier.

| Survival [%] | Rate of medium exchange [1/s] | Fitting coefficient | | Correlation coefficient $R^2$ | Time needed for a $1/e$ drop [min] |
|---|---|---|---|---|---|
| | | A | B | | |
| 0.2 | 1 | 37.5 | 0.115 | 0.96 | 8.7 |
| 9 | 0.62 | 122 | 0.093 | 0.99 | 10.7 |
| 56 | 0.35 | 65.6 | 0.063 | 0.99 | 15.8 |

Table 3.3: The fitting parameters of the exponential decay function to the histograms from Figure 3.7 (strain MJF465, blebbing cells). The fitting was not performed on the last histogram due to an unsatisfactory number of bins. The first bin of the histogram was ignored for the fitting. The time needed to observe a $1/e$ drop for various rates suggests that cells exposed to higher rates tend to show morphological signs leading to cell death earlier compared to cells exposed to an osmotic challenge at lower rates.

## 3.5 Discussion on the rate dependence phenomenon

Long before the discovery of mechanosensitive channels it was known that the exposure of cells to osmotic shock results in the release of various molecular species without a significant loss in cell viability. Moreover, the amount of the material released depends on the rate of shock. Britten and McClure [77] studied the influence of osmotic shock on the proline pool removal. Their results showed that the shock in one step resulted in 90% of the pool release, the shock in four equal steps – 70%, and slow medium concentration change resulted in only 50% of the proline pool loss. Similar results were obtained by Tsapis and Kepes [78] (slow shock resulting in less methyl $-\beta-$ D $-$ thiogalactoside released compared to a fast shock) and Meury *et al.* [130] (the higher the dilution gradient the more $K^+$ ion are released). These results may suggest that not all of the channels were activated during the slower concentration change, or that different types of channels were activated depending on the rate of the shock.

The discovery of mechanosensitive channels [92] solved the mystery of the mechanism of solute release. However, to this date, the survival of cells was studied only after exposure to a step-like change in the medium osmolarity. The results presented in this chapter show the impact of the rate of the osmotic challenge on the survival of MS channel deletion mutants. The classical mutant characterization (by plating assay) is not sufficient to motivate the presence of seven MS channels in an *E. coli*

cell. The method presented in this chapter provides one possible explanation of the existence of a variety of different types of MS channels in *E. coli*, which is protection at different time scales.

The MscS channel was shown experimentally to inactivate even in the presence of the pressure which caused the activation [131]. This suggests that some of the MS channels are sensitive to changes (tension gradients) rather than just to a given arbitrary value of tension. Moreover, Boer *et al.* [120] studied the inactivation of MscS by using patch clamp to simulate channel behavior during an exposure to various osmotic challenges. They showed that in the case of a gradual pressure increase (analogous to a gradual shock) only a fraction of MscS population was activated, whereas in the case of a one-step pressure increase (analogous to a "fast" shock) the fraction of activated channels was much higher (measured by the current amplitude). The inactivation of MscS was observed only in the case of a gradual pressure increase. This may suggest that opening of only a fraction of available MS channels or opening the ones characterized by a smaller conductance in the case of gradual osmolarity change leads to a release of the tension built up and, at the same time, minimizes the losses in the released solutes due to the opening MS channels. In such case one would expect the cell to recover earlier from the osmotic challenge (smaller loss in the electrochemical gradient) compared to cells exposed to a faster osmolarity change.

The observation of various previously unnoticed morphology changes leading to cell death suggests that the exposure to an osmotic shock may damage various parts of the cell envelope. To address this problem, one needs to have a good understanding of the mechanical properties of all layers of the cell envelope. However, as shown in Table 3.4, the measured values of the basic parameters vary a lot. This motivates further studies on the role of cell envelope in protection from osmotic challenge.

The background strain used for the construction of MS channels deletion mutants may also play a role in cell survival [132]. The comparison of the genes disrupted in various wild-type strains leads to the conclusion that the choice of the background strain for the construction of a desired mutant may have an impact on its physiology

| Strain | E [MPa] | Sample | Reference |
|---|---|---|---|
| AB264 | 25 | isolated sacculi | [133] |
| JM109 | 12.8 | whole cells | [134] |
| JM109 | 0.12 | whole cells | [135] |
| JM109 | 0.05 | whole cells + EDTA | [135] |
| DH5$\alpha$ | 2-3 | whole cells | [136] |
| DH5$\alpha$ | 6 | whole cells | [136] |
| NCTC 9001 | 221 | whole cells | [137] |
| NCTC 9001 | 182 | whole cells + COS | [137] |
| BE100 | 32 | whole cells | [32] |
| ATCC 9637 | 2.6 | whole cells | [138] |

Table 3.4: Young's modulus measurements for *E. coli*. Table adapted from [139].

[140]. The genetic comparison of strains MG1655 and NCM3722 suggests that they may react differently to the same osmotic perturbation. For example, strain MG1655 has genes *nmpC* and *wbbL* disrupted. The disruption of these genes may change the mechanical, biophysical, or physiological properties of the cell envelope. The disruption of *nmpC* gene, coding an outer membrane porin, may have an impact on the transport across the cell envelope, whereas the disruption of the *wbbL* gene, which codes lipopolysaccharide biosynthesis protein, may have an impact on the overall outer membrane stability. Strain NCM3722 has multiple genes deleted (*rfbA*, *rfbD*, *rfbB*, *galF*, *wcaM*, *wcaL*, *wcaK*, *wzxC*, *wcaJ*, *cpsG*, *cpsB*, *wcaI*, and *wcaF*). Those genes are related to the lipopolysaccharide and capsule formation. Their deletion may influence the properties of the cell envelope leading to an increased (more elastic) or decreased (less resistant to the mechanical stretching) resistance to mechanical injuries. This aspect, however, needs further investigation and strong experimental evidence for the impact of the background strain on cell survival after an osmotic shock is required.

# Chapter 4

# Counting the number of MscL channels per cell

When the cell is exposed to an osmotic challenge and the tension in the membrane increases, MS channels gate, protecting the membrane from rupturing. At the same time, the opening of the channels (especially MscL, which has the largest pore) leads to a release of multiple molecular species needed for cell functioning and disturbs the electrochemical gradient across the membrane (Figure 4.1). Electrophysiology measurements provide information about the conductance of a given channel (measured in siemens), measured as the ratio of current ($I$, measured in amperes) flowing through the channel to the voltage ($V$, measured in volts) across the membrane. The typical measured current amplitude for an MscL channel is 90 pA. Knowing that 1 ampere is equal to 1 coulomb per second and that 1 $e^-$ is equal to $1.6 \times 10^{-19}$ C, one can calculate that 1 A corresponds to a flow of $6.2 \times 10^{18}$ monovalent ions per second. This number allows us to estimate the number of ions released due to opening of a single channel.

$$\begin{aligned} 90 \text{ pA} &= 90 \times 10^{-12} \text{ A} = 90 \times 10^{-12} \times 6.2 \times 10^{18} \text{ ions/s} \\ &= 5.6 \times 10^{8} \text{ ions/s} = 5.6 \times 10^{5} \text{ ions/ms}. \end{aligned} \tag{4.1}$$

This result indicated that the opening of a single channel for only 1 ms depletes the cell of roughly half a million ions. To get a better understanding of what such a loss means for the cell, let's take potassium ions as an example. The reported concentra-

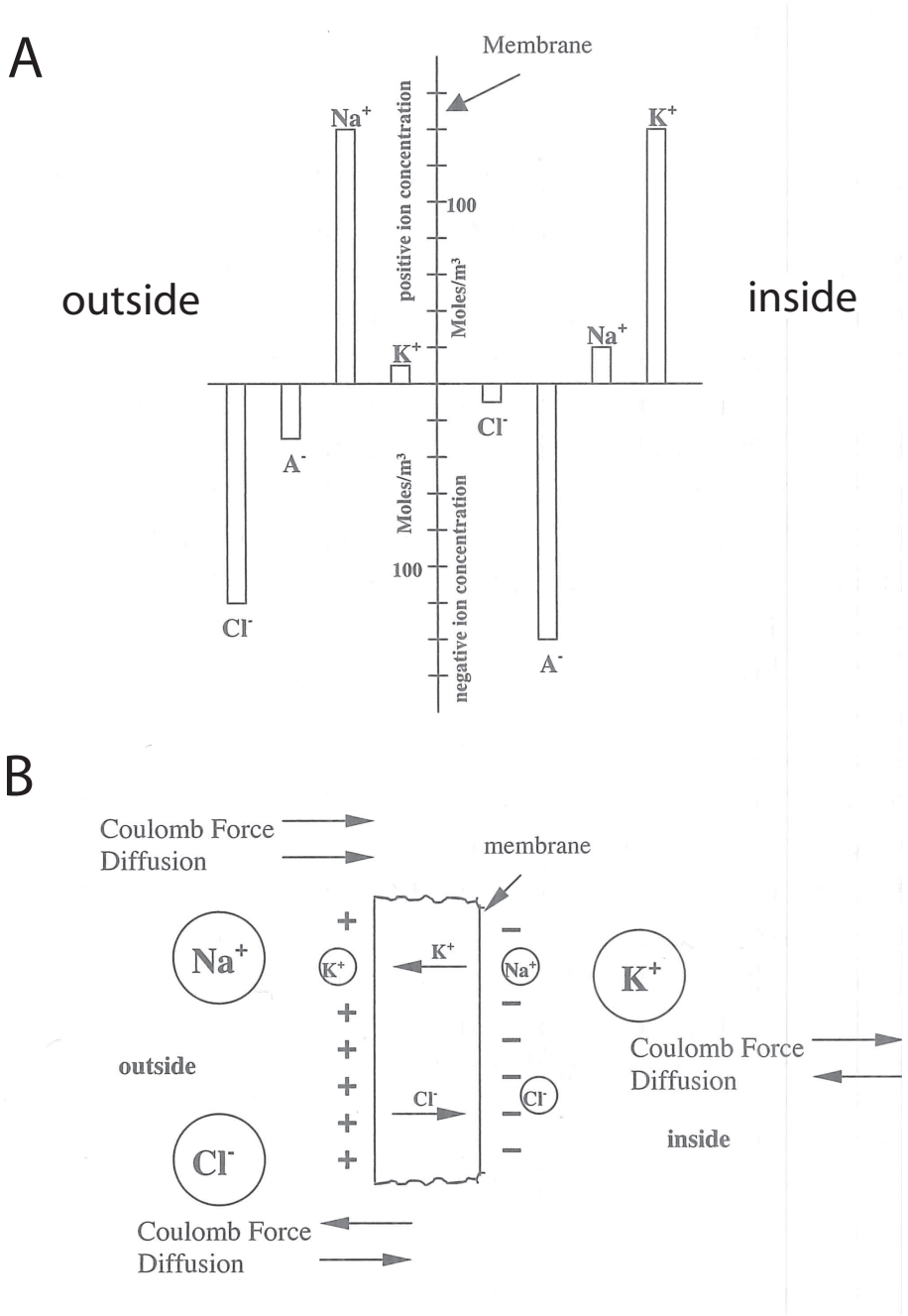


Figure 4.1: Schematic illustration of an electrochemical gradient across the cell membrane. (A) The comparison of negative (below the line) and positive (above the line) ion concentrations outside (left) and inside (right) a cell. The type of ions accumulated inside the cell are significantly different when compared to the outside of the cell. (B) The diffusion of ions across the membrane. The Coulomb force inhibits continuous diffusion down the chemical gradient. Figure adapted from [141].

tion of $K^+$ ions inside the cell is 140 moles/$m^3$ or 0.14 moles per liter. Knowing that the volume of an *E. coli* cell is 1 fL, we can calculate the concentration of $K^+$ ions to be $0.14 \times 10^{-15}$ moles or $0.8 \times 10^8$ $K^+$ ions. This means that the opening of a single MscL channel for only 1 ms depletes the cell of 0.6% of its total number of potassium ions. This number may not seem big; however, the total number of ions lost will depend on the time and number of open channels. This is why, as one might have expected, the number of MS channels may influence the balance between the necessity of releasing the tension from the membrane, and the loss of valuable molecules accumulated in the cell. This balance is crucial for proper and efficient protection. On one hand, not having enough MS channels will provide insufficient protection in the case of an osmotic challenge. On the other hand, opening too many channels will cause a loss of homeostatic balance which may be impossible to recover from. As an example, the work of Simonin *et al.* on the yeast *Saccharomyces cerevisiae* [142] demonstrated that the ratio of transiently depolarized cells (due to the membrane potential loss) to dead cells decreases with increasing degree of osmotic challenge. This result suggests that in the case of a gentle change in osmolarity cells can rebuild the electrochemical gradient across the membrane. However, as the degree of osmotic shock increases, the depletion of ions is too large and the cell dies.

Another important question concerning the number of MS channels is whether it is constant throughout the cell life or is changing dynamically depending on the environmental conditions. The constant number of proteins would suggest that there is a specific level of protein expression that provides protection from the majority of osmotic challenges which a cell could possibly be exposed to. In the case of a dynamic regulation of gene expression, the physiological response of the cell would depend on the number of currently expressed channels for given environmental conditions and could vary significantly from cell to cell. The machinery regulating the number of channels and its induction would allow the cell to modify its physiological response depending on the encountered circumstances.

In order to understand at a deeper level the role of these channels and the conse-

quences of changes in the expression level, many biophysical models were used. The most urgent questions involve estimating how many channels a cell needs for osmotic protection and how much transport occurs through them for a given osmotic challenge [86, 143, 144]. The crucial element needed to build these models is the mean number of channels present in the cell and its variation. Interestingly, the areal density of these proteins was shown to influence channel clustering, gating probability, and cooperative gating [121, 145, 146]. The simplest argument, showing how much the mean number of channels in a cell can influence its chance to survive an osmotic shock, is the dependence of the tension needed to open one channel on the total number of channels present in the cell (Figure 4.2). All these models are very promising for deepening our understanding of cell response to osmotic shock and explaining how this response changes as a function of the mean number of channels. However, these models cannot be verified by experiments without measuring the number of channels, both at the population and single-cell level.

## 4.1 Published results

The question of the mean number of MscL channels per cell was addressed in a few publications (Table 4.1). However, the methods used to perform the measurement were not truly *in vivo*. The counting results were derived on the basis of the number of radio-labeled molecules detected in a purified membrane fraction [147] or through the electrophysiological signal [148, 149, 150]. The number of channels detected within the area of the sample used was then extrapolated to the area of the *E. coli* cell.

The reported numbers vary from 4 to 100 conducting channels per cell. This variation may have its source in the measurement method, especially in the case of the electrophysiological measurements. The sample used for the experiment may also vary a lot from measurement to measurement. In the case of a reconstituted protein one has to assume that its density is comparable to that in the cell. The giant spheroplasts used for the measurement might have been formed by a different number of cells (one of the steps involves using cephalexin, which prevents cells from dividing).

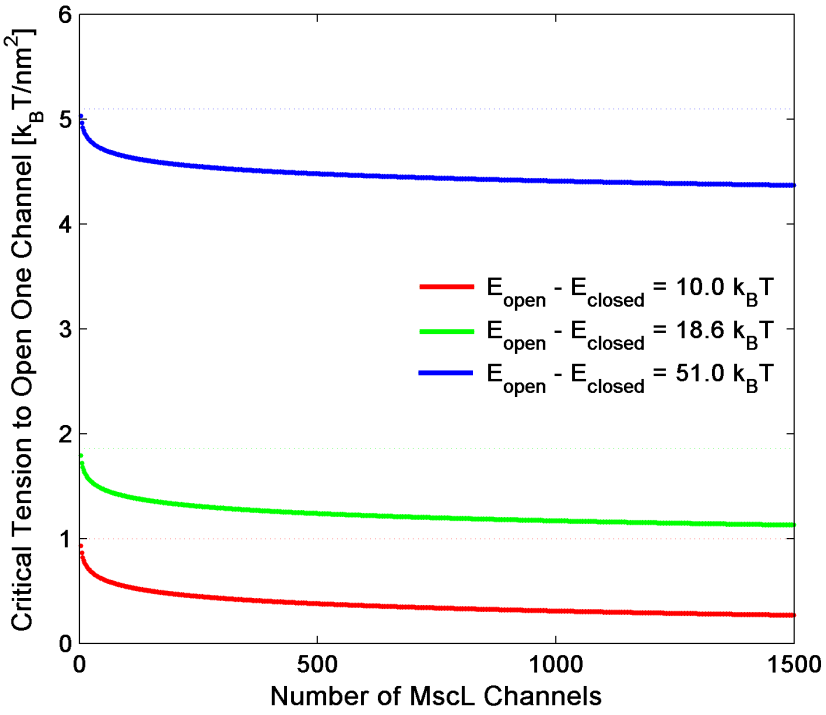


Figure 4.2: The dependence of the critical tension needed to open a single channel on the total number of channels expressed in the cell. As the number of channels present in the cell increases, the gating tension needed to open the first channel decreases. This suggests that the probability of finding an open channel for a given tension value increases with increasing mean number of channels per cell [116].

| Number | Method | Reference |
|---|---|---|
| 50/cell | radiolabeling | [147] |
| 10 - 100/cell | electrophysiology | [148] |
| 4 - 5/cell | electrophysiology | [149] |
| 10 - 15/cell | electrophysiology | [150] |

Table 4.1: Summary of previously published results on the counting of MscL proteins in an *E. coli* cell. These numbers were measured using electrophysiological or radiolabelling techniques. The values differ by an order of magnitude.

Since in both cases the preparation of the samples rely on adding some chemicals to the cell culture or mechanically disrupting the cell in the case of protein purification, one does not know how many channels might have been inactivated or denatured. The work of van den Bogaart *et al.* [72] provides an estimate of the reconstitution

efficiency. The number of liposomes with inactive channels was estimated based on the coincidence of the signal from fluorescently labeled lipid and molecules. The fact that after the activation of MscL these two signals coincided in 40 to 70 % of liposomes was interpreted as the lack of release of the molecules from the liposome due to absence of a functional MscL channel. Based on the MscL to lipid reconstitution ratio and the number of liposomes with inactive channels, the authors estimated that 90% of the protein was lost or not functionally incorporated during reconstitution. Similar reconstitution efficiencies were reported earlier [109, 114, 151]. Also, the lipid environment is known to influence the activation of MS channels [108]. The glass pipette used for the recording may vary in size from measurement to measurement, which would influence the area of the patch from which the signal is collected and/or the geometry of the patch. This in turn, would change the tension sensed by the channels. Last but not least, MscL is known to activate at a tension similar to that at which the membrane ruptures [111]. The number of activated channels increases with increasing tension (pressure). To count the number of all channels in a patch one should keep increasing the tension to the moment where there are no more new activities observed. However, the application of high pressure will most probably rupture the membrane before one can reach a state in which the increase in tension does not increase the number of active channels. This makes the activation of all MscL channels in the patch very hard, if possible at all. For all of the above mentioned reasons, the previously published results are not quantitative enough. Especially those using electrophysiology as a counting technique can give, at best, only an estimate of the number of active channels rather than the total number of channels per cell. To obtain more quantitative results, we performed an absolute MscL census *in vivo*, i.e., the measurement of the total number of channels, both active and inactive.

## 4.2 Regulation of MscL expression

The gene coding the MscL protein (*mscL*) was identified in 1994 [95]. However, our knowledge about the regulation of the *mscL* expression and the identification of the

main factors influencing the abundance of MscL channels in a cell membrane remains limited. The previously published work [149] demonstrated that MscL expression is enhanced by the production of the sigma factor RpoS.

RpoS, known also as $\sigma^{s}$ or $\sigma^{38}$, is a sigma subunit of the RNA polymerase holoenzyme. It is known to be a master regulator of general stress response [152]. It is not necessary for exponential growth, however, it is indispensable upon entry into stationary phase. The *rpoS* gene was discovered independently by a few research laboratories as an important gene in many independent cellular processes [153], which illustrates best its non-specificity to a single target. Accumulation of $\sigma^{s}$ may be triggered by a variety of factors (entry into stationary phase, starvation, high osmolarity, high or low temperature, acidic pH) and it causes changes in cell physiology and morphology that increase cellular resistance to stress by preventing the potential damage rather than repairing the damage that has already occurred. The induction of *rpoS* expression varies with the applied stress, as it might be modified by activation of other genes or factors as well, and it is reversible at any point if the stress factor disappears. The situation is further complicated by the fact that *rpoS* expression is regulated at multiple levels: transcription, translation, and protein stability [154, 155] (Figure 4.3).

So far, over fifty genes under the control of RpoS have been discovered and they are mainly involved in the regulation of the stress tolerance, structural and morphological rearrangements, redirection of the metabolism, and virulence [156, 157]. RpoS is a close relative of the sigma factor $\sigma^{70}$ (RpoD) known as the vegetative ("housekeeping") sigma factor necessary for cell growth. Both of these factors recognize similar promoter sequences *in vitro*. However, the concentration of RpoS is always lower than RpoD ($\sigma^{s}$ can reach up to 30% of the $\sigma^{70}$ level) [158], the affinity of the core polymerase is significantly lower for $\sigma^{s}$ when compared with that for $\sigma^{70}$, the holoenzyme form of RNA polymerase with $\sigma^{s}$ ($E\sigma^{s}$) is more tolerant to deviations from the consensus and less strict in recognition of the -35 part of the promoter, and they control different genes ($\sigma^{70}$ can't compensate for the absence of $\sigma^{s}$) [152].

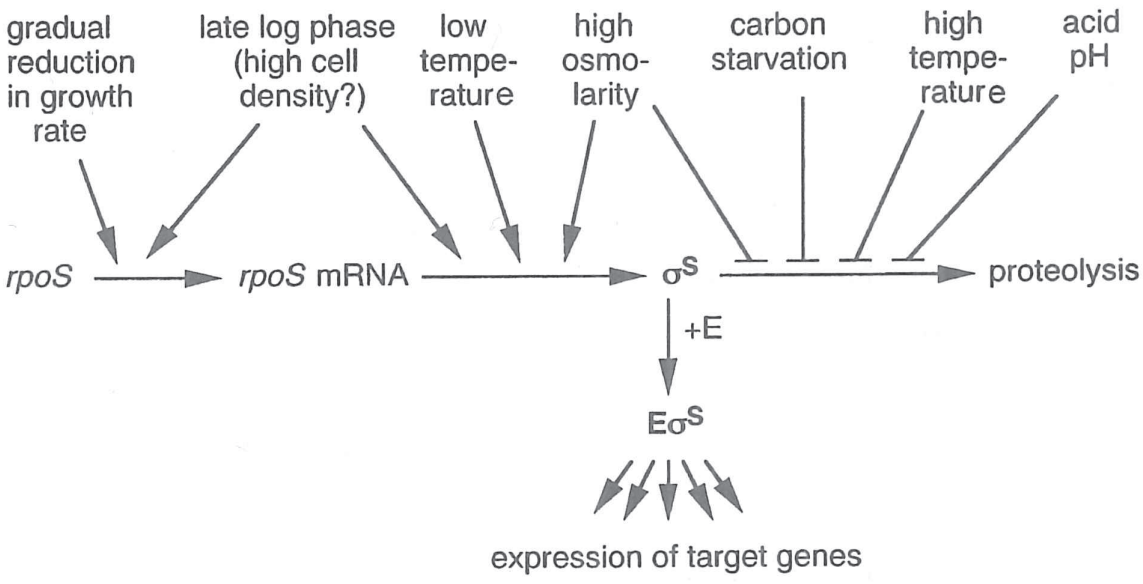


Figure 4.3: Regulation of RpoS expression. Various stress factors affect the amount of RpoS present in the cell: cell density, temperature, osmolarity of the medium, and availability of the carbon source (starvation). The regulation of RpoS level occurs at all stages of expression: transcription, translation, and/or stability of the protein (inhibition of proteolysis). Figure adapted from [152].

Interestingly, *in vitro* preference for E$\sigma^{s}$ over E$\sigma^{70}$ can be enhanced for some of the promoters depending on the presence of salts, DNA supercoiling, or the presence of trehalose [159, 160, 161]. The three most important factors for this work influencing *rpoS* expression are: entry into stationary phase, salt induction, and starvation.

The osmotic induction of *rpoS* expression not only increases the level of the Rpos protein, but its concentration can increase as a function of time. The presence of salt stimulates *rpoS* translation and it increases the half-life of the protein from 3 to 50 minutes [155]. As mentioned earlier, the presence of salt in the medium can alter the promoter recognition by E$\sigma^{S}$ [159]. $K^{+}$ glutamate, which is accumulated when the cell is exposed to a hyperosmotic shock, also seems to stimulate the activity of E$\sigma^{S}$ towards $\sigma^{S}$-dependent promoters [162]. The detailed mechanism of osmotic induction is not well-understood; however, the experimental data suggest that osmotic regulation of *rpoS* happens at the posttranscriptional level [155]. Another response, particularly interesting for this work, is related to the carbon source of the media.

Media associated with slower growth rates have been observed to induce elevated RpoS levels [163]. The same publication suggested that some of the genes (but not all) upregulated during starvation are associated with metabolism and transport.

All of these facts allow us to predict that the mean number of MscL channels should change with the growth conditions: density of the culture ($OD_{600}$), carbon source, and osmolarity of the culture medium.

It is very probable, although not experimentally proven, that RpoS is not the only protein that regulates the *mscL* expression. The work by Bianchi and Baneyx [164] suggests that exposure to high osmolarity induces not only $\sigma^{\mathrm{S}}$, but also heat shock promoters and $\sigma^{\mathrm{E}}$ dependent genes. The presence of NaCl may also increase supercoiling in *E. coli* [165], which can influence cell survival in a NaCl rich medium. It is well known that the DNA topology changes gene expression [166]. The starvation for glucose or phosphate and the entry into stationary phase in a rich medium induces the expression of the universal stress proteins *UspA*, *UspC*, *UspD*, *UspE*, and *UspG* [167]. All of these proteins have overlapping, but biologically distinct functions.

## 4.3 Strain construction and counting methods

In order to avoid major uncertainties due to sample preparation and the method used for counting, we used a complementary approach to electrophysiology. In our approach, a mutant expressing MscL-GFP fusion protein under the control of a native promoter is used to estimate the number of MscL proteins in a single cell and the mean number of channels at the population level. To construct such a strain, we replaced the native MscL coding region of a wild-type *E. coli* strain (MG1655) with a sequence coding MscL fused to a super-folder green fluorescent protein (sfGFP) [168], creating the strain MLG910 (the details of chromosomal integration strategy can be found in Appendix C). To establish that our fusion is functional, we integrated MscL fused to sfGFP into the MJF612 strain, which had four mechanosensitive channel genes knocked out (ΔmscL, ΔmscS, ΔmscK, and ΔybdG) [100] and performed an osmotic

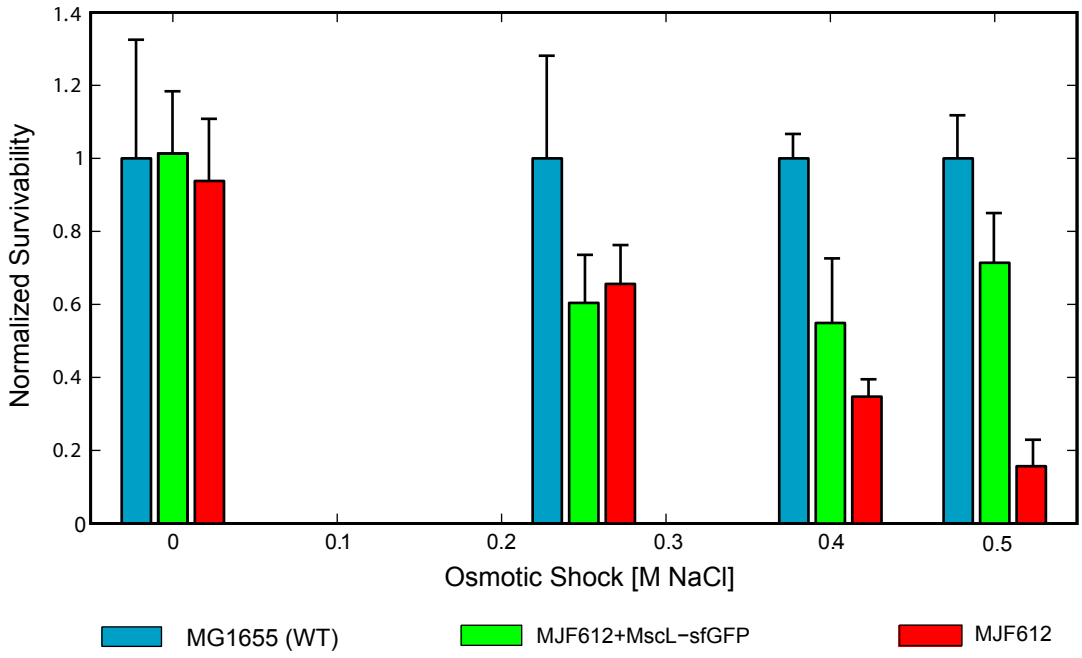


Figure 4.4: Osmotic shock assay results for various strains: wild-type MG1655, MJF612 ($\Delta mscL\ \Delta mscS\ \Delta mscK\ \Delta ybdG$) and MJF612 expressing chromosomally integrated MscL-sfGFP fusion. Mean survival rate after exposure to 0.5 M NaCl osmotic challenge is normalized to colony forming units from the MG1655 strain. The error bars are the standard deviation of five trials [116].

shock survivability assay (Figure 4.4). We observed a considerably higher survival rate for cells expressing our fusion for a 0.5 M NaCl osmotic shock as compared to the rate from the MJF612 strain (75% and 15%, respectively), but a lower survival rate as compared to that of the WT strain MG1655 (defined as 100%). We concluded that our fusion is functional. To check for the proper insertion of the MscL-sfGFP fusion in the cell membrane we used confocal microscopy and fluorescence recovery after photobleaching (FRAP) [169]. We concluded that the majority of the fusion proteins are mobile in the membrane (Figure 4.5). Based on the results from the survival assay and FRAP measurement we interpret that the MLG910 fusion strain is a fair representation of the wild-type MG1655 strain.

The measurement of the number of MscL channels per cell was performed under various culturing conditions using quantitative Western blots and single-molecule calibrated fluorescence microscopy. These methods allow us to measure the variation in

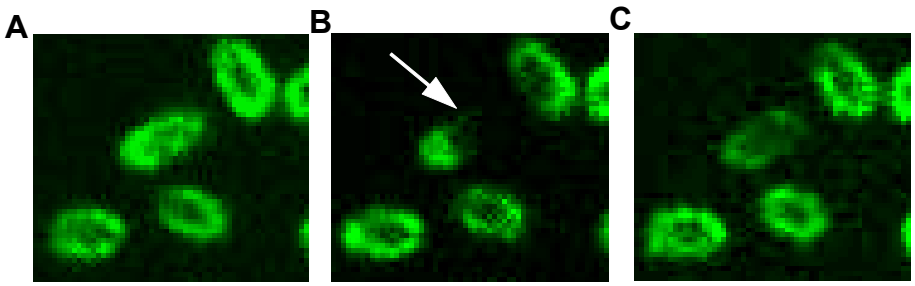


Figure 4.5: Confocal images demonstrating FRAP (Fluorescence Recovery After Photo-bleaching) performed on a single cell expressing chromosomally integrated MscL-sfGFP construct (strain MLG910). (A) Before photo-bleaching (0 s). (B) Photo-bleaching (0.7 s), an arrow indicates the photo-bleached region of the cell. (C) Recovery of the fluorescent signal (8.4 s). The slow recovery of fluorescence is consistent with diffusion rates typical for fluorescent proteins mobile in the cell membrane, as opposed to the sub-second recovery times which are characteristic for free proteins expressed in the cytoplasm [116].

the mean number of channels for different growth conditions, as well as the cell-to-cell variability for a given condition.

### 4.3.1 Western blots

We prepared the lysates derived from various strains, grown in three different media (LB-Miller, M9 supplemented with glucose, and M9 supplemented with glycerol, where the nutritionally poorer glycerol reduced the growth rate by a factor of two or more) to an early exponential ($OD_{600}$ of 0.3) and stationary phase ($OD_{600}$ of 1.2 - 1.7). Known volumes of the lysates were run alongside the purified protein references (either MscL or MscL-sfGFP) of known concentration. The references were diluted in MJF612 (ΔmscL ΔmscS ΔmscK ΔybdG) lysate to keep the total non-specific protein loaded similar to the whole cell lysates. Reference proteins and lysates were separated by the SDS PAGE, transferred to nitrocellulose membranes, and immunostained with primary antibodies for either MscL (polyclonal, generous gift from S. Sukharev) or GFP. Detection of the bands was achieved by imaging the chemiluminescence resulting from the horseradish peroxidase (HRP) labeled secondary antibodies. By measuring the relative intensity of the bands and comparing them to the purified protein reference bands, we determined the mean number of channels per cell for a

given condition.

The quantitative measurement of the number of MscL channels per cell requires that the MscL fusion protein is expressed at a native level. To ensure that the sfGFP tag does not alter the native expression level (despite being under the control of a native promoter), the mean expression levels of MscL-sfGFP to wild-type MscL was compared using quantitative Western blots. For this comparison, we used antibodies that recognize MscL protein (Figure 4.6). The expression levels for the two strains were comparable and, in many conditions, within the accuracy of our technique.

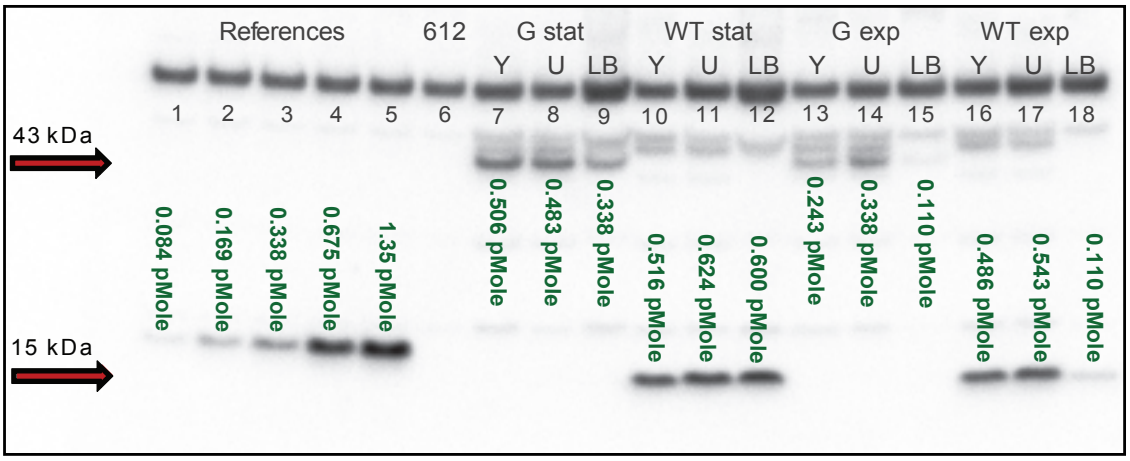


Figure 4.6: Detection of MscL (15 kDa) and MscL-sfGFP (43 kDa) proteins with MscL antibody. Arrows indicate the protein of interest. Other bands are the result of non-specific binding. Lysate from the MJF612 strain (612, lane 6) was used as a negative control (the *mscL* gene is deleted in this strain). The cells used for lysate preparations were cultured to exponential (exp) and stationary phase (stat) in LB-Miller (LB), M9 + glucose (U), and M9 + glycerol (Y). Lanes 1 - 5 are reference loads of purified MscL protein (in picomoles). Lanes 7 - 9 and 13 - 15 are MscL-sfGFP levels in MLG910 strain (MLG). Lanes 10 - 12 and 16 - 18 are MscL levels in MG1655 (WT) stain. The amount of protein in the lysate lanes (7-18) was determined based on a comparison with the calibration curve obtained based on the reference band intensities [116].

To establish the mean number of MscL channels per cell and to measure how it is impacted by stress factors, we used quantitative Western blots with a monoclonal GFP antibody (Figure 4.7). Our measurements show much higher MscL expression levels compared to previously published results (Table 4.1). In LB-Miller medium, we did not observe a significant increase in the MscL levels with increasing density of the

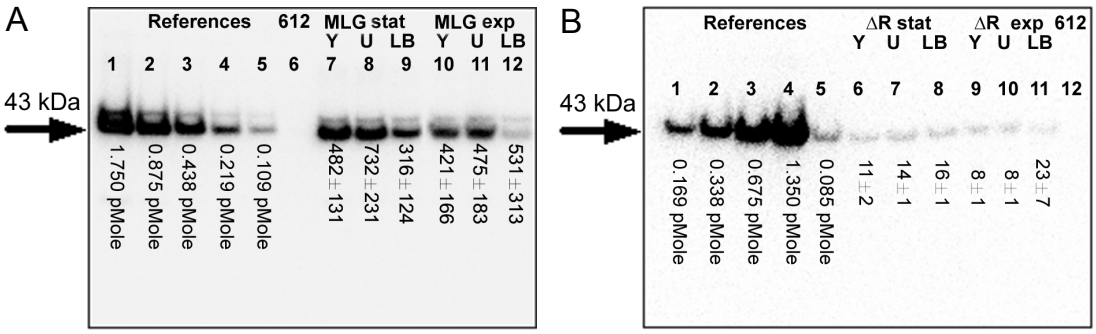


Figure 4.7: Representative Western blots showing the expression of MscL-sfGFP. Arrows indicate the protein of interest. Other bands are the result of non-specific binding. The strains of interest (MLG910 and MLG910 ΔrpoS) were cultured to exponential (exp) and stationary (stat) phase in LB-Miller (LB), M9 + glucose (U), and M9 + glycerol (Y). In (A) and (B), lanes 1 through 5 are the concentration series of a known number of purified channels diluted into the lysate from the MJF612 strain (References). The numbers under lanes 7 through 12 (A) and 6 through 11 (B) represent the average number of channels from three independent Western blots for the respective conditions. The total error of each measurement includes contributions from the standard deviation of three repetitions and the systematic uncertainties in the absolute calibration related to chemiluminescence linearity, initial cell culture density, and lysis efficiency. Lysate from the MJF612 strain (612) was used as a negative control (lane 6 in (A) and lane 12 in (B)). (A) Lanes 7 through 12 show the MscL-sfGFP levels in the MLG910 strain (MLG). (B) Lanes 6 to 11 show the MscL-sfGFP levels in the MLG910 ΔrpoS strain (ΔR) [116].

culture ($OD_{600}$) (lanes 9 and 12 in A). However, in the slower growth-rate M9-based media, the number of MscL channels per cell increased by nearly two to three fold during the transition period from exponential to stationary growth phase (lanes 7 and 8 vs. 10 and 11 in A). These results demonstrate that the carbon source and the associated growth rate influence the amount of upregulation of MscL during the transition from exponential to stationary growth phase.

Earlier work has examined how the expression of mechanosensitive channels is affected by RpoS expression [149] and we have explored this as well. We measured the level of MscLsfGFP protein in the MLG910 strain where the *rpoS* gene had been knocked out (MLG910 ΔrpoS). As expected, the expression of MscL-sfGFP protein in the MLG910 ΔrpoS strain was significantly lower (Figure 4.7B). In contrast to the previous results for the MG1655 and MLG910 strains, we observed neither an increase in the channel expression upon entry into stationary phase nor a change in

the expression level due to different carbon sources. We interpret these results such that the MscL expression in the ΔrpoS strain represents the baseline level of MscL expression in the absence of any stress.

### 4.3.2 Fluorescence microscopy

To conduct a single-cell based census of MscL channels, we used epi-fluorescence excitation microscopy to image the MLG910 strain under various growth conditions and stages. The cells were imaged in laser-excited (473 nm) epi-fluorescence mode at 100x magnification using an electron multiplying CCD camera. For each sample, we imaged multiple fields of view, typically analyzing more than 1000 immobilized bacterial cells per condition. Fluorescent microscopy images were analyzed using a customized MATLAB program based on the SCHNITZCELL segmentation program (a generous gift from M. Elowitz's lab). Images were median filtered to reduce spurious pixel noise. Next, a threshold mask was created for every frame by hand setting a threshold value for each sample. These masks were used to segment out individual cells from the original images and the total fluorescence of each segmented cell could be recorded. The last stage of manual selection was made on the segmented cells, where the selection criteria were based on morphology. The total integrated number of fluorescence counts of each cell was determined and converted into the total number of fully assembled channels by using a calibration factor of the fluorescence-counts-per-sfGFP, explicitly assuming that the fluorescence of each sfGFP represents a single channel subunit and that five subunits form a fully assembled channel [96]. We calibrated the number of fluorescent counts associated with a single sfGFP protein by measuring the average size of the single-step photobleaching events of purified MscL-sfGFP protein [170] (Figure 4.8). In order to maximize signal-to-noise ratio, the fluorescent samples were excited with laser-based TIRF illumination. Movies of the photobleaching molecules were recorded at 4 frames per second. Individual molecules were segmented with a modified version of the MATLAB based PolyParticle-Tracker program [171]. The traces were manually selected and fit to step functions (Figure

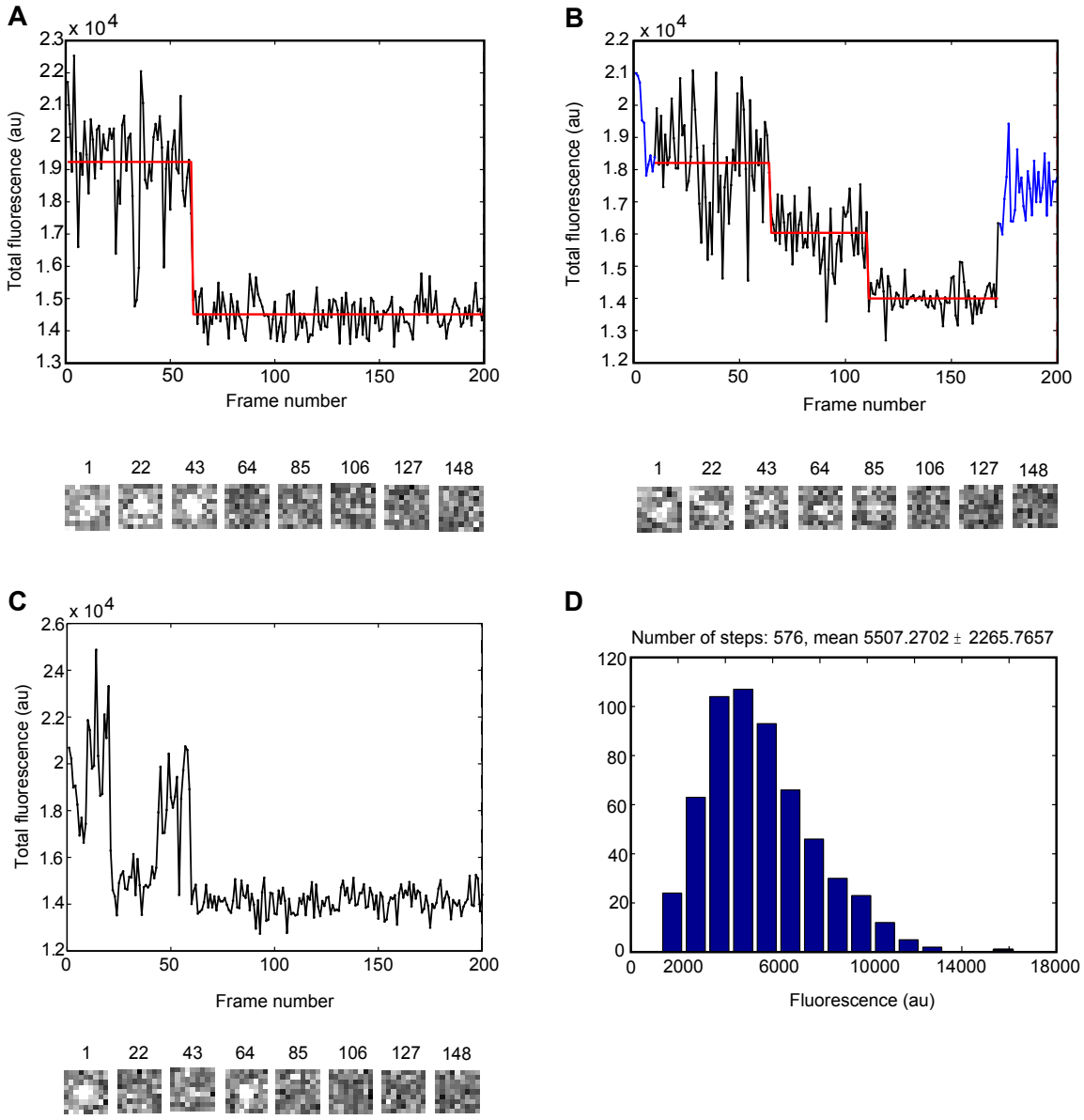


Figure 4.8: Typical single molecule traces and histogram of counts used for calibration of the number of fluorescent counts associated with a single sfGFP protein by measuring the average size of single-step photobleaching events. (A) A trace with one photo-bleaching step. (B) A region of the trace with two photo-bleaching steps. The data points not used for fitting are marked in blue. (C) An example of a single molecule trace that was rejected. (D) Histogram of counts used to calculate the mean value of a photobleaching step [116].

4.8). A histogram of counts was constructed and the mean signal was calculated. The mean value was multiplied by a TIRF/epi-fluorescence calibration factor. In order to calculate a calibration factor between the signal in TIRF and the signal in epi-fluorescence, we collected the images of 50 fields of view of a solution of 40 nm yellow-green fluorescent microspheres in both TIRF and epi-fluorescence. The PolyParticle-Tracker program was used to find the TIRF/epifluorescence ratio for single beads. The number of MscL subunits per cell was obtained by dividing the total fluorescence signal from a given cell by the mean fluorescence counts from a single sfGFP molecule. To determine the number of channels, we assumed there were five subunits per channel. In agreement with the quantitative Western blots, these measurements indicate that the media and the age of the culture affected the expression level of MscL-sfGFP (Figure 4.9).

## 4.4 Results

### 4.4.1 Mean number

The fluorescence microscopy measurements indicate that the mean number of channels per cell determined by the total integrated fluorescence is on the order of 300 to 1400, depending on the culturing conditions. The number of channels increased in M9 minimal media compared to cells grown in LB-Miller media (Figure 4.10, panel A and B compared to C). Depending on the carbon source, there was a 2.5-fold (M9 supplemented with glycerol) or a 1.5-fold (M9 supplemented with glucose) increase in the number of MscL-sfGFP channels per cell in the early exponential phase of growth. Interestingly, as the M9-media-grown cells entered stationary phase, they reached similar expression levels for both carbon sources (Figure 4.10, panel D). We also observed that the number of channels per cell increased steadily with the salt concentration (Figure 4.10, panel E), presumably demonstrating an osmotic induction related to the increased osmolarity of the media. During the exponential phase, cells grown in the M9 medium supplemented with various amounts of salt – 100

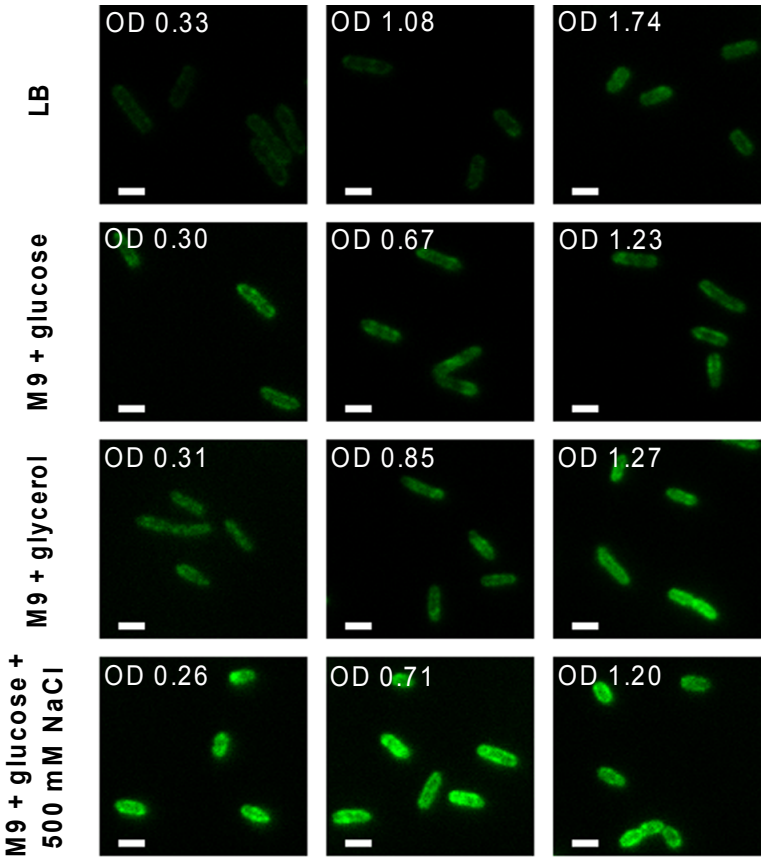


Figure 4.9: Typical fluorescence microscopy images of MLG910 strain (MG1655 expressing chromosomally integrated MscL-sfGFP construct) for various growth conditions. The fluorescence signal intensity (interpreted as the increase in the expression level) increases with increasing density of the culture ($OD_{600}$) and is influenced by the quality of the culture medium (salt content and the carbon source). The white scale bar is 2 $\mu$m long. The relative contrast of the individual images has been unaltered. The contrast of the overall composite image has been adjusted for clarity [116].

mM NaCl (342 m Osm/kg), 250 mM NaCl (529 mOsm/kg) and 500 mM NaCl (886 mOsm/kg) – showed a two to three-fold increase in protein expression, as compared to cells grown in M9 media without supplemented salt (234 mOsm/kg). Cells grown to stationary phase in the various salt-supplemented media appear to be approaching a common expression level of $\sim$ 1300 channels per cell, nearly twice the maximum level seen in M9 media without salt ($\sim$ 700 channels per cell). The age of the culture ($OD_{600}$) also influenced the mean number of MscL proteins per cell. In the presence of 100 mM or 250 mM NaCl salt, the cells showed a characteristic increase in the

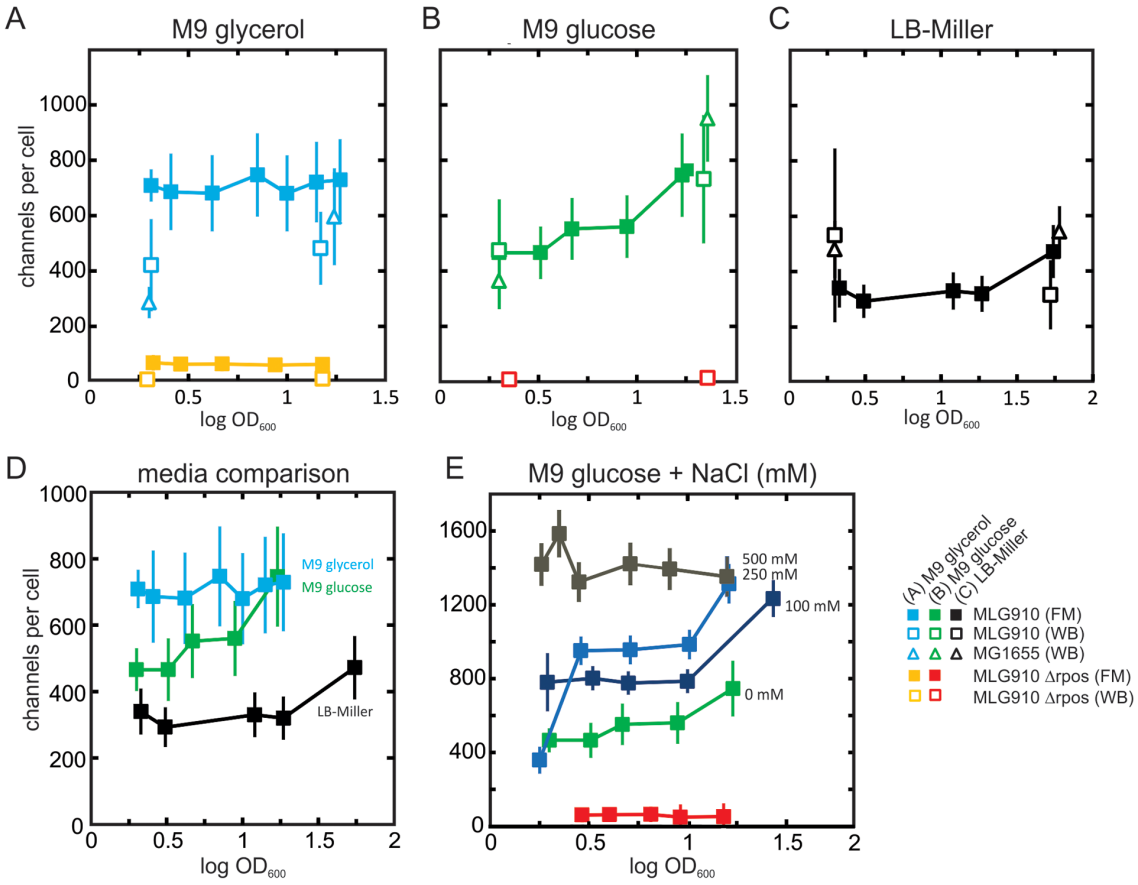


Figure 4.10: Mean channel counts per cell determined by fluorescence microscopy (FM) for various media versus $OD_{600}$. In panels A, B, and C the corresponding mean number of channels determined by Western blots (WB) (open symbols) are shown for reference. The error bar of each fluorescence microscopy results measurement is dominated by systematic uncertainties in the absolute calibration related to single-molecule fluorescence calibration. The standard error of the mean of the uncalibrated fluorescence counts per cell is typically less than 5% of the total error bar. (A) MLG910 strain with (light blue squares) and without RpoS (yellow squares) in M9 medium supplemented with glycerol. (B) MLG910 strain with (green squares) and without RpoS (red squares) in M9 medium supplemented with glucose. (C) MLG910 strain with RpoS in LB-Miller medium. (D) Comparison of fluorescence microscopy results from MLG910 strain grown in three different media. (E) Comparison of fluorescence microscopy results from MLG910 strain grown in M9 medium supplemented with glucose and four different NaCl concentrations: 0 mM (green squares), 100 mM (dark blue squares), 250 mM (gray-blue squares), and 500 mM (dark gray squares)[116].

expression level around $OD_{600}$ equal to 1, which can be interpreted as arising from the stress associated with the transition to stationary phase. However, cells grown in the presence of 500 mM NaCl did not show this tendency. Instead, we observed a

fairly-constant, relatively-high level of expression, which may represent a maximum level of MscL expression in response to salt and growth.

To summarize, the results from both experimental methods discussed above show a general trend of increasing MscL levels as the quality of the media carbon source was decreased (in going from LB-Miller to M9+glycerol), and as the cultures entered stationary phase. The agreement between the mean values found from fluorescence microscopy and quantitative Western blots is shown in Table 4.2.

| Condition | | Western blot | | Fluorescence microscopy | |
|---|---|---|---|---|---|
| Strain | Media | $OD_{600}$ | Mean number | $OD_{600}$ | Mean number |
| MG1655 | LB-Miller | 0.3 | 480 ± 103 | - | - |
| MG1655 | M9 glucose | 0.3 | 364 ± 102 | - | - |
| MG1655 | M9 glycerol | 0.3 | 286 ± 56 | - | - |
| MLG910 | LB-Miller | 0.3 | 531 ± 313 | 0.33 | 340 ± 68 |
| MLG910 | M9 glucose | 0.3 | 475 ± 183 | 0.3 | 466 ± 64 |
| MLG910 | M9 glycerol | 0.31 | 421 ± 166 | 0.31 | 709 ± 57 |
| MG1655 | LB-Miller | 1.78 | 544 ± 92 | - | - |
| MG1655 | M9 glucose | 1.36 | 951 ± 157 | - | - |
| MG1655 | M9 glycerol | 1.24 | 596 ± 174 | - | - |
| MLG910 | LB-Miller | 1.72 | 316 ± 124 | 1.74 | 472 ± 95 |
| MLG910 | M9 glucose | 1.34 | 732 ± 231 | 1.23 | 746 ± 150 |
| MLG910 | M9 glycerol | 1.17 | 482 ± 131 | 1.27 | 729 ± 147 |

Table 4.2: Comparison of channel counts per cell from quantitative Western blots and fluorescence microscopy. Strains MG1655 (wild-type) and MLG910 (strain expressing chromosomally integrated MscL-sfGFP fusion) were grown in various media (LB, M9 + glucose, and M9 + glycerol) and to exponential and stationary phase (measured as $OD_{600}$) [116].

### 4.4.2 Distribution in the population

In addition to measuring the mean number of fully-assembled channels, $N_{mean}$, we used the fluorescence dataset to determine the population distribution of the MscL monomer subunits expressed under various growth and stress conditions (Figure 4.11). This kind of a systematic analysis, as a function of both the growth media and $OD_{600}$, addresses the important question of the cell-to-cell variability of these channels in

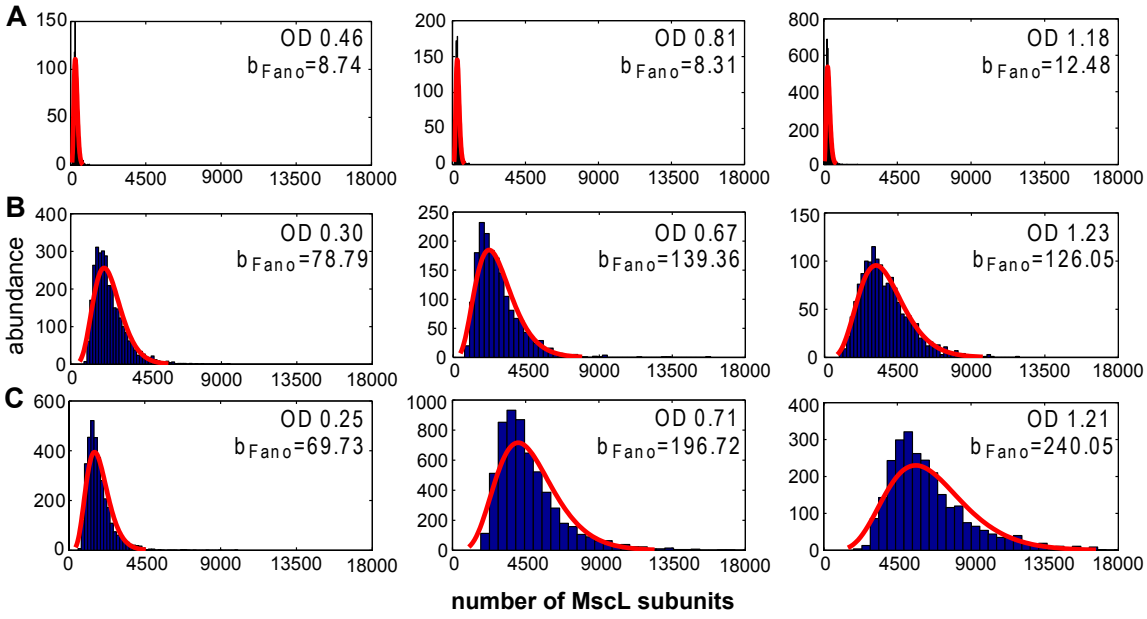


Figure 4.11: Distribution of MscL subunits under different growth conditions at various stages of growth. The red curves show the fitting of the gamma distribution (equation 4.3) to the histograms. The $OD_{600}$ and the Fano factor ($b_{Fano}$, equation 4.2) for a given sample are listed. (A) MLG910-ΔrpoS strain grown in M9 medium supplemented with glucose to $OD_{600}$ 0.46, 0.81, and 1.18, respectively. (B) MLG910 strain grown in M9 medium supplemented with glucose to $OD_{600}$ 0.3, 0.67, and 1.23, respectively. (C) MLG910 strain grown in M9 medium supplemented with glucose and 0.25 M NaCl to $OD_{600}$ 0.25, 0.71, and 1.21, respectively [116].

living bacteria, provides insight into the nature of their regulation under different physiological conditions, and may provide clues about additional physiological roles which these channels might play.

We observed changes in the width and shape of the respective protein distributions under various conditions. To characterize the distribution widths, we determined the standard deviation, $\sigma$, and the Fano factor ($b_{Fano}$) for each distribution, where $b_{Fano}$ is given by

$$b_{Fano} = \frac{\sigma^2}{N_{mean}}. \tag{4.2}$$

The Fano factor is a measure of the non-Poissonian character of the distribution, where a Poisson distributed protein abundance would correspond to $b_{Fano} = 1$.

The MLG910-ΔrpoS strain did not show a wide variation in the Fano factor value with increasing $OD_{600}$ (Figure 4.11). We interpret these Fano factor values as the baseline level of the population variability in the absence of a carbon source or salt-associated stress. There was a dramatic increase in the Fano factor of the RpoS-expressing MLG910 strain distributions compared to the MLG910-ΔrpoS strain. The presence of RpoS alone caused a 10-fold increase in the Fano factor value. In the presence of a 250 mM NaCl, an even larger 10- to 30-fold increase was observed. This increase depended on the $OD_{600}$ of the culture, indicating that the presence of salt introduced further changes in the expression profile.

Numerous theoretical models have linked the steady-state gene expression distribution of a population to stochastic factors describing the transcriptional and translational processes of a single cell. One of the simplest descriptions results in a steady-state distribution described by a gamma distribution of the form

$$p(x) = \frac{1}{b^a \Gamma(a)} x^{a-1} e^{-x/b}, \tag{4.3}$$

where *p(x)* is the probability of an occurrence of $x$ protein subunits, $a$ is a measure of the rate of the transcriptional bursts, and $b$ is the measure of the size of the corresponding translational burst [172]. For this class of models $b = b_{Fano}$. We fit this distribution to our data as a crude gauge of the complexity of the MscL regulation. For the cells expressing RpoS, we observed an increasing trend of both the $a$ and $b$ parameters with growth phase, and/or salt levels (Table D.1). In general, the distributions were reasonably described by such a fit in an early exponential phase, but outside this phase or in the presence of salt, the gamma distribution did not account well for our data (last two panels of Figure 4.11 C).

### 4.4.3 Summary

We presented the results of an absolute MscL channels counting and the impact of various stress factors on the mean number of channels using two methods: quantitative Western blots for bulk measurement and fluorescence microscopy for the mea-

surement at the single-cell level. We obtained similar counting results and general expression trends for both methods. MscL levels can be raised by increasing the salt of a given culture medium or by growing in a medium with a poor carbon source. Our results suggest that carbon source induction mechanisms are, at least, on a comparable scale to salt induction related ones. The relative expression level changes we observe are comparable to the previously published work [149]. We conclude that our results are a good representation of the *in vivo* census within the accuracy of the techniques used. They are at least an order of magnitude higher than the previously published results (Table 4.1). This discrepancy may be caused by the method used for the measurement of the number of MscL channels: our results report the total number of MscL channels, whereas previously published results report number of active channels, measured by, in most of the cases, electrophysiology. It is possible that most of the channels expressed in the cell are inactive due to improper assembly, improper insertion, or misfolding. Another possibility is that the majority of the protein gets inactivated during the sample preparation prior to the electrophysiology measurement. As discussed earlier (section 4.1) the reconstitution efficiency is very low. An additional source of discrepancy might be the fact that the tension needed to activate an MscL channel is close to that when the membrane ruptures, leading to a break of the patch before activating all of the channels. In order to test all of these possibilities one should apply the counting technique presented in this work to the electrophysiological measurement and compare the total number of fluorescently tagged proteins within a patch with the number of active channels.

The measurement at the single-cell level using fluorescence microscopy allowed us to measure the cell-to-cell variability of the MscL expression for various culturing conditions. We described these changes quantitatively by determining the Fano factor from the distributions and by fitting a gamma distribution to the histograms of the MscL monomers at the single-cell level (Figure 4.11, Table D.1). The gamma distribution is derived from a model which assumes the follwing: the mRNA expression level is determined by a single-state, unregulated promoter; the proteins are expressed

in translational bursts from a single copy of mRNA; the number of proteins per burst event is described by an exponential distribution; and the translation events are uncorrelated in time. This model represents our results well for low stress conditions (exponential phase, media without supplemented salt), however, it does not provide a good fit for the measured values in the stationary phase (regulation by RpoS) and in the presence of salt (osmotic induction). We conclude that the induction of the MscL expression is not described well by this simple biophysical model.

The work presented here illustrates the changes in the number of MscL channels per cell depending on the culturing conditions. It does not, however, fully explain the consequences of these changes for cell physiology. As noted before, the number of MscL channels can impact the gating barrier (Figure 4.2). Previously published work has predicted that at sufficiently high protein areal-densities, channels can demonstrate cooperative gating [121]. According to this model, for our measured values, $10^2$ to $10^3$ channels per mm$^2$, the probability of two channels opening at the same time can be equal to or even greater than the probability of one channel opening as the applied tension is increased to values approaching $\tau_{1/2}$ (tension at which channels are open half of the time). The high number of channels may impact not only the gating tension, but also protect the membrane from rupture by adding an extra area to the membrane through the expansion of non-conductive MscL proteins [173] or by increased transport of water and/or osmolytes through open channels [174, 175].

If it is true that a large number of channels leads to higher survival rates, it would be interesting to speculate on how the variability of the cell-to-cell MscL distributions increase substantially with stress (Figure 4.11). It is possible that the increased variability is a survival strategy of the population. The majority of cells would not be required to change their expression profile as a preparation for a potential change in osmotic conditions. In a population of cells there would always be a small percentage of cells in the highest expressing region of the distribution, guaranteeing survival of at least a few cells.

# Chapter 5

# Minimal number of channels needed for survival

## 5.1 Number and variety paradox

As described in chapter 4, we used fluorescence microscopy and quantitative Western blots to perform a counting of MscL channels (in bulk and at the single-cell level). Our measurement results are much larger than those previously published (Table 4.1). This discrepancy raises a question about the source of this more than an order of magnitude difference. Part of the explanation might be the technique used in the previous measurement – electrophysiology (details described in section 4.1). However, the difference in our and previously reported results is so large that it is doubtful it could be explained only on the basis of the imperfection of the technique. This may suggest that only a small fraction of the total number of MscL channels can be activated at the same time. If this is indeed the case, one may wonder why *E. coli* produces so many more copies of the MscL channel. One should also remember that MscL is not the only mechanosensitive channel in *E. coli*. The presence of seven different mechanosensitive channels is experimentally proven [101]. Are all of those channels necessary for proper growth of the cell and protection against osmotic shock?

The techniques demonstrated in chapter 4 may provide means of investigating the connection between survivability and channel expression level. One could image

strains showing different expression levels (measured by fluorescence calibration) before an osmotic shock and correlate it with their fate after the recovery time. Such a measurement would determine, at single-cell resolution, whether the enhanced mean number of channels affects survivability. If survival rates turn out to be weakly dependent on the number of channels, it begs the question of why there is an apparent excess of channels and what their role in cell physiology is.

## 5.2 Bulk results using $\Delta rpoS$ strain

Mechanosensitive channels in *E. coli* are experimentally proven to provide protection against an osmotic shock [22]. However, their mean number is not constant throughout the population growth from exponential to stationary phase, and strongly depends on the culturing conditions [116, 149]. The increase in the mean number of channels upon entry into stationary phase or due to the growth in a high osmolarity medium was interpreted as a preparation for the potential osmotic shock and an additional control against increased stress on the cell envelope in the stationary phase [149]. The basal expression level (exponential phase) of MscS channels was reported as insufficient to provide the required protection against moderate changes in the medium osmolarity [149]. These results lead to a conclusion that the larger the number of MS channels in the cell, the higher the chances for survival.

The claim, according to which changes in the expression level are necessary to modulate the cell's chance for survival, should be reflected in the result of the osmotic challenge experiment. Specifically, cells surviving the shock are expected to have a higher mean number of channels compared to cells which died as a result of a change in medium osmolarity. This assumption can be tested experimentally using strain MJF612 (ΔmscL ΔmscS ΔmscK ΔybdG) with MscL-sfGFP fusion integrated into the chromosome. The absence of MscS, MscK, and YbdG channels guarantees that surviving the osmotic shock will depend mainly on the MscL channels, which can be counted thanks to the presence of a fluorescent reporter (for the counting method see chapter 4). The cells exposed to 0.5 M NaCl shock were divided into

two categories: cells that survived this osmotic challenge and cells that died due to osmolarity change. The fluorescence signal, which can be translated into the number of MscL channels, of each cell was measured and the histogram was constructed for both groups of cells (Figure 5.1).

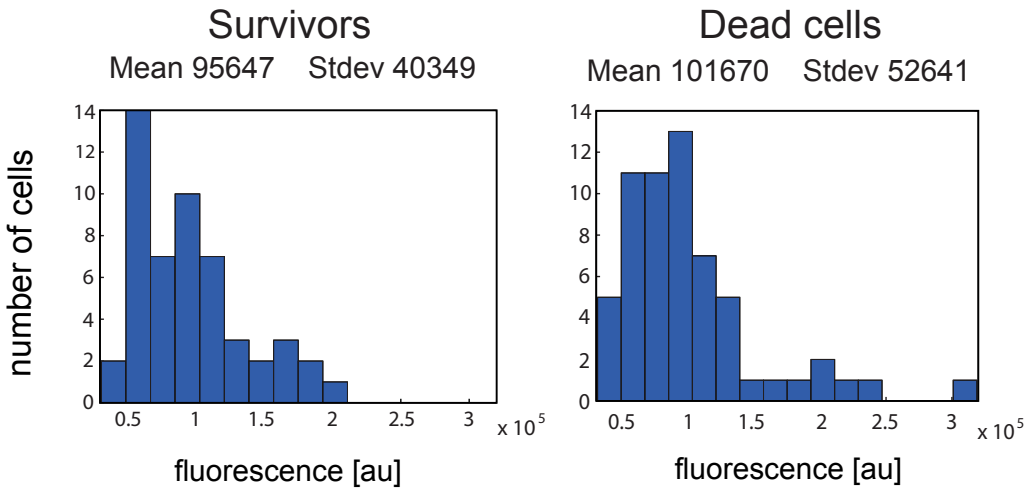


Figure 5.1: Comparison of the MscL expression level between cells that survived and died due to osmotic challenge. Strain MJF612 expressing chromosomally integrated MscL-sfGFP fusion was exposed to a 0.5 M NaCl osmotic shock. The level of MscL channels expression in "survivors" and "dead" cells was measured in arbitrary units as an intensity of the fluorescence. The comparison of the mean fluorescence value (based on histograms) for these two groups of cells does not reveal any significant differences.

Surprisingly, the mean fluorescence level (arbitrary units) for cells in both groups, survivors and dead cells, is very similar. This measurement indicates that, on average, there is no significant difference in the number of expressed channels between survivors and cells that did not survive the shock, at least at the native expression level. The lack of a clear difference in the number of expressed channels between survivors and dead cells puts in doubt the hypothesis of channel up-regulation in order to ensure protection against a potential shock.

Since the difference in the mean number of channels is distinguishable at the native expression level between cells that survive the osmotic challenge and the ones that did not, one can ask the question about the minimal number of channels needed for

survival. It was shown experimentally that the expression of MscL depends strongly on the level of RpoS [116, 149], thus, we used Δ*rpoS* and Δ*mscL* Δ*rpoS* strains to test whether the survival level will be affected by varying the mean number of MscL channels in the strains under examination. Surprisingly, there was no significant difference in the 0.5 M NaCl shock survival between wild-type and Δ*rpoS* strain (Figure 5.2). However, when both the *mscL* and *rpoS* genes are deleted the survival level drops significantly. These results show that lowering the number of channels by an order of magnitude (the mean expression level in wild-type strain is 300 channels, while the mean expression level in Δ*rpoS* strain is 30 [116]) does not seem to influence the cells' ability to survive an osmotic shock. However, the deletion of the *mscL* gene (in addition to *rpoS* deletion) does affect cell survival. This means that the cell needs less than 30 channels for the protection against an osmotic shock and that this critical number of channels is much lower than the native expression level.

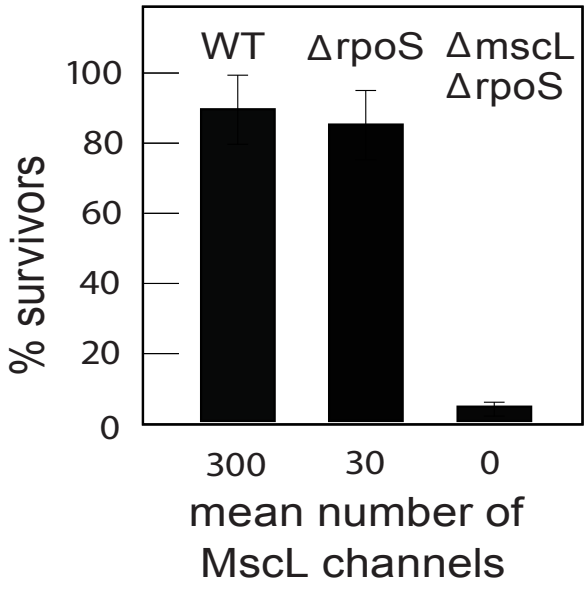


Figure 5.2: Comparison of survival rate as a function of mean number of MscL channels. Strains MG1655 (wild-type, WT), ΔrpoS, and ΔmscL ΔrpoS were exposed to 0.5 M NaCl osmotic shock. Their survival rate was calculated based on the number of cells that were dividing after the recovery phase, normalized by the total number of cells exposed to osmotic challenge.

These results are very interesting and disturbing at the same time if one compares

the native expression level and the critical number of channels needed for protection. However, one should remember that $\Delta rpoS$ strain is not the optimal strain for this type of measurement (for the reasons mentioned below) and further, more detailed analysis is necessary.

As described earlier, RpoS expression may be triggered by various stresses and it regulates the expression of multiple genes in order to prevent potential damage rather than to fix the existing one. In *E. coli*, *rpoS*-dependent genes can be found all over the chromosome [176]. Their function ranges from the DNA repair, protein synthesis, and transport, to the regulation of cell metabolism. The measurements, based on DNA microarray and RT-PCR at the exponential and early stationary phase of growth, show that in the $\Delta rpoS$ mutant 425 genes are down-regulated significantly in the early stationary phase (72 of those are down-regulated in the exponential phase as well) and 208 genes are up-regulated (25 of those are up-regulated in the exponential phase as well) (Figure 5.3). The highest number of up-regulated genes belongs to the transport proteins. The deletion of *rpoS* gene may affect the properties of the cell envelope. The level of RpoS influences the enzymes of fatty acid biosynthesis and phospholipid biosynthesis, enzymes involved in fatty acid degradation, and enzymes modulating the structure of the peptidoglycan layer [176, 177, 178]. The experimental results indicate that $\Delta rpoS$ mutant is less resistant to ampicilin, which may indicate that the cell wall is weaker in the presence of this deletion [179].

## 5.3 RBS modification

The experimental result suggesting that the critical number of MscL channels needed for survival is lower than 30 was obtained with $\Delta rpoS$ strain. In order to avoid potential artifacts introduced by *rpoS* deletion and to control the MscL expression level more quantitatively, a more sophisticated method is necessary. To lower the translation one can change the promoter structure or modify the ribosomal binding site.

A promoter is a region of DNA that initiates transcription of a particular gene.

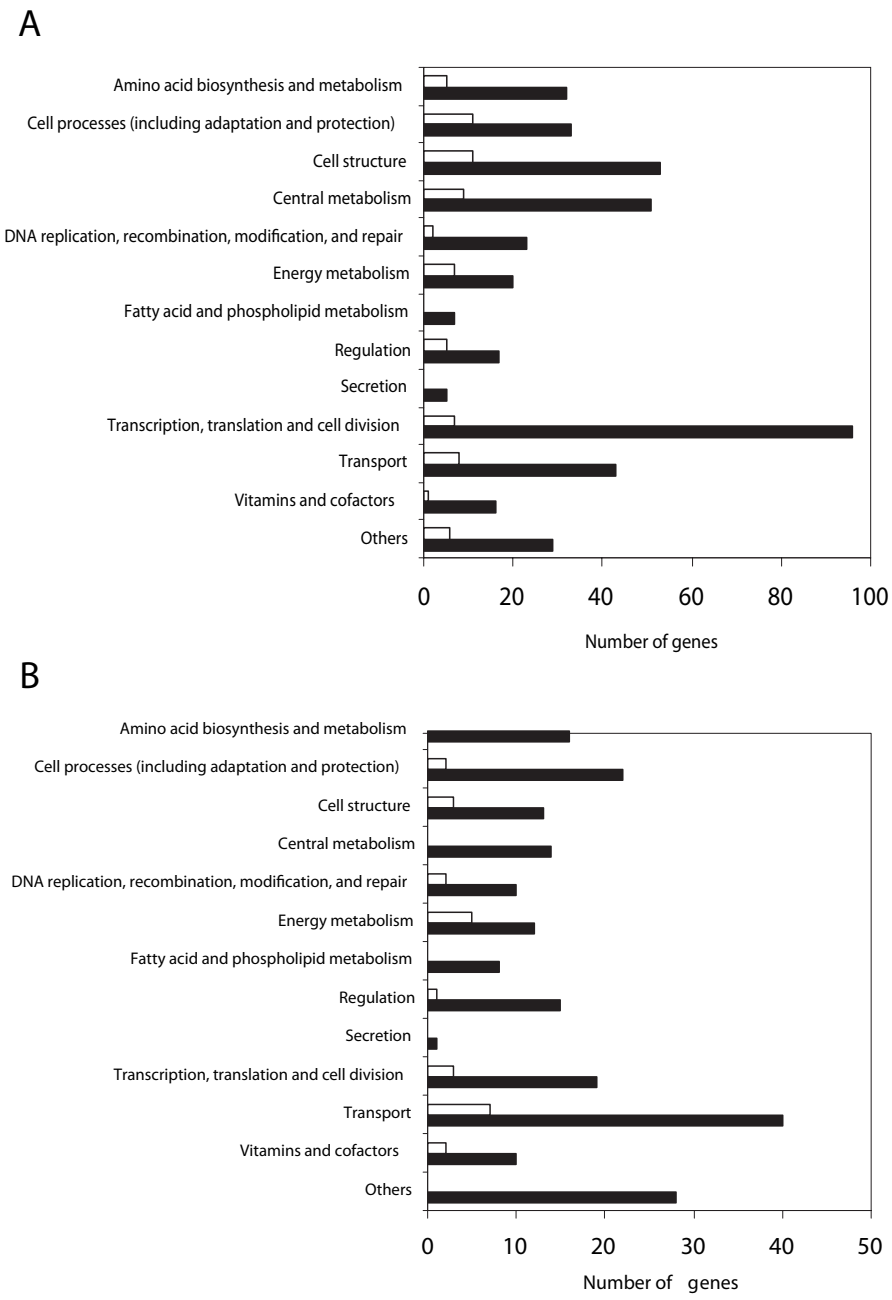


Figure 5.3: Classification and number of genes affected by *rpoS* deletion. Black bars indicate number of genes affected at the early stationary phase, white bars indicate number of genes affected at both late exponential and early stationary phase. Results obtained based on DNA microarray data. (A) Number of genes that were down-regulated by a factor of $< 0.5$; (B) Number of genes that were up-regulated by a factor of $> 2$. Figure adapted from [176].

It is located upstream of the gene it controls. The promoter is a specific DNA sequence that can be easily recognized by the RNA polymerase. At the same time, the promoter sequence can be recognized by proteins called transcription factors (activators and repressors), which influence the expression of a given gene. In bacteria, the promoter contains two short sequence elements: -10 nucleotides upstream from the transcription start site (consensus (most frequent residues) sequence TATAAT) and -35 nucleotides upstream from the transcription start site (consensus sequence TTGACA). However, these sequences are not found in most of the promoters and, on average, only three to four of the six base pairs are found. However, in case of the *mscL* gene not much is known about its promoter sequence or transcription factors [180]. The position of the promoter is predicted to be 23 base pairs upstream of the *mscL* gene [181].

A ribosomal binding site (RBS) is a sequence on mRNA recognized by the ribosome when it binds to mRNA in order to initiate protein translation. It is usually located about six to seven nucleotides upstream of the start codon and is called the Shine–Dalgarno (SD) sequence (consensus sequence AGGAGG) [182]. To reduce expression by modifying the translation efficiency, one can change the Shine–Dalgarno sequence and/or add a spacer between the RBS and the coding region. In general, ribosome binding sites similar to the Shine–Dalgarno sequence will result in high rates of translation and sequences very different from the Shine–Dalgarno sequence will result in low translation rates [183]. The insertion of the spacer between the RBS and the start codon changes the RBS strength (the binding affinity) by limiting the accessibility of the RBS to the ribosome. This can be achieved by using a spacer which, after transcription, will form RNA secondary structure [184]. The translation rates can be predicted based on the mRNA sequence using RBS calculators [185] (Figure 5.4).

Through the replacement of the native spacer with poly-A, poly-AC, or poly-AT spacers of various lengths, one can modulate the translation rate. Based on the prediction, insertion of AT repeats allows an exploration of the widest range of modu-

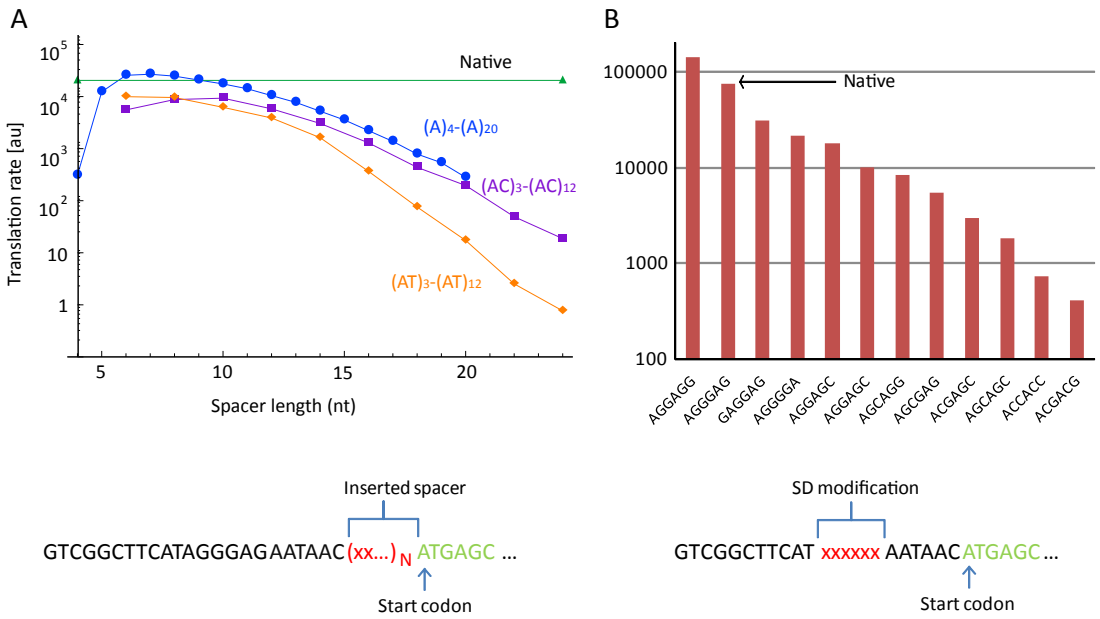


Figure 5.4: Predicted translation rates for MscL after RBS modification. (A) Spacer modification by embedding mono- ((A)n) or dinucleotide ((AC)n, (AT)n) simple sequence repeats (SSR), where $n$ is the number of repeats of a single or a pair of nucleotides; (B) Shine-Dalgarno (SD) sequence modification. The predictions were generated using the RBS calculator [186].

lated expression levels (Figure 5.4 A). We generated a library of plasmids with various spacer lengths. We embedded the dinucleotide simple sequence repeats (AT)$n$, where $n$ is the number of repeats of a pair of nucleotides, between the native Shine-Dalgarno sequence and the constitutive promoter of the *mscL* gene with fluorescent protein fusion (sfGFP). The protein expression is predicted to decrease with increasing spacer length. However, the degree of the decrease has to be experimentally verified. The work of Rob Egbert and Eric Klavins [187] found that the influence of the spacer length on the expression level can agree well with the prediction. However, the rate at which the translation decreases depends on the composition of nucleotides used to create the spacer and may be sensitive to the background strain (host). Moreover, the authors noticed that the stability of the inserted SSRs may vary depending on the length and type of the spacer. The reported mutation rate is $10^{-5}$ – $10^{-4}$ insertions/deletions per base pair per generation. The instability of the spacer may be a

very disadvantageous feature of this method and should be controlled experimentally for a given set of constructs. However, this potential flaw can be used as a powerful tool to study the evolution of the system. Since the insertion of the spacer influences significantly the level of gene expression, the host organism is expected to focus mutations on this element in order to optimize the performance and enhance the functionality of the gene of interest. Tandem repeats are known to play an important role in the occurrence of some diseases (e.g., Huntington disease) and contribute to the phenotypic variability facilitating organism evolvability [188]. Some bacteria use these repeats within the reading frame or in the promoter of a given gene(s) to modulate their interaction with the host by enhancing fitness [189]. Using this strategy in the case of mechanosensitive channels would allow us to study the evolution of a given strain depending on the environmental conditions and selection for an optimal mean number of MS channels expressed. It could also help us answer the question regarding the amount of selection existing in a given environment, e.g., in a high osmolarity medium. To correlate the level of expression with the fitness of a given strain, two previously described methods will be used: counting of the number of protein copies (chapter 4) and single-cell survivability tests (chapter 3).

# Chapter 6

# Hypothesis of an alternative function of MS channels

## 6.1 Overexpression of one type of MS channel guarantees survival

From the moment of their discovery, mechanosensitive channels were proposed to provide protection from osmotic shock [92]. The experimental assay demonstrating their function in cell physiology showed that the presence of MscL or MscS channels, can provide enough protection against a 0.5 M NaCl shock for the cell to survive at the level comparable to that of a wild-type [22]. This result suggests that the other channels contribute very little (if at all) to cell survival and raised a question about the redundancy of the MS channels, especially after the experimental demonstration that *E. coli* possesses seven different channels [101]. The situation got even more intriguing after the discovery that overexpression of any of the channels in *E. coli* (even in the absence of other channels) leads to a very high survival [100, 101] (Figure 6.1).

Not only the variety, but also the number of channels of one type raises some doubts that osmoprotection is the only function of these channels. The quantitative counting of the number of MscL channels expressed per cell [116] revealed that there is at least an order of magnitude more channels than previously estimated (Table 4.1) and it can change depending on the growth conditions. From previous work it is known that MscL is not the most abundant channel in *E. coli* [149]. Such a high

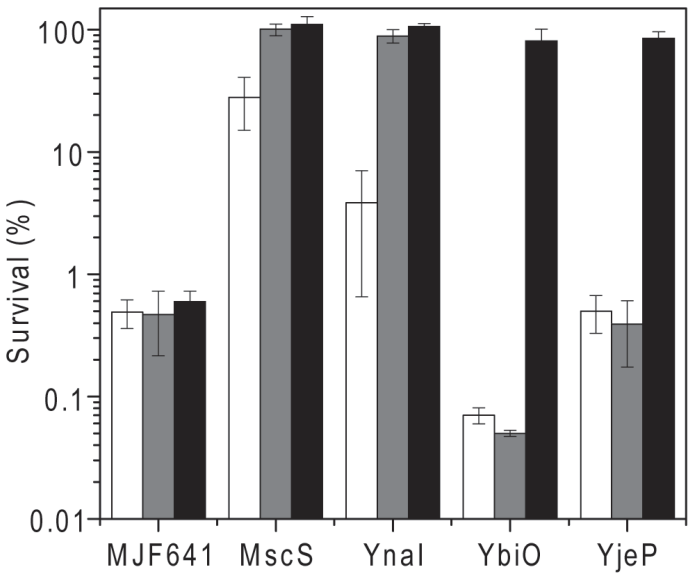


Figure 6.1: Protection of various MscS homologs against osmotic shock. The proteins were expressed in MJF641 strain (all seven channels deleted) from a plasmid induced by IPTG: basal expression level (white bars), 0.3 mM IPTG for 30 min (gray bars) and 0.3 mM IPTG for 2.5h (black bars). Adapted from [101].

abundance of channels is very surprising, especially in comparison to the results of MD simulations, suggesting that a single MscL channel provides enough protection [86]. In addition, the survival rate turns out to be weakly dependent on the number of channels (Figure 5.2), which suggests that there is over-abundance in the type and number of channels not contributing to a better osmoprotection. All of these facts suggest that *E. coli* may not need all of these channels solely for protection against osmotic shock, and the apparent excess of channels (and their upregulation under stress conditions) serves other purposes. If this is indeed the case, what other role could these channels have?

## 6.2 Experimental hints at an alternative function of MS channels

Homologs of MS channels have been identified across all kingdoms of life [12]. The activities of channels responding to tension were discovered in the membranes of various cell types in many plant species. It was proposed that they play a role in sensing gravity, touch, and temperature, as well as controlling the turgor (which is important for cell growth, movement (e.g., guard cells), structure and shape of cells) and the localized gradient of $Ca^{2+}$ ions required for pollen tubes and root hairs growth [190]. However, the best characterized is the family of 10 MSL channels in *Arabidopsis thaliana* (Figure 6.2).

The double deletion mutants, *msl2-1; msl3-1*, and *msl9-1; msl10-1*, show clear phenotypic changes. However, the physiological role of MSL9 and MSL10, localized in the plasma membrane of root cells, remains unknown [14, 191]. MSL2 and MSL3, localized in the plastid envelope, control organelle morphology. The double deletion mutant *msl2-1; msl3-1* has enlarged and abnormally shaped leaf epidermal plastids [13]. These small plastids, in contrast to plastids in leaf mesophyll responsible for photosynthesis, import energy from the cytoplasm needed for several metabolic reactions, e.g., synthesis of amino acids and fatty acids, storage of lipids and pigment molecules [192]. The presence of this phenotype under normal growth conditions leads to the conclusion that plastids are under hypoosmotic stress, and MSL2 and MSL3 channels are necessary to release this stress. This phenotype can be suppressed by growth in high osmolarity conditions or when subjected to hyperosmotic shock [193]. In addition, MSL2 and MSL3 may be components of the chloroplast division machinery [194, 195]. They colocalize with MinE, the protein responsible for restricting the division site to the middle of the cell, at the poles of plastids. When both MSL2 and MSL3 are deleted, chloroplasts have multiple Filamentous temperature sensitive Z (FtsZ) rings. A similar phenotype can be observed in the MJF465 ($\Delta mscL$ $\Delta mscS$ $\Delta mscK$) *E. coli* strain treated with cephalexin [194]. Surprisingly, the MSL8 mutant

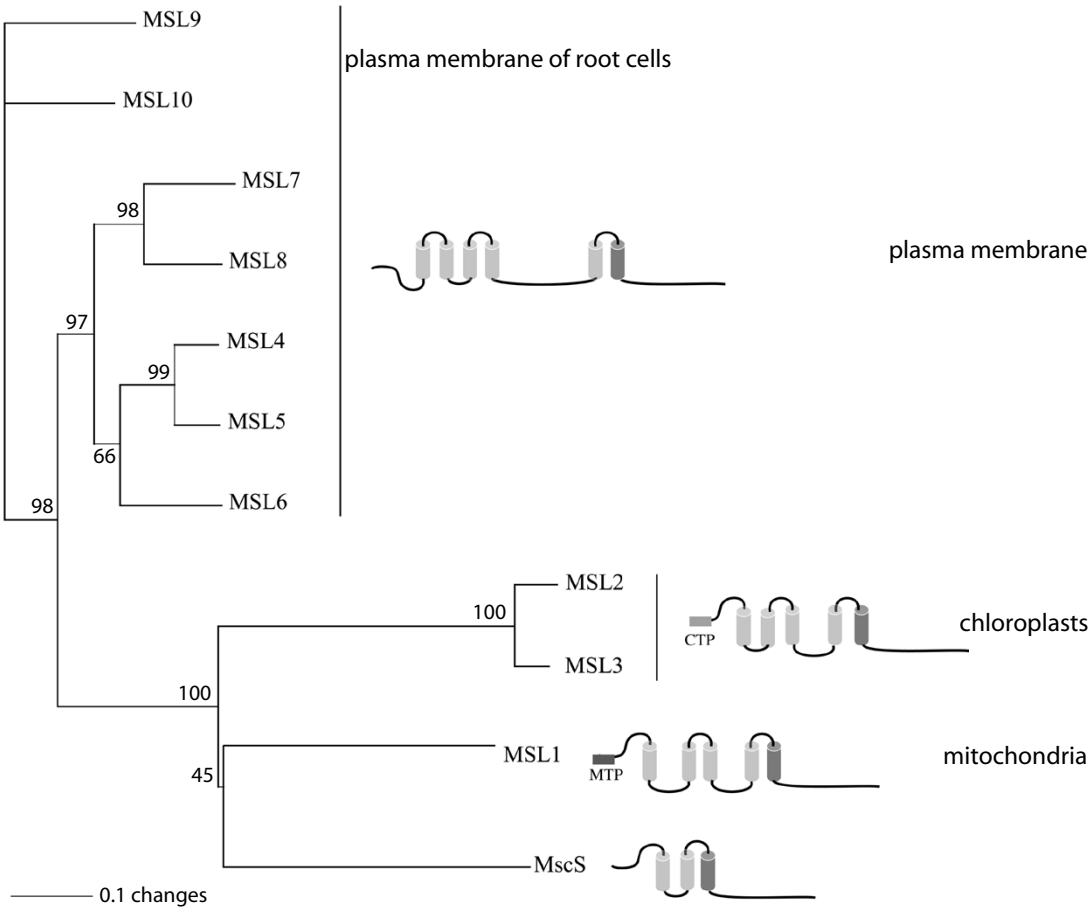


Figure 6.2: Phylogenetic tree of the MscS-like (MSL) channels in *Arabidopsis thaliana* with predicted topologies. Members of this family can be found in a variety of structures in the plant: mitochondria (MSL1), chloroplasts (MSL2 and MSL3), plasma membrane (MSL4 - MSL8), and plasma membrane of root cells (MSL9 and MSl10). MTP, mitochondrial transit sequence; CTP, chloroplast transit sequence. Figure adapted from [190].

showed a significantly higher level or germination when compared to wild-type, and also many "burst" pollen, suggesting that it may play a role in proper germination [196]. When tested in *Bacillus subtilis*, mechanosensitive channels did not show any significant role in the sporulation or germination of spores [197, 198, 199].

MscL and MscS homologs in freshwater cyanobacterium *Synechocystis* sp. PCC 6803 also have alternative functions. PamA, a homolog of MscS [200], was proven experimentally to interact with the PII protein [201]. This protein is known to play

a role in the coordination of carbon and nitrogen metabolism. In addition, the *pamA* deletion mutant is unable to grow in a medium containing glucose. This suggest that the MscS homolog PamA plays a role in controlling cell metabolism. Comparison of $Ca^{2+}$ release between wild-type and *mscL* deletion mutant revealed that the rate of calcium efflux is much slower in the mutant and, in contrast to wild-type, temperature independent [202]. These results suggest that MscL may play a role in $Ca^{2+}$ homeostasis regulation under temperature stress conditions and that it can be activated by different stress factors (depolarization of the plasma membrane and temperature).

Some of the MscS homologs, in contrast to *E. coli* non-specific MscS, are believed to transport specific molecular species. BspA, a MscS homolog in *Erwinia chrysanthemi*, is believed to be necessary for the accumulation of glycine betaine. It may sense the intracellular glycine betaine concentration and the osmolarity of the growth medium. Mutants with *bspA* gene deleted grow poorly in high salt media, especially in the presence of glycine betaine or its analogues. However, there is no experimental evidence that BspA shows a mechanosensitive channel activity [203]. Another example is MscCG protein of *Corynebacterium glutamicum*. It has been experimentally tested that this channel mediates glutamate efflux in response to an hypoosmotic shock or a penicillin treatment. It is hypothesized to play a role in osmoregulation by controlling the concentration of compatible solutes [204, 205].

There is no experimental proof of MS channels in *E. coli* having any additional functions. However, there are indirect data suggesting that they may play a role in various processes other than osmoprotection. Nichols *et al.* [206] reported results of a high-throughput fitness measurement. More than 4000 single gene deletion mutants were profiled in more than 300 physiologically relevant stresses and drug challenges. Quantitative growth scores were assigned to each strain under a given condition based on the growth profile. Mutant strains were grown on agar plates in the presence of chemical/stress and the size of a colony was measured for every strain under all stress conditions. This strategy allows the linkage of the deleted gene with a phenotype and the study of the gene function in a given stress environment. Around 80% of

the phenotypes had negative score (cells are more sensitive to a given stress or drug after the deletion of a gene), around 20% were positive (deletion of a gene led to a higher resistance to a given stimulus). This strategy has more advantages than assigning gene function only on the basis of homology to known genes. Some of the genes, despite being homologous to previously studied ones, may have some specialized functions that can be revealed only under specific circumstances, e.g., only when the cell is exposed to a particular stress. Moreover, based on the response to a given set of conditions, one can find a correlation between phenotypes resulting from deletion of different genes. Such a correlation may indicate a functional connection between genes.

The search in this database for single MS channels deletion mutants revealed a few interesting hints concerning potential additional functions these channels may have in cell physiology. The first surprise comes from the comparison of the reaction of three different strains ($\Delta mscL$, $\Delta mscS$, and $\Delta ybdG$) to a few chosen conditions (Figure 6.3). If the only function of MS channels in *E. coli* is protection from osmotic shock, one would expect them to react in a similar way to all other stresses. However, this is not the case. Not only do these three mutants react differently to a given stimulus (e.g., EGTA), but also a given strain reacts in a very different way to various stresses (e.g., the deletion of the *ybdG* gene is advantageous in the case of growth in the presence of EGTA, but is disadvantageous in the case of growth in the presence of cholate).

The comparison of the reaction of a single MS gene deletion mutant across all applied stresses also reveals some interesting trends. The deletion of the *mscL* gene causes moderate changes in growth. However, one can notice a gentle increase in the growth rate in the presence of chemicals causing DNA (phenazine methosulfate (PMS), mitomycin C, and cisplatin) and membrane damage (SDS, EDTA, and bile salts). As for the decrease in the growth rate in the case of *mscL* gene deletion, there is no apparent trend, but, interestingly, the deletion of this gene causes disadvantage when the cells are grown in the presence of maltose as a carbon source. This result may

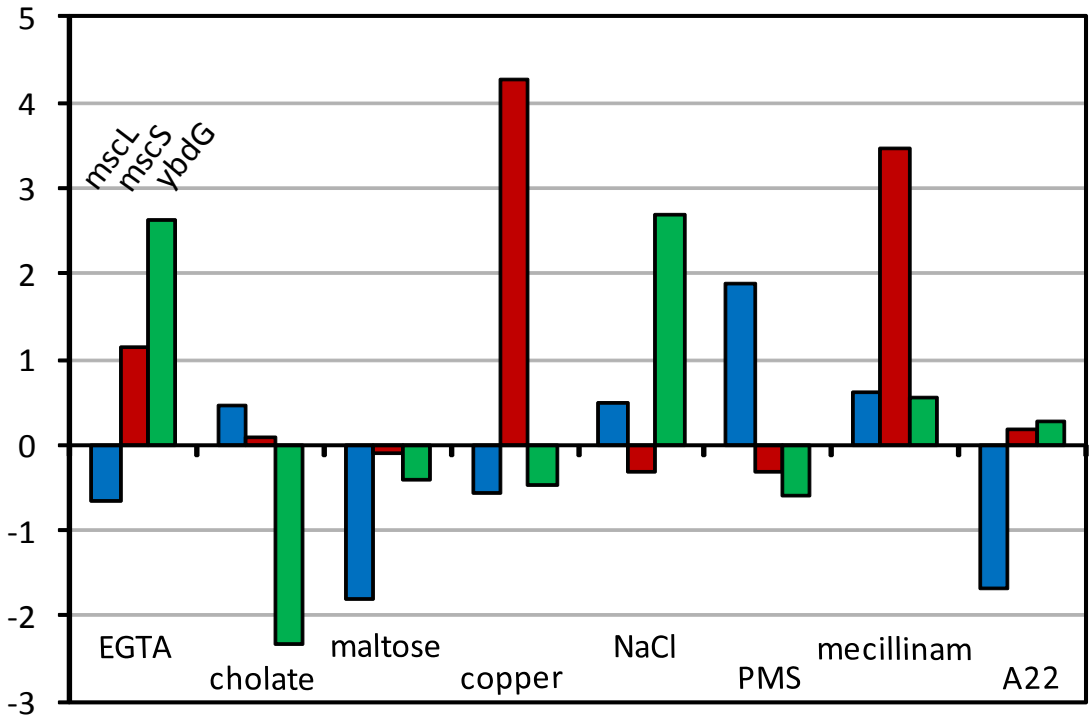


Figure 6.3: Growth profile of strains with *mscL*, *mscS*, or *ybdG* single gene deletion exposed to various stresses. The positive value indicates the growth advantage for a given condition gained after the deletion of the gene, the negative value means the growth impairment in a given condition due to gene deletion. Conditions: EGTA at 0.1 mM, cholate at 2%, maltose at 0.1%, copper at 2 mM, NaCl at 600 mM, phenazine methosulfate (PMS) at 0.02 mM, mecillinam at 0.03 $\mu$g/ml, and A22 at 0.5 $\mu$g/ml. Figure made based on [206].

suggest that MscL channels play a role in carbon metabolism or maltose transport. The effect of *mscS* gene deletion is much more noticeable. This strain grows fastest in the presence of copper chloride, suggesting that in the wild-type cells this metal may poison the cell by being transported through the MscS channel. Also, the presence of chemicals disrupting the integrity of the peptidoglycan layer (mecillinam, ampicillin, tunicamycin, and amoxicillin) seems to be beneficial for the growth of this strain. The decrease in the growth rate is noticeable in the presence of chemicals interfering with the protein synthesis (chloramphenicol, clarythromycin, and tetracycline). The deletion of the *ybdG* gene does not seem to have a clear advantageous trend, but the presence of chemicals causing the disruption of the membrane (cholate, cecropin B, and SDS + EDTA) has a negative impact on the growth of this strain. The presence of

salt has also a very interesting impact on this strain. Depending on its concentration, the change in growth can be very different: the presence of 600 mM NaCl is beneficial, whereas the presence of 450 mM NaCl results in much slower growth.

# Chapter 7

# Future directions

## 7.1 Monitoring channels' activity *in vivo*

The activity of MS channels is traditionally characterized *in vitro* by electrophysiological measurement of the reconstituted protein or giant spheroplasts. These results provide information on the conductance of the channel, the pressure (which can be used to calculate the tension) needed to activate a given channel, the amount of time it spends in an open configuration as a function of applied stimulus, and the potential inactivation. This method, although very accurate, may not represent accurately the behavior of mechanosensitive channels *in vivo*. In case of the reconstituted protein, the lipid environment is known to influence the gating of the channels [108], potentially leading to a big measurement uncertainty depending on the composition difference between *E. coli*'s lipid membrane and that used for the reconstitution. In both cases, the reconstituted protein and giant spheroplasts, the geometry of the membrane is different than that in a living cell. In addition, the membrane in the living cell is being pushed against the peptidoglycan layer, which may also modulate the tension the channels sense. For all of these reasons we designed an experiment which may allow us to study the channel activity *in vivo*, in intact cells, with a high level of accuracy thanks to the merging of a few techniques, with calcium-sensitive proteins used as an indicator of cell physiological state.

### 7.1.1 What are calcium-sensitive proteins?

Fluorescent proteins revolutionized biological and biophysical measurements. They made it possible to tag the protein of interest and observe its localization as well as interactions with other structures. They can also be used for studying gene expression regulation by counting the number of protein/RNA copies in a cell under given conditions. A whole variety of fluorescent proteins is available for experimental use nowadays. They differ in the emission spectrum, brightness, maturation time, and size [207]. One class of special interest is composed of fluorescent proteins used in visualizing the signaling activity in a cell. One example of such proteins are calcium-sensitive proteins. These proteins change the intensity of their fluorescence in response to variations in the calcium ion ($Ca^{2+}$) concentration. Zhao *et al.* [208] engineered a whole family of these proteins (blue, green, red, and ratiometric version, which is excited and emits at different wavelengths depending on whether it has $Ca^{2+}$ ions bound). These proteins are engineered using a few major building blocks: circularly permuted (cp) GFP fused to the calmodulin-binding region of myosin light chain kinase (M13) at the N terminus, and a calmodulin (CaM) at the C terminus (Figure 7.1). Binding of the $Ca^{2+}$ ion by CaM causes conformational change and interaction between M13 and CaM, leading to an increase in fluorescence signal.

### 7.1.2 Preliminary results

The number of channels expressed in the cell is much higher than the the critical number needed for survival (chapter 5). As reported earlier [120], not all of the channels have to be activated during the pressure (tension) change and this number depends on the kinetics and amplitude of the stimulus. These facts raise one of the most intriguing questions about the role of MS channels in cell physiology: how many and which types of channels open in response to physiologically relevant osmotic shock? We believe that the experiment proposed here can be of great help in addressing this question.

Cells expressing fluorescently tagged mechanosensitive channels will be imaged in

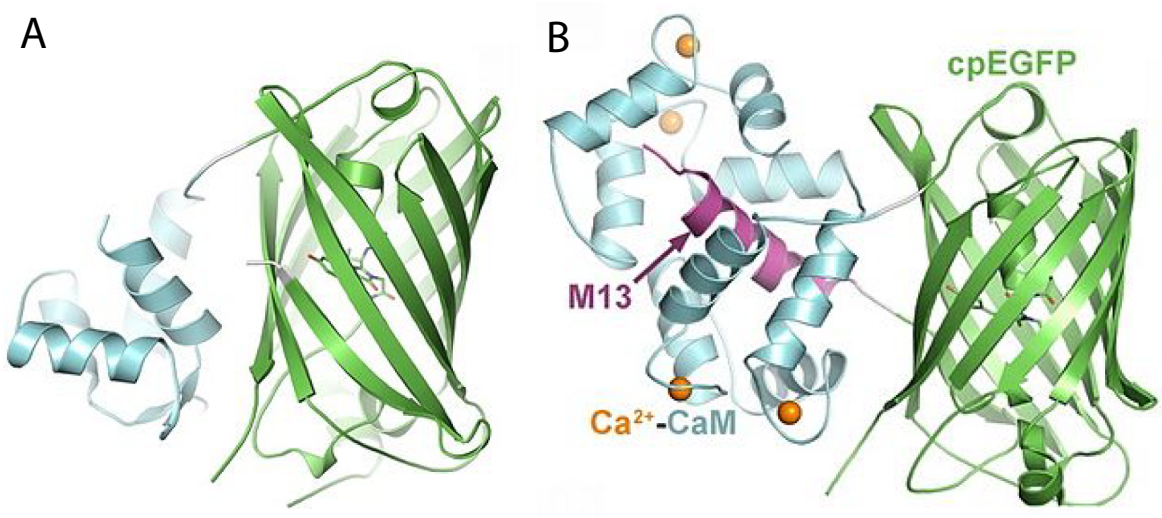


Figure 7.1: A schematic representation of the crystal structure of calcium-sensitive fluorescent protein in "dark" (A) and "bright" (B) state. (A) In the absence of calcium the protein is in the "dark" state; (B) binding $Ca^{2+}$ ions causes CaM (acting as a claw) to bind to M13 (acting as a handle), leading to closure of the structure and increase in fluorescence. CaM: calmodulin, M13: CaM binding region of myosin light chain kinase. Figure adapted from [209].

the flow cell described previously (chapter 3). The fluorescent tag allows us to quantitatively count the number of copies of a given type of channel on a single-cell basis, as discussed in [116] and chapter 4. Performing the experiment in the flow cell allows us to quantitatively calibrate the rate of medium exchange (chapter 3) and measure cell response to varying conditions. Longer imaging (2 – 3 hours) provides information on the number of cells which survived the shock. This can be later correlated with the number of channels which opened during the medium exchange. The presence of a calcium-sensitive fluorescent protein and the use of media with varying calcium concentration allows us to measure the amount of transport that occurs under a given stimulus.

As mentioned earlier, the intensity of the fluorescent signal of calcium-sensitive proteins depends on the calcium ion concentration. In order to measure the amount of mass transfer through the channels during osmotic challenge, one has to correlate the fluorescent protein brightness with the concentration of calcium inside the cell. Such

a calibration can be performed quantitatively with calcium titration buffers [210]. These buffers are prepared by mixing solutions containing EGTA and $Ca^{2+}$ ions in various proportions. As a result, EGTA chelates $Ca^{2+}$ ions and the concentration of free $Ca^{2+}$ is calculated based on the dissociation of the complex. The dissociation constant for the EGTA-$Ca^{2+}$ complex is in the nM to $\mu$M range, which is exactly the physiological range of concentration. The concentration of calcium in the complex medium was measured to be 15 – 30 $\mu$M [211]. The total and the free calcium concentration in *E. coli* was measured to be 0.013 – 1.390 mM and 0.094 – 0.12 $\mu$M, respectively [212]. The calibration curve correlating the fluorescence intensity with the cytosolic calcium concentration can be obtained by measuring the fluorescence signal intensity of the protein in the cell cytoplasm as a function of free $Ca^{2+}$ concentration of the external buffer (Figure 7.2). The fluorescence intensity loss is an effect of the activity of the efflux pump system and can be inhibited by, e.g., carbonyl cyanide m-chlorophenylhydrazone [213].

In summary, knowing the number of each type of MS channels expressed by the strain used in the experiment and its conductance $C$ from electrophysiological measurement [101], as well as the amount of mass transport during osmotic shock (measured as the change in the cytosolic $Ca^{2+}$ concentration $\Delta[Ca^{2+}]$), one can estimate the number of open channels $N_{open}$ as:

$$N_{open} = \frac{\Delta[Ca^{2+}]}{\sum N_x \times C_x}, \tag{7.1}$$

where $x$ denotes the type of MS channels present in the strain used for the measurement. Performing the measurement for strains expressing various combinations of mechanosensitive channels one can count the number of channels, measure when they opened for a given osmotic challenge, and correlate this number with the survival rate.

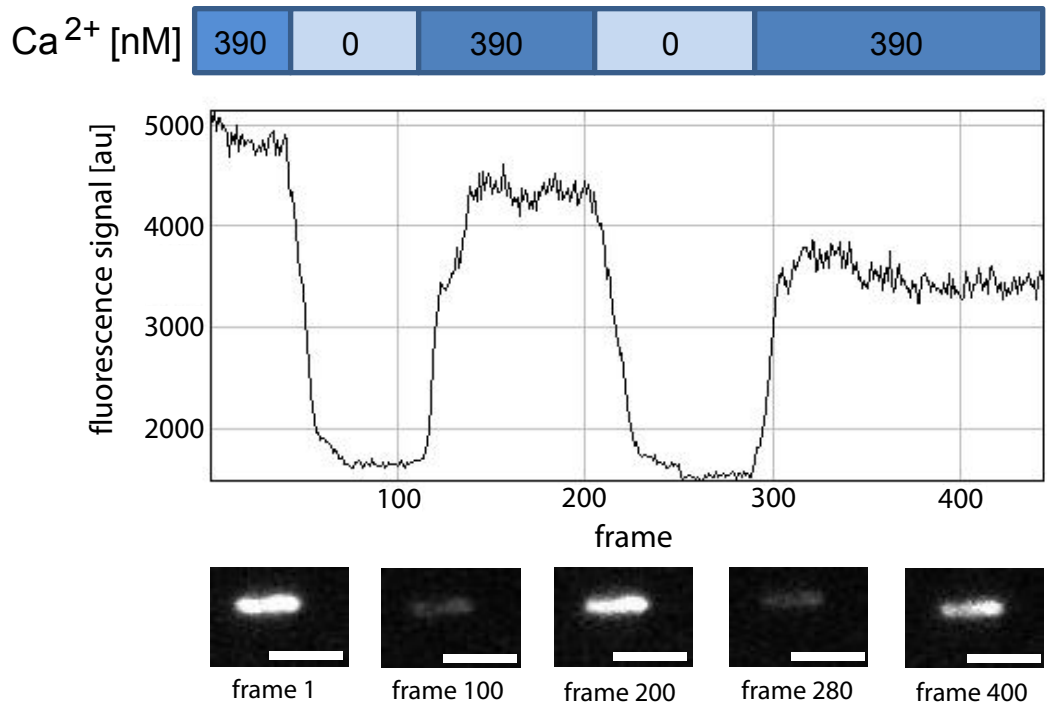


Figure 7.2: Calibration of the response of calcium-sensitive proteins to variations in calcium concentration. Calcium-sensitive proteins inside the permeabilized cells respond to calcium concentration changes (between 0 and 390 nM) by increasing and decreasing the fluorescence signal intensity. The images show the relative fluorescence signal intensities for a cell exposed to cycling changes in $Ca^{2+}$ ion concentration (raw data). Scale bar: 2 $\mu$m.

## 7.2 Volume change measurement

As mentioned earlier, mechanosensitive channels react to changes of the tension in the membrane. Bacteria experience such changes when the osmotic pressure difference between the outside and inside of the cell is fluctuating. The most popular experimental method to study the physiological function of MS channels is the bulk osmotic shock assay. In this assay one studies the osmotic shock survival rate on the basis of the number of cells growing after exposure to osmotic challenge (Figure 2.10).

This method is not very quantitative. It is better suited to study the consequences of the lack of channels rather than their impact on the cell response to a given osmotic shock and the time scale of the reaction. The necessity to plate the cell solution after the shock may introduce a significant error in the measurement

and it certainly masks any stochastic effects which would only be revealed at the single-cell level. The osmolarity difference between the shock medium and the one the plate was prepared from may introduce an additional shock for the cell. On the other hand, if the plate and the shock medium are of the same osmolarity, the results are hard to compare between the shocked sample (grown in a 0.5 M NaCl medium, diluted into 0 M NaCl medium) and the control sample (grown and diluted in a 0.5 M NaCl medium), because the plates of different osmolarities induce a difference in the growth rate of the cells (thus, the recovery time has to be properly adjusted). The number of cells which survived the shock may seem higher due to a possible cryptic growth phenomenon. When a portion of the cells lyses and their content is released, the osmolarity is changed locally, which may influence the chance of survival for the other cells. One can minimize the impact of this phenomenon by a longer incubation period in the shock medium before plating. All of these flaws in the current technique motivate the development of an assay in which the reaction of the cells is directly observed and the osmolarity of the medium is well-controlled.

### 7.2.1 Experimental design

In order to measure the volume change during osmotic challenge, a new single-cell assay was developed as an alternative to the bulk osmotic shock assay. The cells, grown in a high osmolarity medium, are loaded into a flow chamber (described earlier in chapter 3) and immobilized on the cover slip using charged polymer (polyethylene imine, PEI). A well-controlled flow of medium of desired osmolarity (lower salt content in the case of a hypoosmotic shock) exposes the cells in the chamber to different osmotic challenges. The simultaneous recording of cell morphology makes it possible to observe cell swelling as a function of time. This video microscopy data allows for the calculation of volume change during the osmotic shock. The cell volume at a given time point is calculated based on the major and minor axis lengths, area, and perimeter measurements of 2D images (Figure 7.3).

The higher throughput and more complicated (than a single step) sequence of

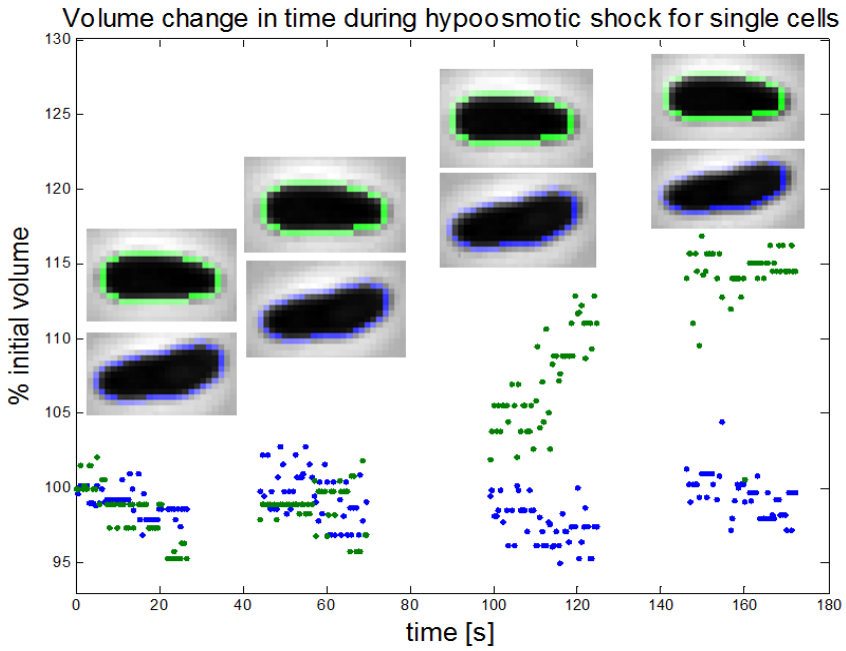


Figure 7.3: The comparison of volume and area change as a function of time for two single cells. The inserts illustrate phase images at discrete time points with an overlayed perimeter measured at $t = 0$. The figure illustrates the importance of a precise image analysis for the interpretation of experimental data. The comparison between the plotted volume change and the area change (inserts) for two single cells illustrates how different the outcome of the experiment may be depending on the data analysis strategy. A 15% volume change indicates an approximately 5% change in one dimension. The major axis of the cell is of the order of 20 pixels, which means that a 5% change is equivalent to 1 pixel. The plotted volume is calculated on the basis of the area, perimeter, major axis length, and minor axis length measurements.

osmolarity changes can be experimentally explored when using an alternative design (Figure 7.4). The chip's architecture allows for a very quick medium exchange in the recording chamber, and, with a computer program controlling the opening and closing of the valves, the exposing of the cell to a wide variety of osmolarities for very short periods of time. Multiple channels and program-controlled flow create a possibility of exposing cells to many different osmotic conditions. The main advantage of this method is the possibility of studying single-cell behavior during an osmotic shock in real time. This design is perfect for addressing questions like "what is the role of MS channels in cell physiology?" and "what is the cell-to-cell response variability upon osmotic shock?".

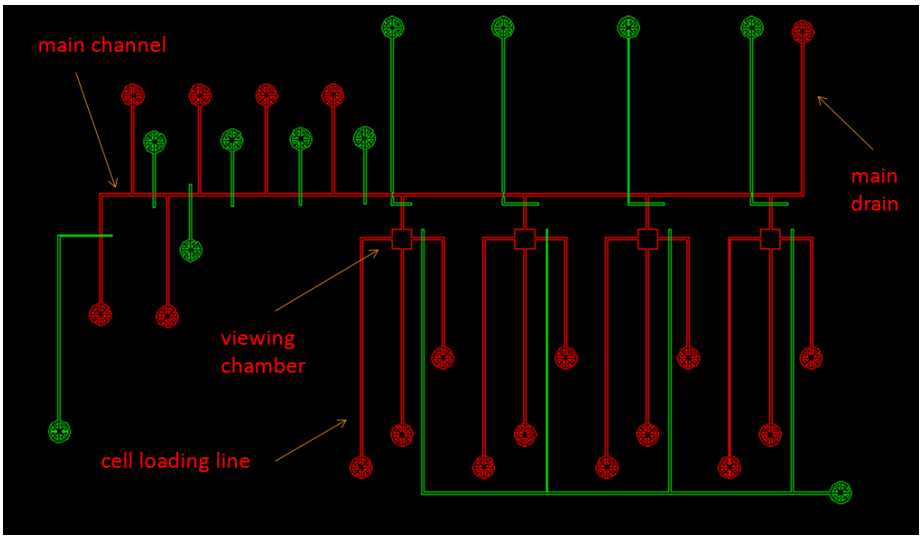


Figure 7.4: Microfluidic chip design showing the main channels (red) and valves (green). The cross structures serve for alignment purposes. A single chip contains four viewing chambers (red squares), each of which is connected with the main channel (the longest red channel) and has a separate line for loading the cells (red channels are connected with the viewing chamber horizontally). Multiple loading lines and valves (left side of the design) allow to perform an osmotic shock with up to five different shock media.

The quantitative measurements of cell volume change as a function of time provide information on the dynamics of cell reaction and the recovery time after the shock. These experiments examine the significance of MS channels in cell physiology when exposed to various and changing stimuli. The comparison of the responses of different strains to an identical osmotic shock makes it possible to investigate the role of various types of MS proteins and measure cell active (opening of MS channels) and passive (flow of water through the membrane) response. The observation of the single-cell reaction to the environmental insult creates the opportunity to compare cell-to-cell variability in a genetically identical population, as well as the differences between various strains. Exposure to changing osmotic conditions provides information on the role and importance of heterogeneity for cell survival. The possibility of growing cells in this experimental setup enables the performance of an observation of the cell recovery time after an osmotic shock. Additionally, the possibility of having a constant flow of the shock medium guarantees that osmolarity is not changed locally.

### 7.2.2 Preliminary results

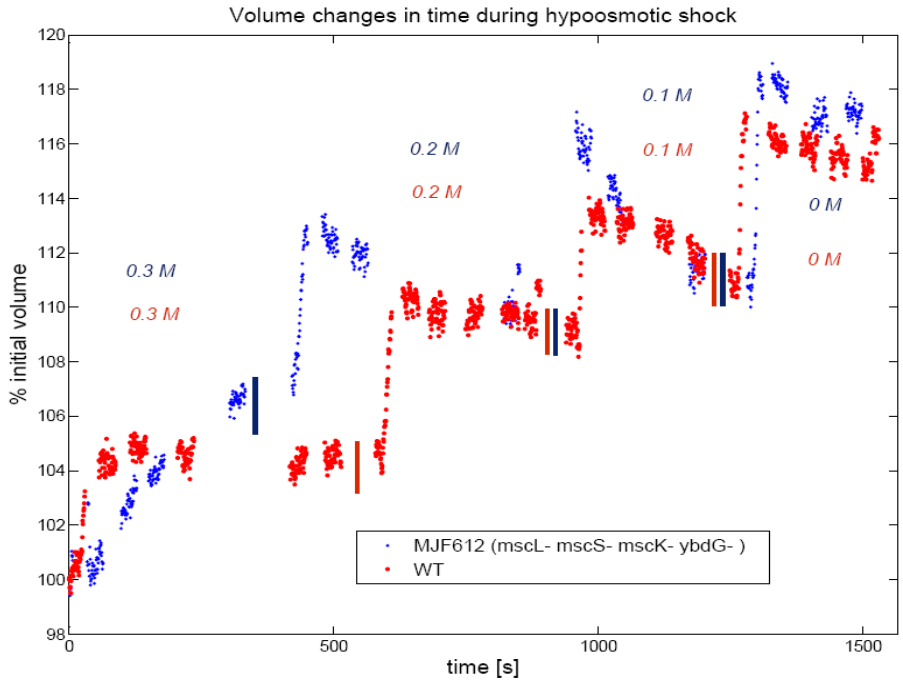


Figure 7.5: Comparison of the volume change between two strains exposed to the same osmotic downshock. Cells were grown in a 0.3 M NaCl medium and downshocked into a 0 M medium in "steps" (every 0.1 M NaCl). Comparison between the MJF612 (*mscL- mscS- mscK- ybdG-*) and wild-type *E. coli*.

As shown in Figure 7.5, wild-type (WT) *E. coli* and the MJF612 mutant $\Delta mscL$ $\Delta mscS$ $\Delta mscK$ $\Delta ybdG$ do not respond to an identical osmotic stimulus in the same way. The increase in volume for the MJF612 strain is larger than the increase for the WT *E. coli*. The character of these changes is also different. WT cells maintain almost constant volume between the increments caused by the osmolarity change. In the case of MJF612 cells the volume does not remain constant; each time it gradually decreases. This comparison may provide information on the cell's "active" response (opening of mechanosensitive channels in WT *E. coli*) and "passive" response (water permeation through the membrane in the $\Delta mscL$ $\Delta mscS$ $\Delta mscK$ $\Delta ybdG$ mutant). As shown in Table 7.1, the final volume may differ depending on the MS channels present in the cell and the cell history (how the shock was performed).

Figure 7.6 shows the volume change as a function of time for four single wild-type

| Strain | Single shock | Shock "in steps" |
|---|---|---|
| WT | 3% | 17% |
| MJF429 (*mscS- mscK-*) | - 3% | 12% |
| MJF465 (*mscL- mscS- mscK-*) | — | 13% |
| MJF612 (*mscL- mscS- mscK- ybdG-*) | 16% | 19% |

Table 7.1: Final volume for four different *E. coli* strains (wild-type, MJF429, MJF465, and MJF612) after exposure to different osmotic shocks (single and multiple steps).

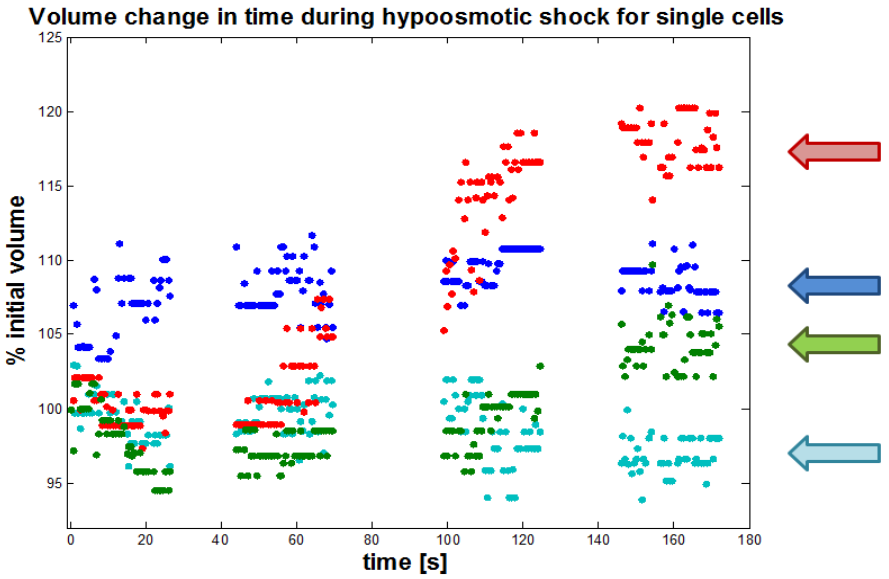


Figure 7.6: Volume change of four wild-type single cells during the osmotic shock at the single-cell level. Cells were grown in a 0.3 M NaCl medium and downshocked into a 0 M medium. Arrows indicate the final volume reached by every cell.

cells under a severe osmotic shock (0.3 M to 0 M medium). The results for single cells differ from each other indicating that genetically identical cells show various reactions to the same stimulus.

It has been shown [214] that when the survivors of a long period of stress are recultured, they exhibit an identical distribution of physiological variants as the members of the culture they were derived from. This phenomenon indicates that the source of heterogeneity is non-genetic, it tells us how important it is for cell survival when encountering an inhospitable niche, and it illustrates how individual cells within isogenic populations exhibit differential sensitivity to stress. This phenomenon could be

predicted on the basis of a viability assay, but only experiments at the single-cell level show heterogeneity of the physiological state of cells. The non-genetic heterogeneity could be fundamental for the survival of organisms. Assuming that the MS channels act as safety valves modulating the tension in the membrane (and that this is their only function), a direct correlation between the variation in the relative volume change and the level of expression of MscL protein should be observed. In such a case, the distributions of these two parameters should have the same character (assuming that the same percentage of the total number of channels gets activated in each cell).

The source of heterogeneity may arise from a variation in the number of MS channels or other proteins per cell. If one assumes that the expression of genes coding mechanosensitive channels is purely stochastic, the distribution of proteins among the cells in a given population is not homogeneous. The studies of other stress protection systems revealed that the expression regulation has multiple and overlapping control systems [214]. Designing a tighter control over these mechanisms would eliminate the problem of overlapping paths, but, on the other hand, the cell would have to sacrifice its ability to adapt to different conditions.

The principal cell variable in exponential phase cultures is the cell cycle stage, which is characterized by fluctuations in the transcriptional activity and cell volume. The cell's "age" may also play a role. *E. coli* divides symmetrically, which means that every daughter cell inherits one pole from the mother cell (old pole) and one formed during the division process (new pole). As was shown in [215], younger cells (the ones with relatively new poles) grow faster and show higher stress resistance compared to the old ones (the ones with an old pole, which was formed many divisions before).

### 7.2.3 Possible variations

It is known that *E. coli* changes the fatty-acid composition of membrane lipids as a function of the temperature of growth [216], which impacts the lipid bilayer's fluidity. This phenomenon is known as "homeoviscous adaptation". Los and Murata [217] re-

ported that hyperosmotic stress might have an impact on membrane fluidity similar in its consequences to low-temperature stress. The dependence of membrane fluidity on the degree of unsaturation of fatty acids is a well-known phenomenon, so one may expect that the rigidity of the membrane in hyperosmotically shocked cells is a result of desaturation of fatty acids, as was shown for *Bacillus subtilis* [217]. When the lipid membranes of the cultures grown in LB medium with and without a 1.5 M NaCl were compared, the difference in viscosity and cardiolipin (CL) content was apparent [218]. Interestingly, membrane fluidizers cause very similar effects to hyperosmotic stimulation [219]. Morein *et al.* [220] reported that the addition of a 0.1 M NaCl to a lipid extract from an inner and outer membrane of *E. coli* grown at 37°C caused a 15 – 20°C decrease in the temperature at which the phase transition occurred.

The facts listed above indicate that the salt content in the growth medium may have an impact on membrane fluidity and, as a consequence, on mechanosensitive channels. The degree of impact of salt on functioning of MS channels may be tested by a series of volume change measurements performed on cells grown in media of different salt concentrations and exposed to an identical osmotic shock (e.g., osmotic shock from 0.5 M to 0.2 M and from 0.3 M to 0 M). The hypothesis of salt indirect impact on MS channels could also be proven by showing that the "temperature effect" may be reversed by the "salt effect".

The most common solute used to change the osmolarity of the medium is NaCl. However, it was reported [221] that salt may have an impact on peptidoglycan contraction. This appeared to be the effect of the electrostatic interaction with the peptidoglycan rather than cell volume change due to the osmotic effect. Isolated peptidoglycan showed a similar behavior: upon addition of water it released protons and, as a result, the structure shrank (however, intact cells and extracted peptidoglycan do not show sensitivity to salt in well-buffered media). Interestingly, this effect was not observed when sucrose was used instead of salt. The salt content may also have an impact on the peptidoglycan geometry: in high-salt media cells are smaller and shorter compared to the ones grown in a low-salt medium.

The presence of PEG (polyethylene glycol) in the growth medium (used to change the osmolarity of the medium) caused very severe damage in the cells during the osmotic shock. One could notice the presence of a few inclusion bodies in the cytoplasm, which might have been aggregates of denaturated protein (Figure 7.7). The experiments on cells grown in media of the same osmolarity but in the presence of various solutes would show the role and importance of the peptidoglycan mesh in cell protection from the osmotic shock and any other potential changes in cell physiology due to high concentration of a given solute.

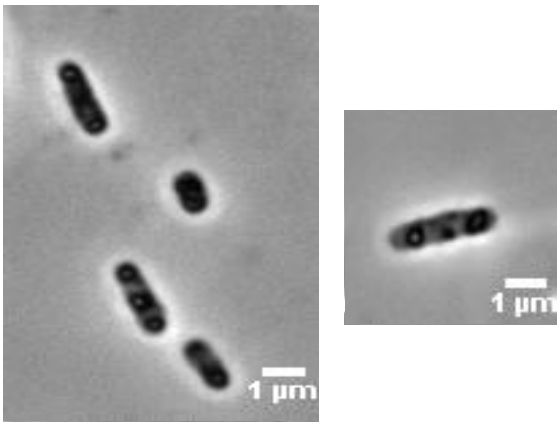


Figure 7.7: Inclusion bodies localization in *E. coli* cells. As reported in [222], such aggregates may appear in the cell growing in the non-stressing environment as natural transcription and translation errors, or in protein overproducing mutants, and as a result of stress conditions. The induced inclusion bodies were found to be located at the cellular poles, in mid- or quarter-cell positions. The results suggest that the presence of the aggregate caused a reduced growth rate. Hence, inclusion bodies appear to act as an intracellular sink for abnormal proteins.

The majority of experiments are done on cells in the exponential phase of growth. Such a solution is believed to be optimal since all cells should be in the same physiological state and their reaction is expected to be identical. However, Makinoshima *et al.* [122] reported that *E. coli* culture in an exponential phase of growth may be separated into at least five discrete subpopulations after the Percoll gradient centrifugation (in stationary phase even ten separate subpopulations may be distinguished). Bacterial populations, even those in an exponential phase of growth, show some heterogeneity.

The physiology of a bacterial cell changes upon transition into a stationary phase. The two most meaningful parameters (from the osmotic shock survival point of view) are structural modification of the peptidoglycan and changes in gene expression. It was reported that murein from cells in a stationary phase of growth is more cross-linked compared to that from an exponential phase. However, the length of the glycan chains was longer in the peptidoglycan from the cells in the exponential phase of growth, compared to that from cells in a stationary phase [223].

All the changes described above may modify the cell response to a given stress. The results of experiments performed on cells in an exponential phase of growth separated in the Percoll gradient centrifugation may indicate the importance of the overall cell density on survival of osmotic shock. If the variation in cell density (or size) is the main source of heterogeneity, separation of cell population in the Percoll gradient and then exposure of each subpopulation to an identical osmotic shock is expected to result in a much lower cell-to-cell variation among the cells from a given subpopulation.

## 7.3 High resolution imaging: cryo-EM

High resolution imaging is a very powerful tool. One such technique, cryo-electron microscopy (cryo-EM), became very popular for studying the detailed structure of biological specimens. The biggest advantage of this method is that the specimen does not have to be stained, fluorescently labeled or fixed in any way, which avoids potential conformational changes. The sample is prepared by flash-freezing, which guarantees it is imaged in its physiological environment and its integrity is not perturbed.

All layers of the Gram-negative cell envelope (inner membrane, peptidoglycan layer, and the outer membrane) have been studied extensively. However, the imaging of these structures separately is a great challenge due to the bacterial size. Cryo-EM is a method that overcomes this limitation.

The turgor pressure presses the cytoplasmic membrane against the peptidoglycan

layer. What happens when a bacterium experiences a sudden drop or increase in osmotic pressure and water is being transferred across the cell envelope? What is the reaction of these three layers? To answer these questions we imaged wild-type MG1655 cells exposed to a 0.5 M NaCl change in the external osmolarity (Figure 7.8). These cells were grown to exponential phase in M9 minimal medium (cells exposed to hyperosmotic shock and unshocked cells) or in M9 minimal medium supplemented with 0.5 M NaCl (cells exposed to hypoosmotic shock). Next, they were pelleted at 37°C and resuspended to a final $OD_{600}$ of 0.6 in prewarmed M9 minimal medium (cells exposed to a hypoosmotic shock and unshocked cells) or in M9 minimal medium supplemented with 0.5 M NaCl (cells exposed to hyperosmotic shock). All samples were frozen immediately after resuspension.

Osmotically unchallenged cells (Figure 7.8A) have a smooth cell envelope with a regular-in-size periplasmic space. All three layers of the cell envelope are close to each other and no sign of disruption or irregularity is visible. The cytoplasm is dense, but homogeneously spread across the whole cell. The morphology of the cell envelope of cells exposed to hyperosmotic shock is very different (Figure 7.8B). The cytoplasmic membrane is detached from the peptidoglycan layer and the inner membrane. The cytoplasmic material is inhomogeneously distributed in the cell with characteristic plasmolysis spaces along the cell circumference, especially enlarged at the polar region. The inner membrane is irregular in shape. Small membrane vesicles can be observed near the cytoplasmic membrane (especially at the plasmolysis spaces); some of them are detached, the others are attached to the inner membrane. These vesicles in osmotically shocked cells have been observed previously [224, 225]. Their presence was justified by a small compressibility of the membrane. When cells are exposed to an increase in osmolarity, water rushes into the external medium and the cytoplasmic membrane is no longer under turgor pressure. Due to small compressibility its surface is deformed with many invaginations. This extra membrane area is believed to dissipate in the form of membrane vesicles. A similar phenomenon was observed in cholesterol-free giant lipid vesicles [226]. The reversible shape transition and budding was observed in lipid vesicles as the hydrostatic pressure was released. The formation

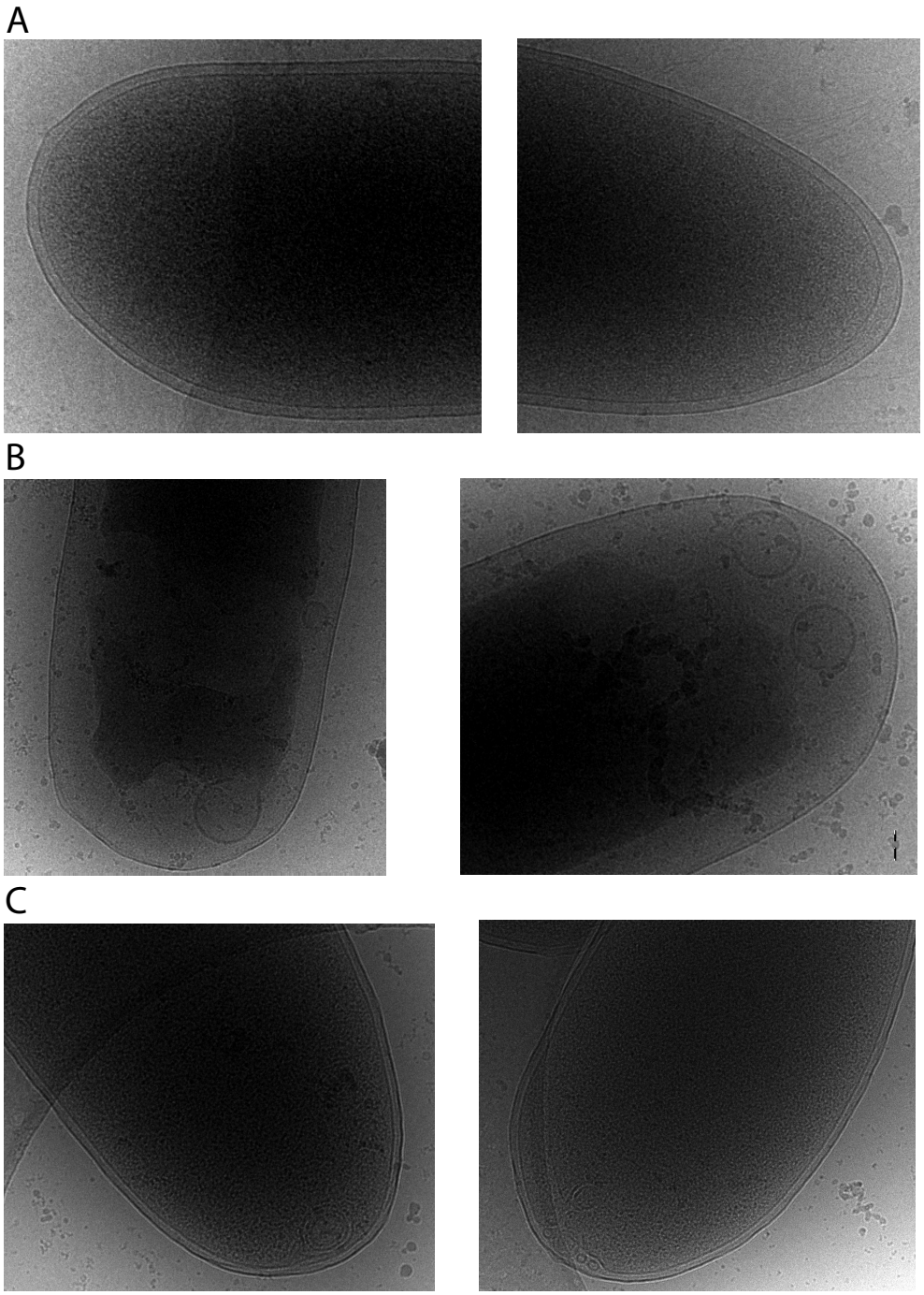


Figure 7.8: MG1655 (wild-type) cells imaged with cryo-electron microscopy. Cells were grown to exponential phase in M9 minimal medium and imaged immediately after medium exchange. (A) Cells not exposed to osmotic challenge; (B) Cells exposed to 0.5 M NaCl hyperosmotic shock; (C) cells exposed to 0.5 M NaCl hypoosmotic shock. Imaging by Morgan Beeby.

of these membrane vesicles was proposed to contribute to the cell lysis during rehydration [227]. Since the area of the cytoplasmic membrane decreases due to vesicle formation, it cannot recover to its initial volume during the fast rehydration and the cell membrane ruptures. Surprisingly, the cells exposed to hypoosmotic shock (Figure 7.8C) also show some inner membrane irregularities, smaller than the vesicles in hyperosmotically challenged cells, but also concentrated mainly at the poles. To our knowledge, such a morphological feature in cells exposed to hypoosmotic shock has not been previously reported.

We also employed cryo-EM microscopy to evaluate the periplasmic space width after exposure to osmotic challenge (Figure 7.9). MG1655 (wild-type) and MJF612 ($\Delta mscL$ $\Delta mscS$ $\Delta mscK$ $\Delta ybdG$) strains were grown in a 0.3 M NaCl NC medium to exponential phase. They were pelleted by centrifugation and resuspended in a 0 M NaCl NC medium to a final $OD_{600}$ of 0.6. Samples were frozen immediately after resuspension.

The width of the periplasmic space of the imaged strains was measured at the pole and in the middle of the cell using the program ImageJ. The measurement was performed for 53 MG1655 (wild-type) cells and 37 MJF612 cells. Two histograms were made for each strain, one for the distribution of the widths measured at the pole, the second one for the distribution of "normalized" widths (the width measured at the pole divided by the width measured in the middle of the cell). The comparison of the polar periplasmic width between the wild-type (Figure 7.9A) and the MS channel deletion mutant (Figure 7.9C) shows that it is roughly 25% smaller for the MJF612 strain. This discrepancy may be explained by the fact that the MJF612 strain lacks four mechanosensitive channels and, thus, cannot release the osmotic pressure build-up due to osmotic shock. As a result, the turgor pressure in the mutant is expected to be higher compared to the wild-type strain, and as a result the inner membrane is being pushed more against peptidoglycan layer. To avoid a potential bias due to the measurement in the polar region, we normalized the values obtained by the periplasmic width in the middle of the cell. The mean value for the

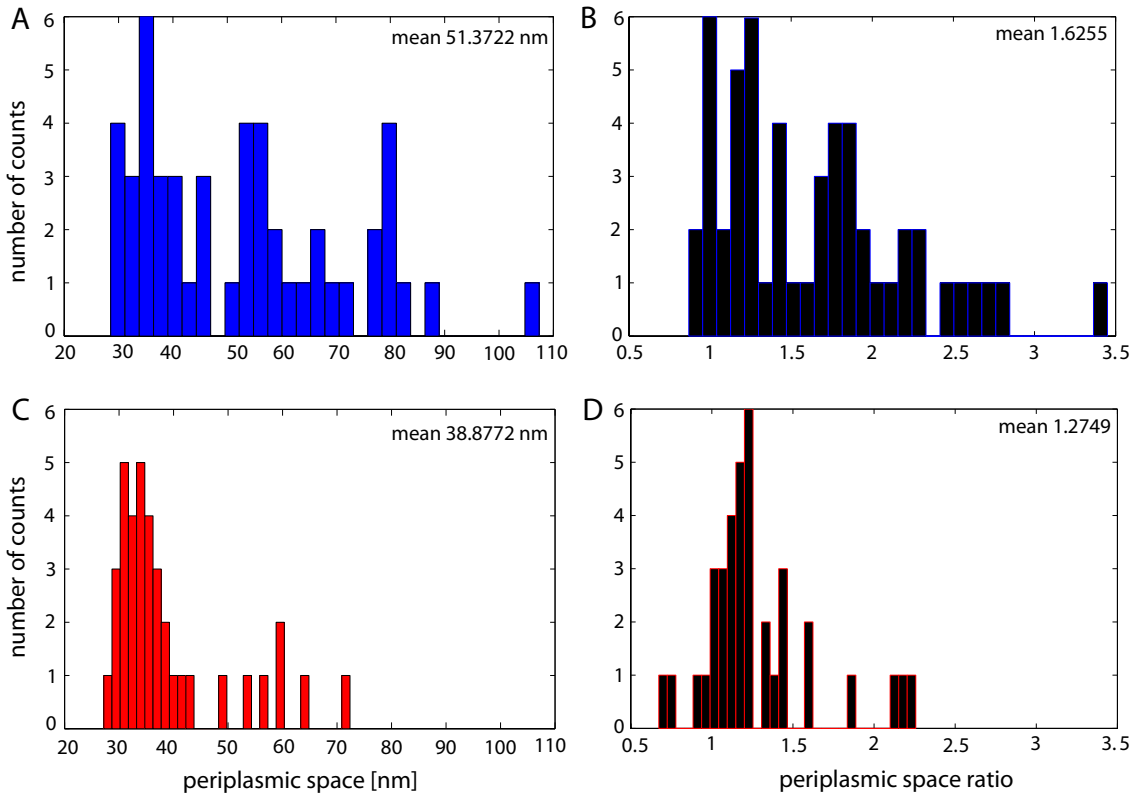


Figure 7.9: Width of the periplasmic space after exposure to a 0.3 M NaCl osmotic shock. (A) Width of the periplasmic space at the polar region, MG1655 strain (wild type); (B) Width of the periplasmic space at the polar region normalized by the width of the periplasmic space in the middle of the cell, MG1655 strain; (C) Width of the periplasmic space at the polar region, MJF612 strain ($\Delta mscL$ $\Delta mscS$ $\Delta mscK$ $\Delta ybdG$); (D) Width of the periplasmic space at the polar region normalized by the width of the periplasmic space in the middle of the cell, MJF612 strain. Images used in this analysis collected by Alasdair McDowall.

mutant (Figure 7.9D) was roughly 20% smaller compared to the value for the wild-type strain (Figure 7.9B). The similar difference between these two strains for both measurements (normalized and not normalized) suggests that the inner membrane of the MJF612 strain is under higher turgor pressure and, as a result, the width of the periplasmic space is homogeneously smaller along the cell perimeter.

# Chapter 8

# Conclusions

The isolation of *Escherichia coli* by Theodor Escherich in 1885 revolutionized many fields of study. The ease of culturing and a relatively short doubling-time very quickly brought this organism to scientific attention, a position it has maintained until this day. Over the years, we have gained a deep understanding of this bacterium, and it has served as one of the origins of many discoveries in modern biology. Thanks to the availability of molecular biology tools, it became an ideal model for studies on various aspects of cell physiology, one of them being the reaction to changes in the osmolarity of the surrounding environment. It is now apparent that mechanosensitive channels are crucial for the survival of osmotic challenge. However, the precise understanding of their function *in vivo* and their role in single-cell physiology still requires much investigation. In this thesis we present an alternative to previously used methods for studying the molecular basis of mechanosensation in bacteria.

One of the major discoveries presented in this work is that the survival of various mechanosensitive channel deletion mutants depends strongly on the rate of medium exchange. Our systematic study of the fate of individual cells after an osmotic challenge with different rates revealed a potential explanation for the existence of seven different types of mechanosensitive channels in *E. coli*. We have also found that some of them may play a larger role than previously assumed. We argue that using just a standard plating assay may be misleading for the holistic description of the function of these channels, and that both quantitative regulation of the rate of medium exchange as well as direct single-cell observation of the morphology are necessary for the fully

quantitative description of the functioning of these channels *in vivo*. We have also described morphologically distinct types of injuries as well as the time distribution of cell death due to osmotic change in the medium. These results should be particularly important for further studies on the contribution of the mechanical properties of the cell envelope on cell resistance to rupture.

We have additionally performed single-cell census of MscL (Mechanosensitive channel of Large conductance) channels as a function of growth conditions. The comparison between our results and those previously reported revealed a large discrepancy, which can be explained as the result of the choice of the measurement method: electrophysiology measures only active channels, whereas quantitative Western blots in combination with fluorescence microscopy measure all MscL proteins expressed in the cell. The comparison of the distribution of the MscL expression levels revealed that they are subject to large cell-to-cell variability exhibiting strong correlation with the presence of stress factors (phase of growth, medium, and osmolarity). This abundance mystery led us to think about the minimal number of channels needed for survival. Using a strain with reduced level of MscL channels expressed, we have shown that the number of channels needed for survival is lower than the basally expressed. A key component that must be used in order to fully understand the relation between the number of expressed channels and the protection of the cell against osmotic shock is the quantitative regulation of the MscL protein expression through the RBS modification.

Finally, we have also discussed a possible new approach to studing the activity of mechanosensitive channels *in vivo*, which involves the use of a calcium-sensitive protein and a volume change measurement. The combination of our single-cell assay with a well-controlled rate of medium exchange and quantitative measurement of the number of expressed proteins is ideally suited to determine the amount of transport occurring through these channels. Our preliminary results illustrate the accessibility of both these methods. An equally interesting issue is the variation in the volume of the periplasmic space and the observation of the morphology of the cell envelope lay-

ers. We present preliminary data obtained with a high resolution cryo-EM imaging.

We hope that the results presented in this thesis, as well as our discussion on the possible alternative functions of mechanosensitive channels, will inspire a new way of thinking about mechanosensation in bacteria. We believe that a deeper understanding of the relation between these channels and the other structures in the cell will result in many more surprising discoveries.

# Appendices

# Appendix A

# Modified protocol for the plating assay

The original protocol was written by Susan Black. The version presented here contains minor modifications and comments.

- Inoculate 2 mL of LB (5g/L NaCl) in a round-bottom 14 mL culture tube with a single colony of the desired strain. Using the Miller variant of LB (10g/L NaCl) throughout the assay will result in slightly lower ($\sim$ 10%) cell survival.

- The next morning prewarm plates and media, and prepare all the aliquots needed for the subsequent steps in the protocol.

- Measure $OD_{600}$ of the overnight culture and dilute to $OD_{600}$ 0.05 into 10 mL of prewarmed LB in a 50 mL conical tube. Leave the cap loose and secure it with a piece of lab tape. Incubate with shaking at 37°C. If the assay is performed for more than one strain, prepare dilutions every 30 minutes. Diluting all strains at the same time will result in some of them growing above the desired $OD_{600}$, as the various MS deletion mutants have slightly different doubling times.

- When the culture reaches $OD_{600}$ 0.3 (after about 2 hours) dilute it 1:10 into a 10 mL prewarmed LB supplemented with 0.5 M NaCl and incubate with shaking at 37°C.

- Monitor $OD_{600}$ of the culture. Using $OD_{650}$ for the optical density measurement

will result in a slightly higher number of cells compared with the measurement using $OD_{600}$.

- When the culture reaches $OD_{600}$ 0.2 – 0.3 (preferably $OD_{600}$ 0.25) perform the osmotic shock (the cells are at the desired $OD_{600}$ after about an hour after the dilution). Using cells at $OD_{600}$ lower than 0.3 is critical for the consistency of the assay [228].

- To osmotically challenge the cells, dilute 0.5 mL of high salt culture into 9.5 mL of prewarmed LB without additional salt (shock sample) and 9.5 mL of prewarmed LB supplemented with 0.5 M NaCl (control). Cells should be added into the center of the medium volume. Layering them on top of the medium will result in a higher survival. The pipette used when making these dilutions will also affect final survival. The highest survival rate can obtained by using serological pipette and adding cells slowly to the medium. A lower survival rate will be obtained when using 1 mL regular pipette and adding cells quickly into the medium. These dilutions are made in 50 mL conical tubes. After the addition of cells make sure to mix the content of the tube.

- Incubate for 10 minutes at 37°C. No difference was noticed for static incubation versus incubation with shaking.

- After the incubation, serially dilute cells 1:10 to a final dilution $1 : 10^4$ in media of the same osmolarity (LB supplemented with 0.5 M NaCl for the control and LB without addition of NaCl for the shock sample). These dilutions are made by adding 50 $\mu$L or cell dilution into 450 $\mu$L of previously aliquoted medium in the 1.7 mL Eppendorf tube and mixed by gentle vortexing. Preparing these dilutions in a 37°C room will result in higher survival compared to the dilutions prepared at room temperature.

- Plate 5 $\mu$L of the original cell dilution and all the subsequent dilutions in five repetitions on agar plate. For the shock sample use plates made of regular LB

(no additional salt), for the control sample use plates made of LB supplemented with 0.5 M NaCl. Let the plates dry.

- Incubate the plates for a few hours. The counting of the colonies should be done when they are barely visible with a naked eye. Use a microscope with 4x magnification to find a row which gives 20 – 30 colonies and count them. Counting colonies early will result in a better consistency of the assay, as they tend to merge when getting bigger.

# Appendix B

# Flow cell assembly

Materials:

- Cole-Parmer tygon microbore tubing, ID 0.02 in, OD 0.06 in
- Corning glass microslides, 3" × 1", plain
- coverslips, VWR 22 x 50 mm, No. 1 1/2
- double sided sticky tape, Grace Bio-Labs Secure-Seal Adhesive, 0.1 mm thick, precut, with a T-shape channel cut out
- 5-minute epoxy
- plated diamond flat-tip drill bit, CRLaurence, 1.50 mm
- razor blade
- blunt needles, Warner Instruments
- valves, Cole-Parmer, stopcock 1 way male lock
- syringes, BD
- syringe pump, New Era Pump System, NE-1000

Assembly:

- Using a diamond-tipped drill bit, drill three holes in a stack of glass slides immersed in water (Figure B.1A).

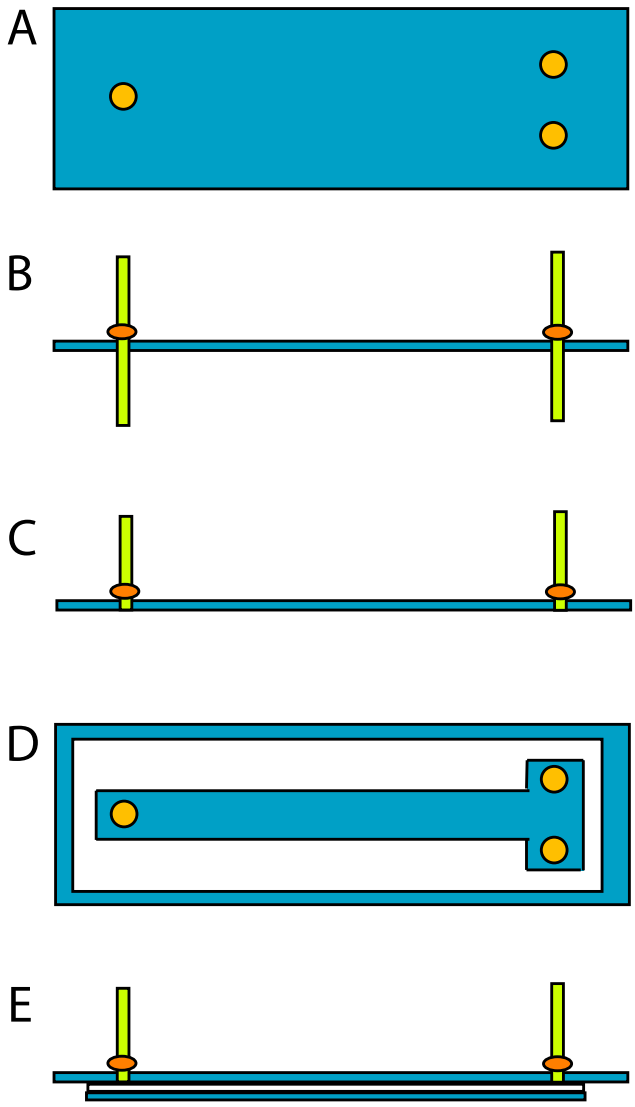


Figure B.1: Schematic picture showing how to assemble a flow cell. (A) Top view of a glass slide with drilled holes; (B) side view of a slide with the tubing pushed through the holes and secured with epoxy; (C) side view of a slide with the spare tubing cut on the inner side of the slide; (D) Top view of a slide (inner side of the chamber) with a double sided sticky tape attached; (E) Side view of an assembled flow cell.

- Clean drilled slides and coverslips by 30 minutes sonication in 1 M KOH, ethanol, and MilliQ water. Dry them by heating on a hot plate.
- Cut (at an angle) two 15.5 cm long pieces of tubing for the input and one 40.5 cm long piece of tubing for the output.

- Push about 0.5 cm of the tubing through the drilled holes and secure with 5-minute epoxy on external side of the flow cell (side where the longer piece of tubing is) (Figure B.1B).
- Let epoxy dry.
- When the epoxy has dried, cut off the 0.5 cm piece of tubing using a razor blade (Figure B.1C).
- Remove one side of the backing from the double-sided tape and carefully attach it on the inner side of the slide. Make sure it does not cover input or output ports (Figure B.1D). Using a pipette tip or the bottom of the eppendorf tube, make sure the tape sticks well to the glass.
- Remove the other backing from the tape and seal the chamber with cleaned and dried coverslip. Once again, make sure that the tape sticks well to the coverslip (Figure B.1E).
- As an additional step you can melt the tape by heating it on a hot plate for less than a minute.
- Prime the flow cell with water.
- Connect the output of the tubing through the blunt needle to the syringe mounted on the syringe pump.
- Flow PEI solution through the chamber, wash the excess with water.
- Connect the inputs of the chamber to syringes containing desired media through blunt needles attached to the valves.
- Prime the input ports with desired medium by flushing it through the chamber.

# Appendix C

# MLG910 strain: chromosomal integration strategy

Figure C.1: The details of chromosomal integration strategy. (A) MscL-sfGFP fusion protein design and sequence. The single letter amino acid sequence for *E. coli* MscL, the linker, and sfGFP are colored in brown, pink, and (fluorescent) green, respectively; (B) Sequences of 23.01 Forward Primer and 23.01R Reverse Primer used for integration; (C) Auxiliary plasmid pZS4*-em7-galK. 4* denotes spectinomycin resistance gene, em7 is a synthetic prokaryotic promoter, and galK is the galactokinase coding gene; (D) Native MscL coding region in *E. coli*; (E) 4*-em7-galK cassette from pZS4*-em7-galK plasmid inserted into MscL coding region by recombineering with lambda Red-mediated homologous recombination [229]; (F) MscL-sfGFP fusion inserted into MscL coding region by recombineering with lambda Red-mediated homologous recombination [229]. The gene is under control of the native MscL promoter. The resulting colonies were screened by a negative selection scheme (growth on agar plates containing 2-Deoxy-D-galactose) to avoid introducing an antibiotic resistance marker in the fusion construct. To verify successful integration, multiple colonies were picked for single colony PCR amplification of the MscL region. The mass of the desired fragment was confirmed by agarose gel electrophoresis. The PCR fragments were purified and sent for DNA sequencing (Laragen) for final verification [116].

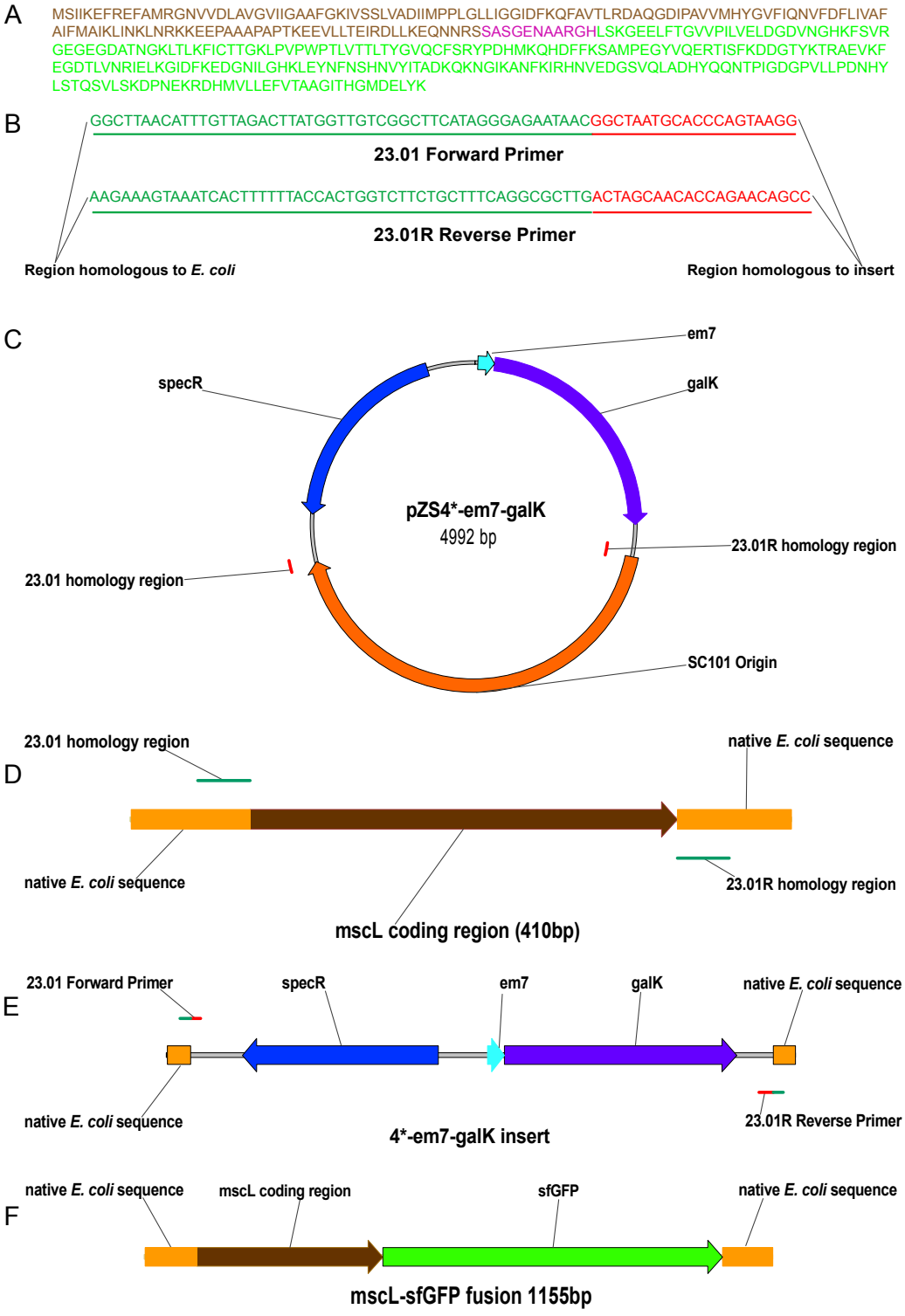
A
MSIIKEFREFAMRGNVVDLAVGVIIGAAFGKIVSSLVADIIMPPLGLLIGGIDFKQFAVTLRDAQGDIPAVVMHYGVFIQNVFDFLIVAF
AIFMAIKLINKLNRKKEEPAAAPAPTKEEVLLTEIRDLLKEQNNRSSASGENAARGHLSKGEELFTGVVPILVELDGDVNGHKFSVR
GEGEGDATNGKLTLKFICTTGKLPVPWPTLVTTLTYGVQCFSRYPDHMKQHDFFKSAMPEGYVQERTISFKDDGTYKTRAEVKF
EGDTLVNRIELKGIDFKEDGNILGHKLEYNFNSHNVYITADKQKNGIKANFKIRHNVEDGSVQLADHYQQNTPIGDGPVLLPDNHY
LSTQSVLSKDPNEKRDHMVLLEFVTAAGITHGMDELYK
B
GGCTTAACATTTGTTAGACTTATGGTTGTCGGCTTCATAGGGAGAATAACGGCTAATGCACCCAGTAAGG
23.01 Forward Primer
AAGAAAGTAAATCACTTTTTTACCACTGGTCTTCTGCTTTCAGGCGCTTGACTAGCAACACCAGAACAGCC
23.01R Reverse Primer
Region homologous to E. coli
Region homologous to insert
C
em7
specR
galK
pZS4*-em7-galK
4992 bp
23.01R homology region
23.01 homology region
SC101 Origin
D
23.01 homology region
native E. coli sequence
native E. coli sequence
23.01R homology region
mscL coding region (410bp)
E
23.01 Forward Primer
specR
em7
galK
native E. coli sequence
native E. coli sequence
23.01R Reverse Primer
4*-em7-galK insert
F
native E. coli sequence
mscL coding region
sfGFP
native E. coli sequence
mscL-sfGFP fusion 1155bp

# Appendix D

# Gamma fitting parameters

| MLG910 | | | | | | |
|---|---|---|---|---|---|---|
| media | OD600 | # of cells | Mean count | Fano factor | $a$ | $b$ |
| LB-Miller | 0.33 | 2503 | 340 | 17.6408611 | 6.7152 | 50.6649 |
| LB-Miller | 0.49 | 2556 | 293 | 68.98253 | 6.1215 | 47.8332 |
| LB-Miller | 1.08 | 788 | 330 | 43.49771 | 9.3501 | 35.3103 |
| LB-Miller | 1.27 | 1555 | 320 | 42.77948 | 8.8456 | 36.1941 |
| LB-Miller | 1.74 | 6165 | 472 | 92.64373 | 6.2285 | 75.8225 |
| M9+glucose | 0.3 | 3084 | 466 | 78.78777 | 7.1114 | 65.5902 |
| M9+glucose | 0.51 | 1221 | 466 | 118.3628 | 5.0172 | 92.9789 |
| M9+glucose | 0.67 | 1756 | 552 | 139.3568 | 4.9949 | 110.4617 |
| M9+glucose | 0.95 | 2559 | 560 | 137.6172 | 4.9512 | 113.0242 |
| M9+glucose | 1.23 | 1520 | 746 | 126.0476 | 6.4454 | 115.7735 |
| M9+glucose +0.1M NaCl | 0.29 | 4280 | 780 | 191.23870 | 4.8270 | 161.5811 |
| M9+glucose +0.1M NaCl | 0.52 | 3663 | 802 | 158.5049 | 6.4774 | 123.8357 |
| M9+glucose +0.1M NaCl | 0.7 | 2019 | 776 | 130.4718 | 7.2173 | 107.5843 |
| M9+glucose +0.1M NaCl | 1 | 3799 | 786 | 141.1716 | 7.1582 | 109.7980 |
| M9+glucose | | | | | | |

| | | | | | | |
|---|---|---|---|---|---|---|
| +0.1M NaCl | 1.43 | 4397 | 1234 | 237.9579 | 6.5788 | 187.5706 |
| M9+glucose +0.25M NaCl | 0.25 | 3429 | 358 | 69.73346 | 6.7773 | 52.8596 |
| M9+glucose +0.25M NaCl | 0.46 | 3976 | 951 | 192.7966 | 6.5631 | 144.9569 |
| M9+glucose +0.25M NaCl | 0.71 | 5971 | 956 | 196.7224 | 6.4514 | 148.2273 |
| M9+glucose +0.25M NaCl | 1.01 | 3569 | 985 | 212.4989 | 6.3969 | 153.9933 |
| M9+glucose +0.25M NaCl | 1.21 | 2684 | 1314 | 240.0539 | 6.9047 | 190.3492 |
| M9+glucose +0.5M NaCl | 0.26 | 1681 | 1419 | 227.7141 | 7.9413 | 178.6636 |
| M9+glucose +0.5M NaCl | 0.35 | 2261 | 1585 | 331.3018 | 6.1975 | 255.8249 |
| M9+glucose +0.5M NaCl | 0.45 | 2540 | 1324 | 215.3837 | 8.0087 | 165.2828 |
| M9+glucose +0.5M NaCl | 0.71 | 3921 | 1422 | 241.854 | 7.4901 | 189.8175 |
| M9+glucose +0.5M NaCl | 0.91 | 1546 | 1394 | 276.4679 | 6.7176 | 207.5572 |
| M9+glucose +0.5M NaCl | 1.2 | 1503 | 1353 | 235.0474 | 7.2670 | 186.2539 |
| M9+glycerol | 0.31 | 2098 | 709 | 112.7239 | 8.2344 | 86.1558 |
| M9+glycerol | 0.41 | 4635 | 686 | 123.8411 | 6.6806 | 102.7219 |
| M9+glycerol | 0.62 | 3248 | 681 | 128.9213 | 6.3772 | 106.8403 |
| M9+glycerol | 0.85 | 4385 | 747 | 150.5265 | 5.9535 | 125.5369 |
| M9+glycerol | 1 | 3227 | 680 | 141.0444 | 6.2205 | 109.3368 |
| M9+glycerol | 1.15 | 4960 | 721 | 145.3868 | 6.1545 | 117.0988 |
| M9+glycerol | 1.27 | 3914 | 729 | 159.2388 | 6.2790 | 116.1648 |
| M9+glycerol | | | | | | |

| | | | | | | |
|---|---|---|---|---|---|---|
| +0.1M NaCl | 0.4 | 3923 | 870 | 184.3223 | 6.2537 | 139.1729 |
| M9+glycerol +0.1M NaCl | 0.76 | 2631 | 827 | 144.6099 | 7.4902 | 110.3775 |
| M9+glycerol +0.1M NaCl | 1.07 | 1949 | 847 | 129.1219 | 8.5798 | 98.7149 |
| M9+glycerol +0.25M NaCl | 0.19 | 3712 | 1013 | 181.4919 | 6.9965 | 144.7469 |
| M9+glycerol +0.25M NaCl | 0.28 | 2426 | 1173 | 228.9686 | 6.6479 | 176.4324 |
| M9+glycerol +0.25M NaCl | 0.33 | 4073 | 1043 | 237.7741 | 5.8768 | 177.4560 |
| M9+glycerol +0.25M NaCl | 0.46 | 2258 | 951 | 192.7966 | 8.1167 | 105.7527 |
| M9+glycerol +0.25M NaCl | 0.56 | 2348 | 1125 | 251.1459 | 5.9777 | 188.1924 |
| M9+glycerol +0.25M NaCl | 0.68 | 1371 | 875 | 149.4666 | 7.7279 | 113.2247 |
| M9+glycerol +0.25M NaCl | 0.71 | 2248 | 866 | 170.2669 | 7.8821 | 109.8916 |
| M9+glycerol +0.25M NaCl | 0.92 | 1497 | 865 | 194.9382 | 6.9831 | 123.8102 |
| M9+glycerol +0.25M NaCl | 1.26 | 2267 | 938 | 168.3297 | 7.5704 | 123.9285 |
| M9+glycerol +0.5M NaCl | 0.19 | 3351 | 1746 | 350.3273 | 6.1965 | 281.7584 |
| M9+glycerol +0.5M NaCl | 0.21 | 3531 | 1511 | 337.0336 | 5.8162 | 259.7950 |
| M9+glycerol +0.5M NaCl | 0.23 | 3230 | 1634 | 287.2615 | 7.3157 | 223.3389 |
| M9+glycerol +0.5M NaCl | 0.46 | 1226 | 1423 | 261.1942 | 6.7470 | 210.8849 |

| | | | | | | |
|---|---|---|---|---|---|---|
| M9+glycerol +0.5M NaCl | 0.5 | 2520 | 1508 | 331.159 | 6.4267 | 236.8047 |
| M9+glycerol +0.5M NaCl | 0.71 | 2727 | 1709 | 425.3123 | 5.0346 | 339.4075 |
| M9+glycerol +0.5M NaCl | 0.83 | 1366 | 1348 | 228.5577 | 7.2754 | 185.2823 |
| M9+glycerol +0.5M NaCl | 0.99 | 1689 | 1501 | 216.2896 | 8.5913 | 174.6689 |
| M9+glycerol +0.5M NaCl | 1.23 | 253 | 1443 | 211.2783 | 8.7255 | 165.4151 |
| MLG910-ΔrpoS | | | | | | |
| media | OD600 | # of cells | Mean count | Fano factor | $a$ | $b$ |
| LB-Miller | 0.24 | 1429 | 108 | 45.0497 | 6.0750 | 17.8172 |
| LB-Miller | 0.42 | 1496 | 109 | 19.63285 | 6.1966 | 17.6530 |
| LB-Miller | 0.65 | 2256 | 80 | 16.39978 | 6.1865 | 12.8821 |
| LB-Miller | 0.86 | 2677 | 89 | 19.31024 | 6.4813 | 13.7722 |
| LB-Miller | 1.01 | 2555 | 95 | 16.09938 | 7.2978 | 12.9749 |
| LB-Miller | 1.2 | 2783 | 115 | 24.8767 | 6.5511 | 17.5012 |
| M9+glucose | 0.46 | 1444 | 64 | 8.742002 | 8.7053 | 7.3483 |
| M9+glucose | 0.6 | 3043 | 65 | 8.490565 | 8.8846 | 7.3159 |
| M9+glucose | 0.81 | 2179 | 66 | 8.306852 | 9.2411 | 7.1535 |
| M9+glucose | 0.96 | 2560 | 56 | 9.410702 | 7.2931 | 7.6971 |
| M9+glucose | 1.18 | 3785 | 58 | 12.48343 | 5.9048 | 9.8834 |
| M9+glycerol | 0.32 | 2932 | 68 | 10.20687 | 8.3619 | 8.1879 |
| M9+glycerol | 0.46 | 1367 | 63 | 8.814788 | 9.2509 | 6.8037 |
| M9+glycerol | 0.67 | 1100 | 64 | 9.418268 | 9.0937 | 7.0203 |
| M9+glycerol | 0.94 | 1000 | 60 | 7.645006 | 9.7265 | 6.1819 |
| M9+glycerol | 1.18 | 1182 | 62 | 7.23113 | 10.4019 | 6.0069 |

Table D.1: A summary of results for channel counts and gamma distribution fitting.

# Bibliography

[1] Raven P. H., Evert R. F. and Eichhorn S. E. (2005) *Biology of Plants* (7th ed.), W.H. Freeman and Company.

[2] Gillespie P. G. and Walker R. G. (2001) *Molecular basis of mechanosensory transduction*, Nature 413, 194-202.

[3] Babinski J. (1896) *Sur le rflexe cutan plantaire dans certaines affections organiques du systeme nerveux central*, Comptes rendus de la Société de Biologie 48, 207-208.

[4] $http://en.wikipedia.org/wiki/File:VFT\_ne1.JPG$.

[5] $http://en.wikipedia.org/wiki/File:CelegansGoldsteinLabUNC.jpg$.

[6] $http://en.wikipedia.org/wiki/File:BabinskiSign.jpg$.

[7] Pohorille A., Schweighofer K., and Wilson M. A. (2005) *The origin and early evolution of membrane channels*, Astrobiology 5, 1, 1-17.

[8] Balleza D. (2011) *Toward understanding protocell mechanosensation*, Orig Life Evol Biosph 41, 281-304.

[9] Kloda A. and Matinac B. (2001) *Molecular identification of a mechanosensitive channel in Archaea*, Biophysical Journal 80, 229-240.

[10] Kloda A. and Matinac B. (2001) *Mechanosensitive channel of thermoplasma, the cell wall-less Archaea*, Cell Biochemistry and Biophysics 34, 321-347.

[11] Kloda A. and Matinac B. (2002) *Common evolutionary origins of mechanosensitive ion channels in Archaea, Bacteria and cell-walled Eukarya*, Archaea 1, 3544.

[12] Pivetti Ch. D., Yen M.-R., Miller S., Busch W., Tseng Y.-H., Booth I. R. and Saier M. H. Jr. (2003) *Two families of mechanosensitive channel proteins*, Microbiology and Molecular Biology Reviews 67, 1, 6685.

[13] Haswell E. S. and Meyerowitz E. M. (2006) *MscS-like proteins control plastid size and shape in Arabidopsis thaliana*, Current Biology 16, 111.

[14] Haswell E. S., Peyronnet R., Barbier-Brygoo H., Meyerowitz E. M. and Frachisse J.-M. (2008) *Two MscS homologs provide mechanosensitive channel activities in the Arabidopsis root*, Current Biology 18, 730734.

[15] Friedman H. C. (2006) *Escherich and Escherichia*, Advances in Applied Microbiology 60, 133-196.

[16] Poulsen L. K., Licht T. R., Rang C., Krogfelt K. A., and Molin, S. (1995) *Physiological state of E. coli BJ4 growing in large intestines of streptomycin-treated mice*, Journal of Bacteriology 177, 5840-5845.

[17] *microbewiki.kenyon.edu/index.php/Escherichia_coli*.

[18] Isaac L. and Ware G. C. (1974) *The flexibility of bacterial cell walls*, J. appl. Bact. 37, 335 - 339.

[19] Wang S., Arellano-Santoyob H., Combs P. A. and Shaevitz J. W. (2010) *Actin-like cytoskeleton filaments contribute to cell mechanics in bacteria*, PNAS 107, 20, 9182-9185.

[20] Koch A. L., Higgins M. L., and Doyle R. J. (1981) *Surface tension-like forces determine bacterial shapes: Streptococcus faecium*, Journal of General Microbiology 123, 151-161.

[21] Csonka L. N. (1989) *Physiological and genetic responses of bacteria to osmotic stress*, Microbiological Reviews 53, 1, 121-147.

[22] Levina N., Totemeyer S., Stokes N. R., Louis P., Jones M. A. and Booth I. R. (1999) *Protection of Escherichia coli cells against extreme turgor by activation of MscS and MscL mechanosensitive channel: identification of genes required for MscS activity*, EMBO Journal 18, 7, 1730-1737.

[23] Erdos T., Butler-Browne G. S., and Rappaport L. (1991) *Mechanogenetic regulation of transcription*, Biochimie 73, 1219-1231.

[24] Walderhaug M. O., Polarek J. W., Voelkner P., Daniel J. M., Hesse J. E., Altendorf K., and Epstein W. (1992) *KdpD and KdpE, proteins that control expression of the kdpABC operon, are members of the two-component sensor-effector class of regulators*, Journal of Bacteriology 174, 2152-2159.

[25] Mitchell P. and Moyle J. (1956) *Osmotic function and structure in bacteria*, in Spooner E. T. C. and Stocker B. A. D. *Bacteria Anatomy*, Cambridge University Press.

[26] Whatmore A. M. and Reed R. H. (1990) *Determination of turgor pressure in Bacillus subtilis: a possible role for $K^+$ in turgor regulation*, Journal of General Microbiology 136, 2521-2526.

[27] Yao X., Walter J., Burke S., Stewart S., Jericho M. H., Pink D., Hunter R., and Beveridge T. J. (2002) *Atomic force microscopy and theoretical considerations of surface properties and turgor pressures of bacteria*, Colloids and Surfaces B: Biointerfaces 23, 213-230.

[28] Walsby A. E., Hayes P. K., and Boje R. (1995) *The gas vesicles, buoyancy and vertical distribution of cyanobacteria in the Baltic Sea*, European Journal of Phycology 30, 87-94.

[29] Holland D. P. and Walsby A. E. (2009) *Digital recordings of gas-vesicle collapse used to measure turgor pressure and cellwater relations of cyanobacterial cells*, Journal of Microbiological Methods 77, 214-224.

[30] Scheie P. (1973) *Osmotic Pressure in Escherichia coli as rendered detectable by lysozyme attack*, Journal of Bacteriology 114, 2, 549-555.

[31] Cayley D. S., Guttman H. J., and Record M. T. (2000) *Biophysical characterization of changes in amounts and activity of Escherichia coli cell and compartment water and turgor pressure in response to osmotic stress*, Biophysical Journal 78, 1748-1764.

[32] Deng Y., Sun M., and Shaevitz J. W. (2011) *Direct measurement of cell wall stress stiffening and turgor pressure in live bacterial cells*, Physical Review Letters 107, 158101-1 - 158101-4.

[33] Stock J. B., Rauch B. and Roeman S. (9177) *Periplasmic space in Salmonella typhimurium and Escherichia coli*, Journal of Biological Chemistry 252, 21, 7850-7861.

[34] Koch A. L. and Suzanne-Pinette M. F. (1987) *Nephelometric determination of turgor pressure in growing Gram-negative bacteria*, Journal of Bacteriology, 169, 8, 3654-3663.

[35] Pinette M. F. S. and Koch A. L. (1987) *Variability of the turgor pressure of individual cells of the Gram-negative heterotroph Ancylobacter aquaticus*, Journal of Bacteriology 169, 10, 4737-4742.

[36] Overmann J., Lehmann S., and Pfennig N. (1991) *Gas vesicle formation and buoyancy regulation in Pelodictyon phaeoclathratiforme (Green sulfur bacteria)*, Archives of Microbiology 157, 29-37.

[37] Arnoldi M., Fritz M., Bauerlein E., Radmacher M., Sackmann E. and Boulbitch A. (2000) *Bacterial turgor pressure can be measured by atomic force microscopy*, Physical Review E 62, 1, 1034-1044.

[38] Roszak D. B. and Colwell R. R. (1987) *Survival strategies of bacteria in the natural environment*, Microbiological Reviews 51, 3, 365-379.

[39] Potts W. T. W. and Parry G. (1964) *Osmotic and Ionic Regulation in Animals*, International Series of Monographs on Pure and Applied Biology, A Pergamon Press Book, the MacMillan Company, New York.

[40] Van Elsas J. D., Semenov A. V., Costa R., and Trevors J. T. (2011) *Survival of Escherichia coli in the environment: fundamental and public health aspects*, The ISME Journal 5, 173-183.

[41] Rozen Y. and Belkin S. (2001) *Survival of enteric bacteria in seawater*, FEMS Microbiology Reviews 25, 513-529.

[42] Nishimuta M., Inoue N., Kodama N., Morikuni E., Yoshioka Y. H., Matsuzaki N., Shimada M., Sato N., Iwamoto T., Ohki K., Takeyama H., and Nishimuta H. (2006) *Moisture and mineral content of human feces. High fecal moisture is associated with*

*increased sodium and decreased potassium content*, Journal of Nutritional Science and Vitaminology 52, 121-126.

[43] Cooke E. M., Ewins S. P., and Shooter R. A. (1969) *Changing faecal population of Escherichia coli in hospital medical patients*, Brtish Medical Journal 4, 593-595.

[44] Cooke E. M. and Ewins S. P. (1973) *Properties of strains of Escherichia coli isolated from a variety of sources*, Journal of Medical Microbiology 8, 107-111.

[45] Garfield L. M. and Walker M. J. (2008) *Water potential changes in faecal matter and Escherichia coli survival*, Journal of Applied Microbiology 105, 1009-1016.

[46] Gerba C. P. and McLeod J. S. (1976) *Effect of sediments on the survival of Escherichia coli in marine waters*, Applied and Environmental Microbiology 32, 1, 114-120.

[47] Davies C. M., Long J. A. H., Donald M., and Ashbolt N. J. (1995) *Survival of fecal microorganisms in marine and freshwater sediments*, Applied and Environmental Microbiology 61, 5, 1888-1896.

[48] Hartz A., Cuvelier M., Nowosielski K., Bonilla T. D., Green M., Esiobu N., McCorquodale D. S., and Rogerson A. (2008) *Survival potential of Escherichia coli and Enterococci in subtropical beach sand: Implications for water quality managers*, Journal of Environmental Quality 37, 898-905.

[49] Nollet, L'Abbé (1748) *Recherches sur les causes du bouillonnement des liquides*, in *Mémoires de Mathématique et de Physique, tirés des registres de l'Académie Royale des Sciences de l'année 1748*, pp. 57-104.
Full text: $http://books.google.com/books?id=0r34MpoStRkC\&pg=RA1-PA101\#v=onepage\&q\&f=false$.

[50] $http://marietietz.girlshopes.com/concentratedurine/$.

[51] Dutrochet, H. (1826) *L'agent immédiat du movement vital dévoilé dans sa nature et dans son mode d'action chez les végétaux et chez les animaux*, Paris, France.
Full text: $http://books.google.com/books?id=WAIAAAAAQAAJ\&pg=PR1\#v=onepage\&q\&f=false$.

[52] Vierordt, K. (1848) *Beschreibung eines verbesserten Endosmometers*, Pogg. Ann., vol. 73, 529.

[53] Graham, T. (1854) *The Bakerian Lecture: On osmotic force*, Philosophical Transactions of the Royal Society of London, vol. 144, 177228.
Full text: http : //ia600504.us.archive.org/35/items/philtrans00286382/00286382.pdf.

[54] Traube, M. (1866) *Über homogene Membranen und deren Einfluß auf die Endosmose*, Zentralblatt fur die medicinischen Wissenschaften, vol. 7, 97-100.
Full text: $http://books.google.com/books?id=p5sEAAAAQAAJ\&pg=PA97\&dq=\%C3\%9Cber+homogene+Membranen+und+deren+Einflu\%C3\%9F+auf+die+Endosmose\&hl=pl\&sa=X\&ei=PPgzUfW5LqnKigKa94HAAw\&ved=0CDEQ6AEwAA\#v=onepage\&q\&f=false$.

[55] Findlay, A. (1913) *Monographs on inorganic and physical chemistry. Osmotic pressure*, Longmans, Green and Co, London, New York, Bombay and Calcutta.

[56] $http://de.academic.ru/dic.nsf/dewiki/358998$.

[57] Pfeffer, W. (1921) *Osmotische Untersuchungen. Studien zur Zellmechanik*, Wilhelm Engelmann, Leipzip.
Full text: http : //ia700305.us.archive.org/9/items/osmotischeunters00pfef/osmotischeunters00pfef.pdf.

[58] Van't Hoff, J. H. (1887) *Die Rolle osmotischen Drucks in der Analogie zwischen Losungen und Gasen*, Zeitschrift fur physikalische Chemie, vol. 1, 481-508.

[59] Morse, H. N. (1914) *Osmotic pressures of aqueous solutions*, Carnegie Institute of Washington, 211-217.
Full text: $http://books.google.com/books?id=MyAWAAAAYAAJ\&printsec=frontcover\&hl=pl\#v=onepage\&q\&f=false$.

[60] Phillips R., Kondev J., Theriot J., Garcia H. G., and Orme N. (2012) *Physical Biology of the Cell*, second edition, Garland Science.

[61] Dick D. A. (1964) *The permeability coefficient of water in the cell membrane and the diffusion coefficient in the cell interior*, Journal of Theoretical Biology 3, 504-531.

[62] Poolman B. and Glaasker E. (1998) *Regulation of compatible solute accumulation in bacteria*, Molecular Microbiology 29, 2, 397-407.

[63] Epstein W. and Schultz S. G. (1965) *Cation transport in Escherichia coli. V. Regulation of cation content*, Journal of General Physiology 49, 221-234.

[64] Epstein W. (1986) *Osmoregulation by potassium transport in Escherichia coli*, FEMS Microbiology Reviews 39, 73-78.

[65] Ajouz B., Berrier C., Garrigues A., Besnard M., and Ghazi A. (1998) *Release of thioredoxin via the mechanosensitive channel MscL during osmotic downshock of Escherichia coli cells*, Journal of Biological Chemistry 273, 41, 26670-26674.

[66] McLaggan D., Naprstek J., Buurman E. T., and Epstein W. (1994) *Interdependence of $K^+$ and glutamate accumulation during osmotic adaptation of Escherichia coli*, Journal of Biological Chemistry 269, 3, 1911-1917.

[67] Record M. T., Courtenay E. S., Cayley D. S., and Guttman H. J. (1998) *Responses of E. coli to osmotic stress: large changes in amounts of cytoplasmic solutes and water*, TIBs 23, 143-148.

[68] Neu H. C. and Hepel L. A. (1965) *The release of enzymes from Kwherichia coli by osmotic shock and during the formation of spheroplasts*, Journal of Biological Chemistry 240, 9, 3685-3692.

[69] Nossal N. G. and Heppel L. A. (1966) *The release of enzymes by osmotic shock from Escherichia coli in exponential phase*, Journal of Biological Chemistry 241, 13, 3055-3062.

[70] Schleyer M., Schmid R., and Bakker E. P. (1993) *Transient, specific and extremely rapid release of osmolytes from growing cells of Escherichia coli K-12 exposed to hypoosmotic shock*, Archives of Microbiology 160, 424-431.

[71] Berrier C., Garriguez A., Richarme G., and Ghazi A. (2000) *Elongation factor Tu and DnaK are transferred from the cytoplasm to the periplasm of Escherichia coli during osmotic downshock presumably via the mechanosensitive channel MscL*, Journal of Bacteriology 182, 1, 248-251.

[72] van den Bogaart G., Krasnikov V., and Poolman B. (2007) *Dual-color fluorescence-burst analysis to probe protein efflux through the mechanosensitive channel MscL*, Biophysical Journal 92, 1233-1240.

[73] Cruickshank C. C., Minchin R. F., Le Dain A. C. , and Martinac B. (1997) *Estimation of the pore size of the large-conductance mechanosensitive ion channel of Escherichia coli*, Biophysical Journal 73, 1925-1931.

[74] Sukharev S. I., Sigurdson W. J., Kung C., and Sachs F. (1999) *Energetic and spatial parameters for gating of the bacterial large conductance mechanosensitive channel, MscL*, Journal of General Physiology 113, 525-540.

[75] Vazquez-Laslop N., Lee H., Hu R., and Neyfakh A. A. (2001) *Molecular sieve mechanism of selective release of cytoplasmic proteins by osmotically shocked Escherichia coli*, Journal of Bacteriology 183, 8, 2399-2404.

[76] Berrier C., Coulombe A. Szabo I., Zoratti M., and Ghazi A. (1992) *Gadolinium ion inhibits loss of metabolites induced by osmotic shock and large stretch-activated channels in bacteria*, European Journal of Biochemistry 206, 559-565.

[77] Britten R. J. and McClure F. T. (1962) *The amino acid pool in Escherichia coli*, Bacteriological Reviews 26, 292-335.

[78] Tsapis A. and Kepes A. (1977) *Transient breakdown of the permeability barrier of the membrane of Escherichia coli upon hypoosmotic shock*, Biochimica et Biophysica Acta 469, 1-12.

[79] Kimmich G. A., Randles J., Brand J. S. (1975) *Assay of picomole amounts of ATP, ADP and AMP using the luciferme enzyme system*, Analytical Biochemistry 69, 187-206.

[80] Jones S. E., Naik R. R., and Stone M. O. (2000) *Use of small fluorescent molecules to monitor channel activity*, Biochemical and Biophysical Research Communications 279, 208-212.

[81] Ewis H. E. and Lu C.-D. (2005) *Osmotic shock: A mechanosensitive channel blocker can prevent release of cytoplasmic but not periplasmic proteins*, FEMS Microbiology Letters 253, 295-301.

[82] Thorstenson Y. R., Zhang Y., Olson P. S., and Mascarenhas D. (1997) *Leaderless polypeptides efficiently extracted from whole cells by osmotic shock*, Journal of Bacteriology 179, 17, 5333-5339.

[83] Dinnbier U., Limpinsel E., Schmid R., and Bakker E. P. (1988) *Transient accumulation of potassium glutamate and its replacement by trehalose during adaptation of growing cells of Escherichia coli K-12 to elevated sodium chloride concentrations*, Archives of Microbiology 150, 348-357.

[84] Lurquin P. F. (1997) *Gene transfer by electroporation*, Molecular Biotechnology 7, 5-35.

[85] Zimmermann U. (1986) *Electrical breakdown, electropermeabilization and electrofusion*, Reviews of Physiology, Biochemistry and Pharmacology 105, 176-256.

[86] Louhivuori M., Risselada H. J., van der Giessen E., and Marrink S. J. (2010) *Release of content through mechano-sensitive gates in pressurized liposomes*, PNAS 107, 46, 19856-19860.

[87] Seeman P. (1967) *Transient holes in the erythrocyte membrane during hypotonic hemolysis and stable holes in the membrane after lysis by saponin and lysolecithin*, Journal of Cell Biology 32, 55-70.

[88] Topazian M. and Binder H. J. (1994) *Factitious diarrhea detected by measurement of stool osmolarity*, The New England Journal of Medicine 330, 20, 1418-1419.

[89] Etheridge R. D., Seerley R. W., and Huber T. L. (1984) *The effect of diet on fecal moisture, osmolarity of fecal extracts, products of bacterial fermentation and loss of minerals in feces of weaned pigs*, Journal of Animal Science 58, 6, 1403-1411.

[90] Bionumbers ID 100804, $http://bionumbers.hms.harvard.edu/bionumber.aspx?\&id = 100804\&ver = 0$.

[91] Braude A. I., Siemienski J., and Lee K. (1968) *Spheroplasts in human urine*, in Guze L. B. *Microbial Protoplasts, Spheroplasts and L-Forms*, the Williams & Wilkins company, Baltimore.

[92] Martinac B., Buechner M., Delcour A. H., Adler J. and Kung C. (1987) *Pressure-sensitive ion channel in Escherichia coli*, Proc. Natl. Acad. Sci. USA, Vol. 84, pp. 2297-2301.

[93] Ajouz B., Berrier C., Garrigues A., Besnard M. and Ghazi A. (1998) *Release of thioredoxin via the mechanosensitive channel MscL during osmotic downshock of Escherichia coli cells*, Journal of Biological Chemistry 273, 41, 26670-26674.

[94] Berrier C., Besnard M., Ajouz B., Coulombe A, and Ghazi A. (1996) *Multiple mechanosensitive ion channels from Escherichia coli, activated at different Thresholds of Applied Pressure*, Journal of Membrane Biology 151, 175-187.

[95] Sukharev S. I., Blount P., Martinac B., Blattner F. R. and Kung C. (1994) *A large-conductance mechanosensitive channel in E. coli encoded by mscL alone*, Nature 368, 265-268.

[96] Chang G., Spencer R. H., Lee A. T., Barclay M. T., Rees D. C. (1998) *Structure of the MscL homolog from Mycobacterium tuberculosis: A gated mechanosensitive ion channel*, Science 282, 2220-2226.

[97] Bass R. B., Strop P., Barclay M., and Rees D. C. (2002) *Crystal structure of Escherichia coli MscS, a voltage-modulated and mechanosensitive channel*, Science 298, 1582-1587.

[98] Wang W., Black S. S., Edwards M. D., Miller S., Morrison E. L., Bartlett W., Dong C., Naismith J. H., and Booth I. R. (2008) *The structure of an open form of an E. coli mechanosensitive channel at 3.45 Å resolution*, Science 321, 1179-1183.

[99] Liu Z., Gandhi C. S., and Rees D. C. (2009) *Structure of a tetrameric MscL in an expanded intermediate state*, Nature 461, 120-124.

[100] Schumann U., Edwards M. D., Rasmussen T., Bartlett W., van West P. and Booth I. R. (2010) *YbdG in Escherichia coli is a threshold-setting mechanosensitive channel with MscM activity*, PNAS 107, 28, 12664-12669.

[101] Edwards M. D., Black S., Rasmussen T., Rasmussen A., Stokes N. R., Stephen T.-L., Miller S., and Booth I. R. (2012) *Characterization of three novel mechanosensitive chanels activities in Escherichia coli*, Channels 6, 4, 1-10.

[102] Li Y., Moe P. C., Chandrasekaran S., Booth I. R., and Blount P. (2002) *Ionic regulation of MscK, a mechanosensitive channel from Escherichia coli*, EMBO Journal 21, 20, 5323-5330.

[103] Wiggins P. and Phillips R. (2004) *Analytic models for mechanotransduction: Gating a mechanosensitive channel*, PNAS 101, 4071-4076.

[104] Wiggins P. and Phillips R. (2005) *Membrane-protein interactions in mechanosensitive channels*, Biophysical JOurnal 88, 880-902.

[105] Reeves D., Ursell T., Sens P., Kondev J., and Phillips R. (2008) *Membrane mechanics as a probe of ion-channel gating mechanisms*, Physical Review E 78, 041901-1 - 041901-11.

[106] Ursell T., Phillips R., Kondev J., Reeves D., Wiggins P. A. (2008) *The role of lipid bilayer mechanics in mechanosensation*, in Kamkin A. and Kiseleva I. *Mechanosensitivity in cells and tissues 1: Mechanosensitive ion channels*, Springer-Verlag.

[107] Delcour A. H., Martinac B., Adler J. and Kung C. (1989) *Modified reconstitution method used in patch-clamp studies of Escherichia coli ion channels*, Biophysical Journal 58, 631-636.

[108] Perozo E., Kloda A., Cortes D. M., and Martinac B. (2002) *Differential effects of lipids and lyso-lipids on the mechanosensitivity of the mechanosensitive channels MscL and MscS*, Nature Structural Biology 9, 9, 696-703.

[109] Moe P. and Blount P. (2005) *Assessment of potential stimuli for mechano-dependent gating of MscL: effects of pressure, tension, and lipid headgroups*, Biochemistry 44, 12239-12244.

[110] Nomura T., Cranfield C. G., Deplazes E., Owen D. M., Macmillan A., Battle A. R., Constantine M., Sokabe M., and Martinac B. (2012) *Differential effects of lipids and lyso-lipids on the mechanosensitivity of the mechanosensitive channels MscL and MscS*, PNAS 109, 22, 8770-8775.

[111] Perozo E. and Rees D. (2003) *Structure and mechanism in prokaryotic mechanosensitive channels*, Current Opinion in Structural Biology 13, 4, 432 - 442.

[112] Martinac B., Adler J. and Kung C. (1990) *Mechanosensitive ion channels of E. coli activated by amphipaths*, Nature 348, 261-263.

[113] Nguyen T., Clare B., Guo W., and Martinac B. (2005) *The effect of parabens on mechanosensitive channels o E. coli*, European Biophysics Jurnal 34, 389-395.

[114] Koçer A., Walko M., Meijberg W., and Feringa B. L. (2005) *A light-actuated nanovalve derived from a channel protein*, Science 309, 755-758.

[115] Folgering J. H. A., Kuiper J. M., de Vries A. H., Engberts J. B. F. N., and Poolman B. (2004) *Lipid-mediated light activation of a mechanosensitive channel of large conductance*, Langmuir 20, 6985-6987.

[116] Bialecka-Fornal M., Lee H. J., DeBerg H. A., Gandhi C. S., and Phillips R. (2012) *Single-cell census of mechanosensitive channels in living bacteria*, PLoS ONE 7, 3, e33077.

[117] Maurer J. A. and Dougherty D. A. (2001) *A high-throughput screen for MscL channel activity and mutational phenotyping*, Biochimica et Biophysica Acta (BBA) Biomembranes 1514, 165-169.

[118] Davey H. M. (2011) *Life, death, and in-between: Meanings and methods in microbiology*, Applied and Environmetal Microbiology 77, 16, 5571-5576.

[119] Powl A. M., East J. M., and Lee A. G. (2003) *Lipid-protein interactions studied by introduction of a tryptophan residue: The mechanosensitive channel MscL*, Biochemistry 42, 14306-14317.

[120] Boer M., Anishkin A., and Skharev S. (2011) *Adaptive MscS gating in the osmotic permeability response in E. coli: The question of time*, Biochemistry 50, 4087-4096.

[121] Ursell T., Huang K. C., Peterson E., Phillips R. (2007) *Cooperative gating and spatial organization of membrane proteins through elastic interactions*, PLoS Computational Biology 3, e81.

[122] Makinoshima H., Nishimura A. and Ishihama A. (2002) *Fractionation of Escherichia coli cell populations at different stages during growth transition to stationary phase*, Molecular Microbiology 43, 2, 269 279.

[123] Poirier I., Marcéhal P.-A., and Gervais P. (2007) *Effects of the kinetics of water potential variation on bacteria viability*, Journal of Applied Micribiology 82, 101-106.

[124] Poirier I., Marcéhal P.-A., Evrard C., and Gervais P. (2008) *Escherichia coli and Lactobacillus plantarum responses to osmotic stress*, Applied Microbiology and Biotechnology 50, 704-709.

[125] Mille Y., Beney L., and Gervais P. (2003) *Magnitude and kinetics of rehydration influence the viability of dehydrated E. coli K-12*, Biotechnology and Bioengineering 83, 578-582.

[126] Booth I. R., Edwards M. D., Black S., Schumann U., Bartlett W., Rasmussen T., Rasmussen A., and Miller S. (2007) *Physiological analysis of bacterial mechanosensitive channels*, Methods in Enzymology 428, 47-61.

[127] Booth I. R., Edwards M. D., Black S., Schumann U., and Miller S. (2007) *Mechanosensitive channels in bacteria: signs of closure?*, Nature Reviews Microbiology 5, 431-440.

[128] Naismith J. H. and Booth I. R. (2012) *Bacterial mechanosensitive channels – MscS: Evolution's solution to creating sensitivity in function*, Annual Reviews of Biophysics 41, 15777.

[129] Pittman J. K., Edmond C., Sunderland P. A., and Bray C. M. (2008) *A cation-regulated and proton gradient-dependent cation transporter from Chlamydomonas reinhardtii has a role in calcium and sodium homeostasis*, Journal of Biological Chemistry 284, 525533.

[130] Meury J., Robin A., and Monnier-Champeix P. (1985) *Turgor-controlled K + fluxes and their pathways in Escherichia coli*, European Journal of Biochemistry 151, 613-619.

[131] Kamaraju K., Belyy V., Rowe I., Anishkin A., and Sukharev S. (2011) *The pathway and spatial scale for MscS inactivation*, JPG 138, 49-57.

[132] Sydney Kustu, personal communication.

[133] Yao X, Jericho M., Pink D., and Beveridge T. (1999) *Thickness and elasticity of Gram-negative Murein sacculi measured by atomic force microscopy*, Journal of Bacteriology 181, 68656875.

[134] Abu-Lail N. I. and Camesano T. A. (2006) *The effect of solvent polarity on the molecular surface properties and adhesion of Escherichia coli*, Colloids and Surfaces B, Biointerfaces 51, 62-70.

[135] Chen Y. Y., Wu C. C., Hsu J. L., Peng H. L., Chang H. Y., and Yew T. R. (2009) *Surface rigidity change of Escherichia coli after filamentous bacteriophage infection*, Langmuir 25, 4607-4614.

[136] Cerf A., Cau J.-C., Vieu C., and Dague E. (2009) *Nanomechanical properties of dead or alive single-patterned bacteria*, Langmuir 25, 5731-5736.

[137] Eaton P., Fernandes J. C., Pereira E., Pintado M. E., and Xavier Malcata F. (2008) *Atomic force microscopy study of the antibacterial effects of chitosans on Escherichia coli and Staphylococcus aureus*, Ultramicroscopy 108, 1128-1134.

[138] Perry C. C., Weatherly M., Beale T., and Randriamahefa A. (2009) *Atomic force microscopy study of the antimicrobial activity of aqueous garlic versus ampicillin against Escherichia coli and Staphylococcus aureus*, Journal of the Science of Food and Agriculture 89, 958964.

[139] Tuson H. H., Auer G. K., Renner L. D., Hasebe M., Tropini C., Salick M., Crone W. C., Gopinathan A., Huang K. C., and Weibel D. B. (2012) *Measuring the stiffness of bacterial cells from growth rates in hydrogels of tunable elasticity*, Molecular Microbiology 84, 874891.

[140] Soupene E., van Heeswijk W. C., Plumbridge J., Stewart V., Bertenthal D., Lee H., Prasad G., Paliy O., Charernnoppakul P., and Kustu S. (2003) *Physiological studies of Escherichia coli strain MG1655: Growth defects and apparent cross-regulation of gene expression*, Journal of Bacteriology 185, 56115626.

[141] Tuszynski J. A. (2007) *Molecular and Cellular Biophysics*, Chapman & Hall/CRC.

[142] Simonin H, Beney L., and Gervais P. (2007) *Sequence of occurring damages in yeast plasma membrane during dehydration and rehydration: Mechanisms of cell death*, Biochimica et Biophysica Acta 1768, 16001610.

[143] Ursell T. (2009) *Bilayer elasticity in protein and lipid organization: Theory and experiments in model systems*, VDM Verlag.

[144] Rob Phillips and Pierre Sens, personal communication.

[145] Grage S. L., Keleshian A. M., Turdzeladze T., Battle A. R., Tay W. C., May R. P., Holt S. A., Contera S. A., Haertlein M., Moulin M., Pal P., Rohde P. R., Forsyth V. T., Watts A., Huang K. C., Ulrich A. S., and Martinac B. (2011) *Bilayer-mediated clustering and functional interaction of MscL channels*, Biophysical Journal 100, 12521260.

[146] Lindén M., Sens P., and Phillips R. (2012) *Entropic tension in crowded membranes*, PLoS Computational Biology, 8(3):e1002431.

[147] Hase C. C., Minchin R. F., Kloda A. and Martinac B. (1997) *Cross-linking studies and membrane localization and assembly of radiolabelled Large mechanosensitive ion channel (MscL) of Escherichia coli*, Biochemical and Biophysical Research Communications, 232, 777-782.

[148] Blount P., Sukharev S.I., Moe P. C., Martinac B. and Kung C. (1999) *Mechanosensitive channels of bacteria*, Methods Enzymol, 294, 458-482.

[149] Stokes N. R., Murray H. D., Subramaniam Ch., Gourse R. L., Louis P., Bartlett W., Miller S. and Booth I.R. (2003) *A Role for mechanosensitive channels in survival of stationary phase: Regulation of channel expression by RpoS*, PNAS vol. 100, no. 26, 15959-15964.

[150] Booth I. R., Edwards M. D., Murray E. and Miller S. (2005) In: *Bacterial Ion Channels and Their Eucaryotic Homologs*, ASM Press Wadhington, D.C., pp 291-312.

[151] Hase C. C., Le Dain A. C., and Martinac B. (1995) *Purification and functional reconstitution of the recombinant large mechanosensitive ion channel (MscL) of Escherichia coli*, Journal of Biological Chemistry 270, 1832918334.

[152] Hengge-Aronis R. (2000) *The general stress response in Escherichia coli*, in Storz G. and Hengge-Aronis R. *Bacterial Stress Responses*, ASM Press, Washington, D.C.

[153] Kolter R. (1999) *Growth in studying the cessation of growth*, Journal of Bacteriology 181, 697-699.

[154] Lange R. and Hengge-Aronis R. (1994) *The cellular concentration of the $\sigma^S$ subunit of RNA polymerase in Escherichia coli is controlled at the levels of transcription, translation, and protein stability*, Genes & Development 8, 1600-1612.

[155] Muffler A., Traulsen D. D., Lange R., and Hengge-Aronis R. (1996) *Posttranscriptional osmotic regulation of the $\sigma^S$ subunit of RNA polymerase in Escherichia coli*, Journal of Bacteriology 178, 6, 1607-1613.

[156] Hengge-Aronis R. (1996) *Regulation of gene expression during entry into stationary phase*, in Neidhardt F. C., Curtiss III R., Ingraham J. L., Lin E. C. C., Low K. B., Magasanik B., Reznikoff W. S., Riley M., Schaechter M., and Umbarger H. E., *Escherichia coli and Salmonella: Cellular and Molecular Biology*, 2nd edition, ASM Press, Washington, D.C.

[157] Loewen P. C., Hu B., Strutinsky J., and Sparling R. (1998) *Regulation in the rpoS regulon of Escherichia coli*, Canadian Journal of Microbiology 44, 707-717.

[158] Jishage M. and Ishihama A. (1995) *Regulation of RNA polymerase sigma subunit synthesis in Escherichia coli: intracellular levels of $\sigma^{70}$ and $\sigma^{38}$*, Journal of Bacteriology 177, 23, 6832-6835.

[159] Ding Q., Kusano S., Villarejo M., and Ishihama A. (1995) *Promoter selectivity control of Escherichia coli RNA polymerase by ionic strength: differential recognition of osmoregulated promoters by $E\sigma^D$ and $E\sigma^S$ holoenzymes*, Molecular Miccrobiology 16, 649-656.

[160] Kusano S., Ding Q., Fujita N., and Ishihama A. (1996) *Promoter selectivity of Escherichia coli RNA polymerase $E\sigma^{70}$ and $E\sigma^{38}$ holoenzymes: effect of DNA supercoiling*, Journal of Biological Chemistry 271, 1998-2004.

[161] Kusano S. and Ishihama A. (1997) *Stimulatory effect of trehalose on formation and activity of Escherichia coli RNA polymerase E$\sigma^{38}$ holoenzyme*, Journal of Bacteriology 179, 3649-3654.

[162] Hengge-Aronis R. (1996) *Back to log phase: $\sigma^S$ as a global regulator in the osmotic control of gene expression in Escherichia coli*, Milecular Microbiology 21, 5, 887-893.

[163] Liu M. Durfee T., Cabreras J. E., Zhao K., Jin D. J., and Blattner F. R. (2005) *Global transcriptional programs reveal a carbon source foraging starategy by Escherichia coli*, Journal of Biological Chemistry 280, 16, 15921-15927.

[164] Bianchi A. A. and Baneyx F. (1999) *Hyperosmotic shock induces the $\sigma^{32}$ and $\sigma^E$ stress regulons of Escherichia coli*, Molecular Microbiology 34, 5, 1029-1038.

[165] Conter A. (2003) *Plasmid DNA supercoiling and survival in long-term cultures of Escherichia coli: role of NaCl*, Journal of Bacteriology 185, 17, 5324-5327.

[166] Ni Bhriain N., Dorman C. J., and Higgins C. F. (1989) *An overlap between osmotic and anaerobic stress responses: a potential role for DNA supercoiling in the coordinate regulation of gene expression*, Molecular Microbiology 3, 933-942.

[167] Siegele D. A. (2005) *Guest commentaries: Universal stress proteins in Escherichia coli*, Journal of Bacteriology 187, 18, 6253-6254.

[168] Pedelacq J. D., Cabantous S., Tran T., Terwilliger T. C., and Waldo G. S. (2006) *Engineering and characterization of a superfolder green fluorescent protein*, Nature Biotechnology 24, 79-88.

[169] Snapp E. L., Altan N., Lippincott-Schwartz J. (2003) *Measuring protein mobility by photobleaching GFP chimeras in living cells*, Current Protocols in Cell Biology, chapter 1, Unit 21.1.

[170] Garcia H. G., Lee H. J., Boedicker J. Q., and Phillips R. (2011) *Comparison and calibration of different reporters for quantitative analysis of gene expression*, Biophysical Journal 101, 535-544.

[171] Rogers S. S., Waigh T. A., Zhao X., and Lu J. R. (2007) *Precise particle tracking against a complicated background: polynomial fitting with Gaussian weight*, Physical Biology 4, 220-227.

[172] Friedman N., Cai L., and Xie X. S. (2006) *Linking stochastic dynamics to population distribution: an analytical framework of gene expression*, Physical Review Letters 97, 168302.

[173] Boucher P. A., Morris C. E., and Joos B. (2009) *Mechanosensitive closed-closed transitions in large membrane proteins: osmoprotection and tension damping*, Biophysical Journal 97, 2761-2770.

[174] Steinbacher S., Bass R., Strop P., Rees D. C. (2007) *Structures of the prokaryotic mechanosensitive channels MscL and MscS*, in Hamill O.P. *Current Topics in Membranes, Mechanosensitive Ion Channels, Part A*, London, Academic Press, 1-24.

[175] Ursell T., PhD thesis, *Stretching the definition of a lipid bilayer : elasticitys role in protein and lipid organization*, 2009, California Institute of Technology.

[176] Rahman M., Hasan M. R., Oba T., and Shimizu K. (2005) *Effect of rpoS gene knockout on the metabolism of Escherichia coli during exponential growth phase and early stationary phase based on gene expressions, enzyme activities and intracellular metabolite concentrations*, Biotechnology and Bioengineering 94, 585-595.

[177] Dougherty T. J. and Pucci M. J. (1994) *Penicillin-binding proteins are regulated by rpoS during transitions in growth states of Escherichia coli*, Antimicrobial Agents and Chemotherapy 38, 205-210.

[178] Lessard I. A. D., Pratt S., McCafferty D. G., Bussiere D. E., Hutchins C., Wanner B. L., Katz L., and Walsh C. T. (1998) *Homologs of the vancomycin resistance D-Ala-D-Ala dipeptidase VanX in Streptomyces toyocaensis, Escherichia coli and Synechocystis: attributes of catalytic efficiency, stereoselectivity and regulation with implications for function*, Chemistry & Biology 5, 489-504.

[179] Huang Y.-M., Kan B., Lu Y., and Szeto S. (2009) *The effect of osmotic shock on RpoS expression and antibiotic resistance in Escherichia coli*, Journal of Experimental Microbiology and Immunology 13, 13-17.

[180] $http://regulondb.ccg.unam.mx/operon?term=ECK120028312\&format=jsp\&organism=ECK12\&type=operon$

[181] Mendoza-Vargas A., Olvera L., Olvera M., Grande R., Vega-Alvarado L., Taboada B., Jimenez-Jacinto V., Salgado H., Jurez K., Contreras-Moreira B., Huerta A. M., Collado-Vides J., and Morett E. (2009) *Genome-wide identification of transcription start sites, promoters and transcription factor binding sites in E. coli*, PlosOne 4(10):e7526.

[182] Shine J. and Dalgarno L. (1975) *Determinant of cistron specificity in bacterial ribosomes*, Nature 254, 34-38.

[183] $http://partsregistry.org/Help:Ribosome\_Binding\_Sites/Mechanism.$

[184] $http://partsregistry.org/Ribosome\_Binding\_Sites/Catalog.$

[185] Salis H. M., Mirsky E. A., and Voigt C. A. (2009) *Automated design of synthetic ribosome binding sites to control protein expression*, Nature Biotechnology 27, 946-952.

[186] $https://salis.psu.edu/software/RBSLibraryCalculatorSearchMode.$

[187] Egbert R. G. and Klavins E. (2012) *Fine-tuning gene networks using simple sequence repeats*, PNAS 109, 1681716822.

[188] Gemayel R., Vinces M. D., Legedre M., and Verstrepen K. J. (2010) *Variable tandem repeats accelerate evolution of coding and regulatory sequences*, Annual Review of Genetics 44, 445-477.

[189] Moxon R., Bayliss C., and Hood D. (2006) *Bacterial contingency loci: The role of simple sequence DNA repeats in bacterial adaptation*, Annual Review of Genetics 40, 307-333.

[190] Haswell E. S. (2007) *MscS-like proteins in plants*, Current Topics in Memebranes 58, 329-358.

[191] Peyronnet R., Haswell E. S., Barbier-Brygoo H., and Frachisse J.-M. (2008) *AtMSL9 and AtMSL10. Sensors of plasma membrane tension in Arabidopsis roots*, Plant Signaling & Behavior 3, 726-729.

[192] Veley K. M. and Haswell E. S. (2012) *Plastids and pathogens: Mechanosensitive channels and survival in a hypoosmotic world*, Plant Signaling & Behavior 7, 668-671.

[193] Veley K. M., Marshburn S., Clure C. E., and Haswell E. S. (2012) *Mechanosensitive channels protect plastids from hypoosmotic stress during normal plant growth*, Current Biology 22, 408-413.

[194] Wilson M. E., Jensen G. S., and Haswell E. S. (2011) *Two mechanosensitive channel homologs influence division ring placement in Arabidopsis chloroplasts*, The Plant Cell 23, 29392949.

[195] Wilson M. E. and Haswell E. S. (2012) *A role for mechanosensitive channels in chloroplast and bacterial fission*, Plant Signaling & Behavior 7, 157-160.

[196] Elizabeth Haswell, personal communication.

[197] Wahome P. G. and Setlow P. (2006) *The synthesis and role of the mechanosensitive channel of large conductance in growth and diVerentiation of Bacillus subtilis*, Archives of Microbiology 186, 377-383.

[198] Wahome P. G. and Setlow P. (2008) *Growth, osmotic downshock resistance and diVerentiation of Bacillus subtilis strains lacking mechanosensitive channels*, Archives of Microbiology 189, 49-58.

[199] Wahome P. G., Cowan A. E., Setlow B., and Setlow P. (2009) *Levels and localization of mechanosensitive channel proteins in Bacillus subtilis*, Archives of Microbiology 191, 403-414.

[200] Haswell E. S., Phillips R., and Rees D. C. (2012) *Mechanosensitive channels: What can they do and how do they do it?*, Structure 19, 1356-1369.

[201] Osanai T., Sato S., Tabata S., and Tanaka K. (2005) *Identification of PamA as a PII-binding membrane protein important in nitrogen-related and sugar-catabolic gene expression in Synechocystis sp. PCC 6803*, Journal of Biological Chemistry 280, 3468434690.

[202] Nazarenko L. V., Andreev I. M., Lyukevich A. A., Pisareva T. V., and Los D. A. (2003) *Calcium release from Synechocystis cells induced by depolarization of the plasma membrane: MscL as an outward $Ca^{2+}$ channel*, Microbiology 129, 1147-1153.

[203] Touze T., Gouesbet G., Boiangiu C., Jebbar M., Bonnassie S., and Blanco C. (2001) *Glycine betaine loses its osmoprotective activity in a bspA strain of Erwinia chrysanthemi*, Molecular Microbiology 42, 87-99.

[204] Börngen K., Battle A. R., Möker N., Morbach S., Marin K., Martinac B., and Krämer R. (2010) *The properties and contribution of the Corynebacterium glutamicum MscS variant to fine-tuning of osmotic adaptation*, Biochimica et Biophysica Acta 1798, 21412149.

[205] Becker M., Börngen K., Nomura T., Battle A. R., Marin K., Martinac B., and Krämer R. (2013) *Glutamate efflux mediated by Corynebacterium glutamicum MscCG, Escherichia coli MscS, and their derivatives*, Biochimica et Biophysica Acta 1828, 1230-1240.

[206] Nichols R. J., Sen S., Choo Y. J., Beltrao P., Zietek M., Chaba R., Lee S., Kazmierczak K. M., Lee K. J., Wong A., Shales M., Lovett S., Winkler M. E., Krogan N. J., Typas A., and Gross C. A. (2011) *Phenotypic landscape of a bacterial cell*, Cell 144, 143-156.

[207] Shaner N. C., Steinbach P. A., and Tsien R. Y. (2005) *A guide to choosing fluorescent proteins*, Nature Methods 2, 905-909.

[208] Zhao Y., Araki S., Wu J., Teramoto T., Chang Y.-F., Nakano M., Abdelfattah A. S., Fujiwara M., Ishihara T., Nagai T., and Campbell R. E. (2011) *An expanded palette of genetically encoded $Ca^{2+}$ indicators*, Science 333, 18881891.

[209] Akerboom J., Rivera J. D., Guilbe M. M., Malavé E. C., Hernandez H. H., Tian L., Hires S. A. , Marvin J. S., Looger L. L., Schreiter E. R. (2009) *Crystal structures of the GCaMP calcium sensor reveal the mechanism of fluorescence signal change and aid rational design*, Journal of Biological Chemistry 284, 6455-6464.

[210] Grynkiewicz G., Poenie M., and Tsien R. Y. (1985) *A new generation of $Ca^{2+}$ indicators with greatly improved fluorescence properties*, Journal of Biological Chemistry 260, 3440-3450.

[211] Wee S. and Wilkinson B. J. (1988) *Increased outer membrane ornithine-containing lipid and lysozyme penetrability of Paracoccus denitrificans grown in a complex medium deficient in divalent cations*, Journal of Bacteriology 170, 3283-3286.

[212] Gangola P. and Rosen B. P. (1987) *Maintenance of intracellular calcium in Escherichia coli*, Journal of Biological Chemistry 262, 12570-12574.

[213] Bohnert J. A., Karamian B., and Nikaido H. (2010) *Optimized nile red efflux assay of AcrAB-TolC multidrug efflux system shows competition between substrates*, Antimicrobial Agents and Chemotherapy 54, 37703775.

[214] Booth I. R. (2002) *Stress and the single cell: intrapopulation diversity is a mechanism to ensure survival upon exposure to stress*, International Journal of Food Microbiology 15, 78, 19-30.

[215] Stewart E.J., Madden R., Paul G. and Taddei F. (2005) *Aging and death in an organism that reproduces by morphologically symmetric division*, Plos Biology 3, 2, e45, 295-300.

[216] M. Sinensky (1974) *Homeoviscous adaptation – A homeostatic process that regulates the viscosity of membrane lipids in Escherichia coli*, Proc. Nat. Acad. Sci. USA 71, 2, 522-525.

[217] Los D. A. and Murata N. (2004) *Membrane fluidity and its roles in the perception of environmental signals*, Biochimica et Biophysica Acta 1666, 142- 157.

[218] Lopez C. S., Heras H., Garda H., Ruzal S., Snchez-Rivas C. and Rivas E. (2000) *Biochemical and biophysical studies of Bacillus subtilis envelopes under hyperosmotic stress*, International Journal of Food Microbiology 55, 1-3, 137-142.

[219] Tokishita S. and Mizuno T. (1994) *Transmembrane signal transduction by the Escherichia coli osmotic sensor, EnvZ: intermolecular complementation of transmembrane signalling*, Molecular Microbiology 13(3), 435-444.

[220] Morein S., Andersson A.-S., Rilfors L. and Lindblom G. (1996) *Wild-type Escherichia coli cells regulate the membrane lipid composition in a "window" between gel and non-lamellar structures*, Journal of Biological Chemistry 271, 12, 6801-6809.

[221] Marquis R. E. (1968) *Salt-induced contraction of bacterial cell walls*, Journal of Bacteriology 95, 3, 775 - 781.

[222] Lindner A.B., Madden R., Demarez A., Stewart E. J. and Taddei F. (2008) *Asymmetric segregation of protein aggregates is associated with cellular aging and rejuvenation*, PNAS 105, 8, 3076 - 3081.

[223] Pisabarro A. G., de Pedro M. A. and Vazquez D. (1985) *Structural modifications in the peptidoglycan of Escherichia coli assosiated with changes in the state of growth of the culture*, Journal of Bacteriology 161, 1, 238 - 242.

[224] Schwarz H. and Koch A. L. (1995) *Phase and electron microscopic observations of osmotically induced wrinkling and the role of endocytotic vesicles in the plasmolysis of the Gram-negative cell wall*, Microbiology 141, 161-3 170.

[225] Beney L., Mille Y., and Gervais P. (2004) *Death of Escherichia coli during rapid and severe dehydration is related to lipid phase transition*, Applied Microbiology and Biotechnology 65, 457464.

[226] Beney L., Perrier-Cornet J.-M., Hayert M., and Gervais P. (1997) *Shape modification of phospholipid vesicles induced by high pressure: Influence of bilayer compressibility*, Biophysical Journal 72, 1258-1263.

[227] Mille Y., Beney L., and Gervais P. (2002) *Viability of Escherichia coli after combined osmotic and thermal treatment: a plasma membrane implication*, Biochimica et Biophysica Acta 1567, 41 48.

[228] Sezonov G., Joseleau-Petit D., and D'Ari R. (2007) *Escherichia coli physiology in Luria-Bertani broth*, Journal of Bacteriology 189, 87468749.

[229] Sharan S. K., Thomason L. C., Kuznetsov S. G., Court D. L. (2009) *Recombineering: a homologous recombination-based method of genetic engineering*, Nature Protocols 4, 206223.